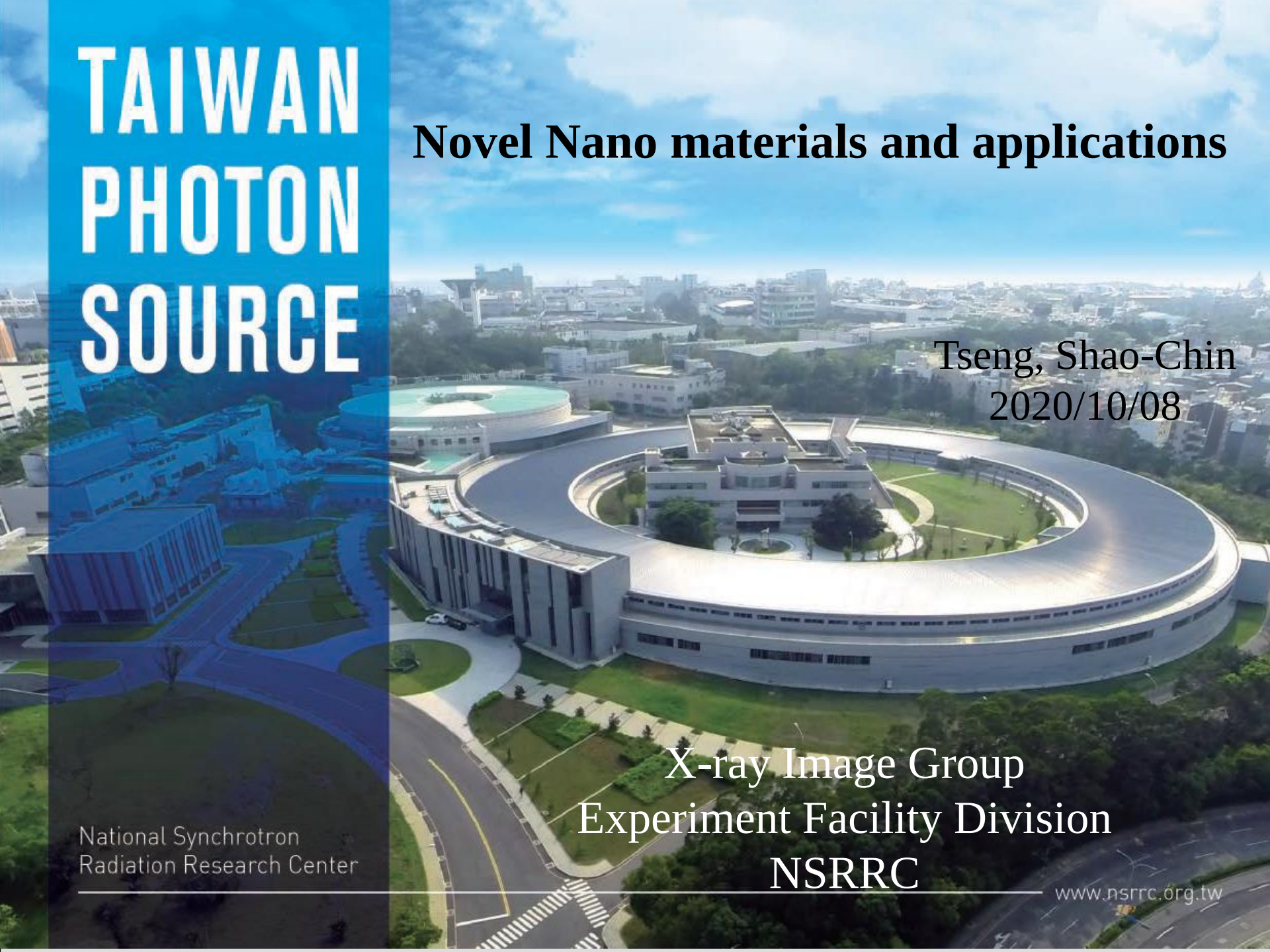

Novel Nano materials and applications

Tseng, Shao-Chin
2020/10/08

X-ray Image Group
Experiment Facility Division
NSRRC

Outline

- Advantage of materials in nanometer dimensions
- Nanomaterial analysis technology

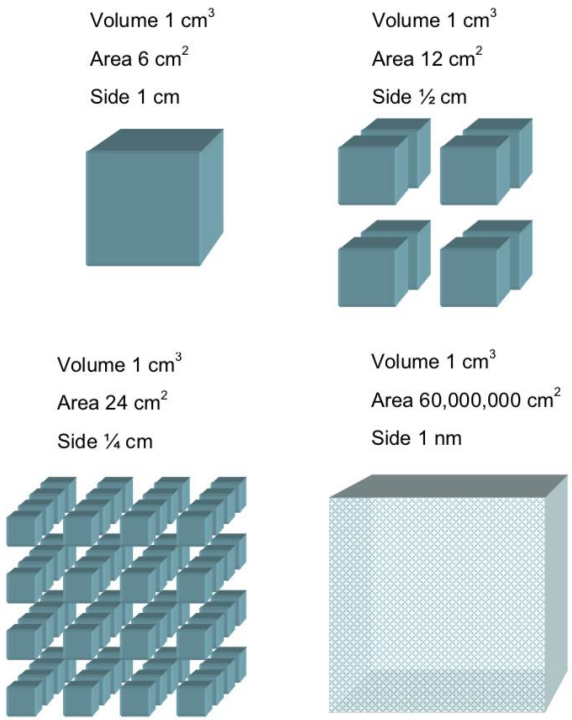

What is the nanotechnology? The term nanotechnology is employed to describe the creation and exploitation of materials with structural features in between those of atoms and bulk materials, with at least dimension in the nanometer range (1 nm = 10^{-9} m).

There are many uses and applications available using nanotechnology that are not possible using conventional materials which make it unique. For applications that use a substance's chemical properties, substantially less nanomaterial may be required to do the job of a conventional material. The chemical reactivity of a material is related to its surface area compared to its volume and the surface area for a nanoparticle is enormous per unit volume. The diagram below illustrates how surface area increases when a material is dissected into nano-sized particles.

Methods of controlling the NPs size

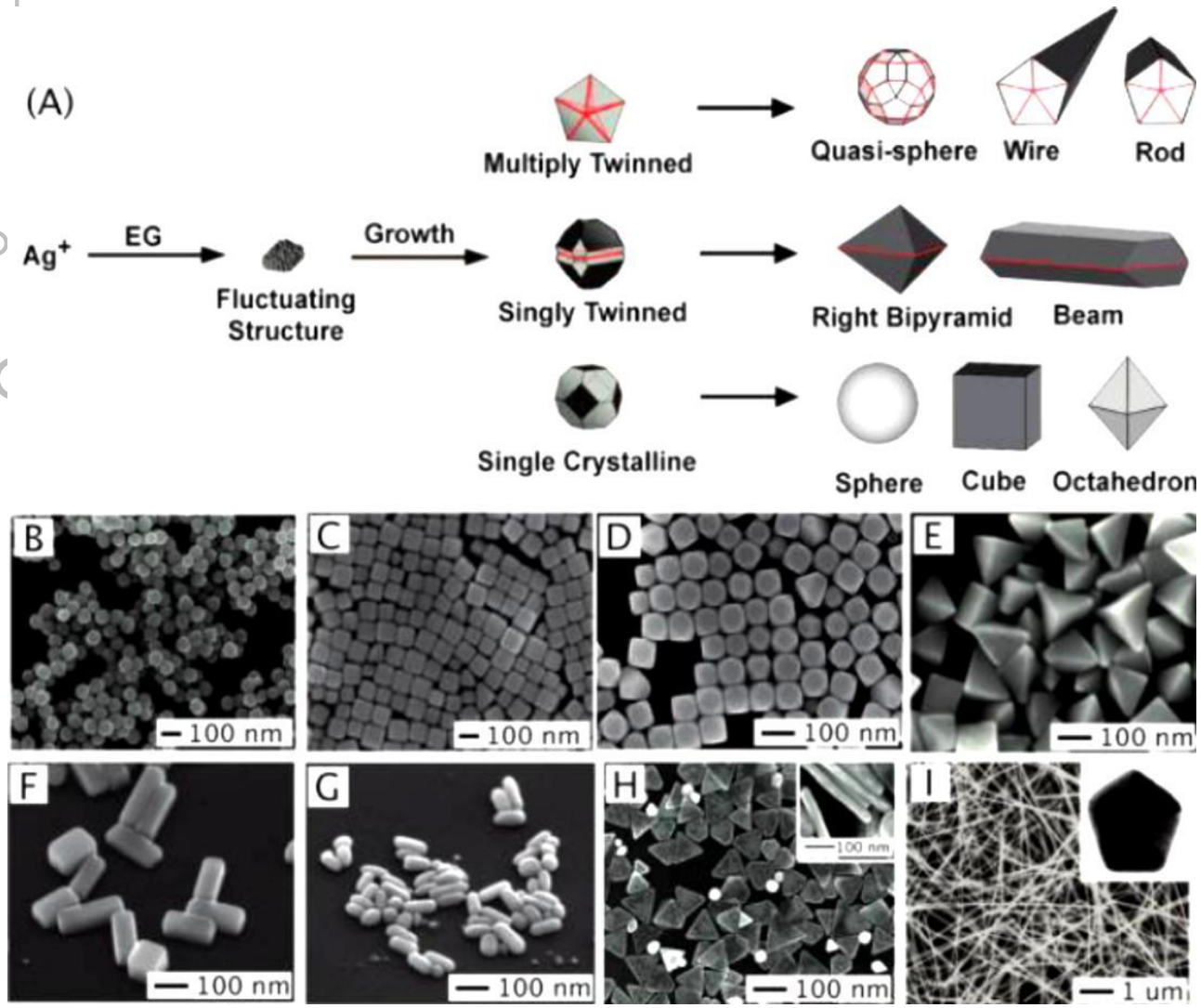

Since NPs exhibit special properties and these properties vary with the size of NPs, controlling the NPs sizes becomes an important issue. Changing the size of NPs in chemical synthesis methods is usually carried out by precisely controlling the synthesis process and concentration of reactants.

NC arrays fabricated by Chemical self-assembly

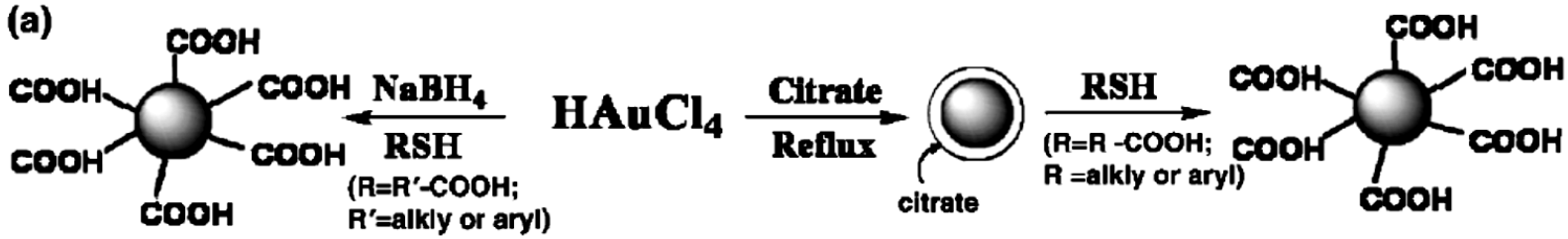

NCs of different sizes have been synthesized from $AuCl_4^-$, predominantly, using either citrate or sodium borohydride as reducing agents.

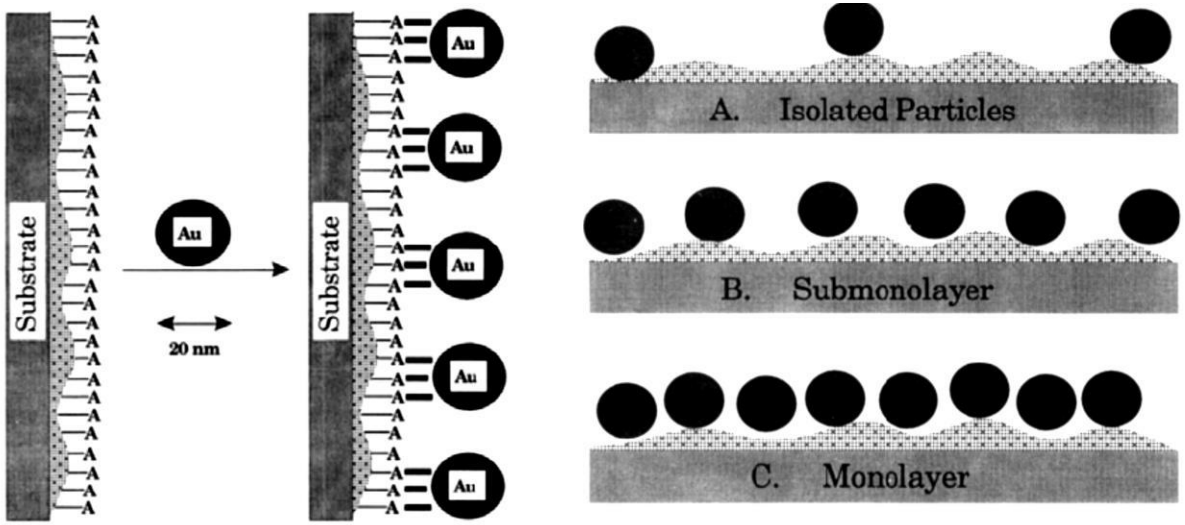

Hydroxyl/oxide groups on the substrate (e.g., glass, quartz, Si) surface provide active sites for the attachment of an alkoxysilane possessing functional group A, where A has a high affinity for gold.

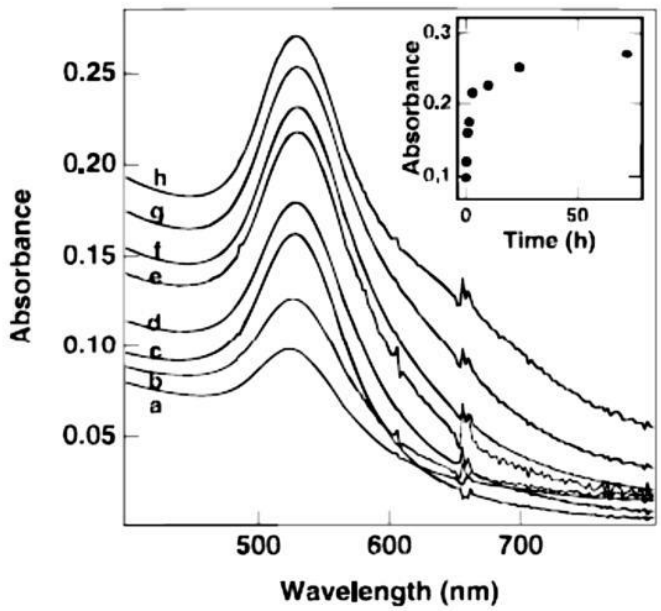

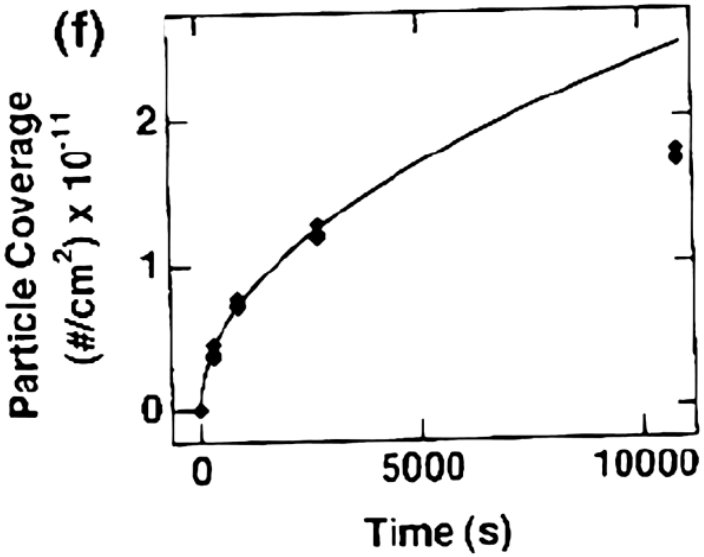

The absorbance spectra and particle coverages for glass slides immersed in 15-nm-diameter colloidal Au solution as a function of time.

Nanocluster arrays fabricated by laser annealing

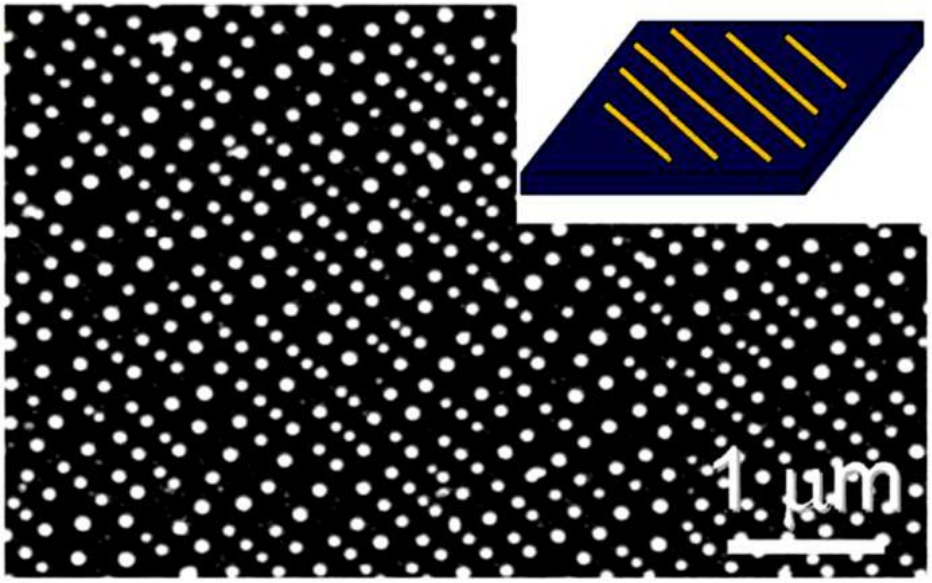

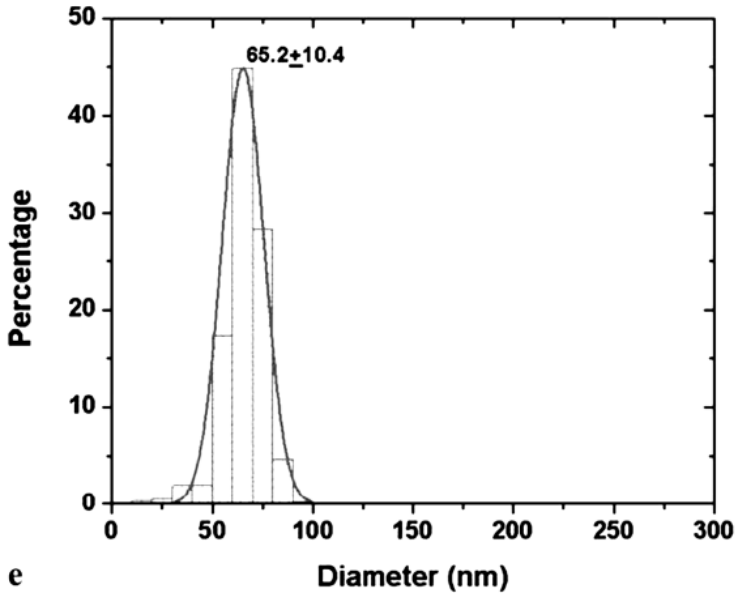

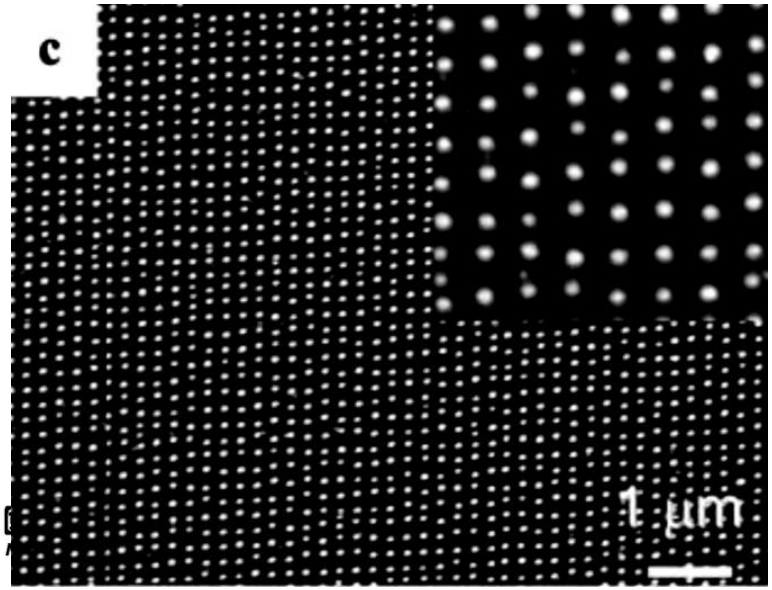

The method starts with a thin metal lines deposited on a substrate, followed by melting using a single excimer laser pulse.

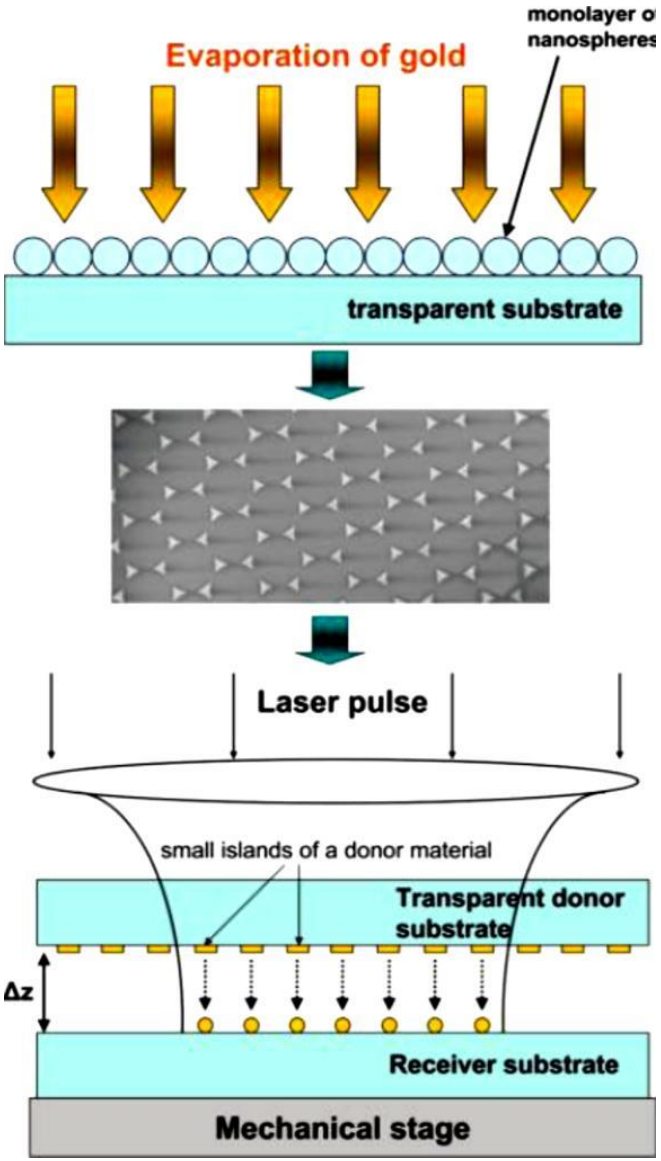

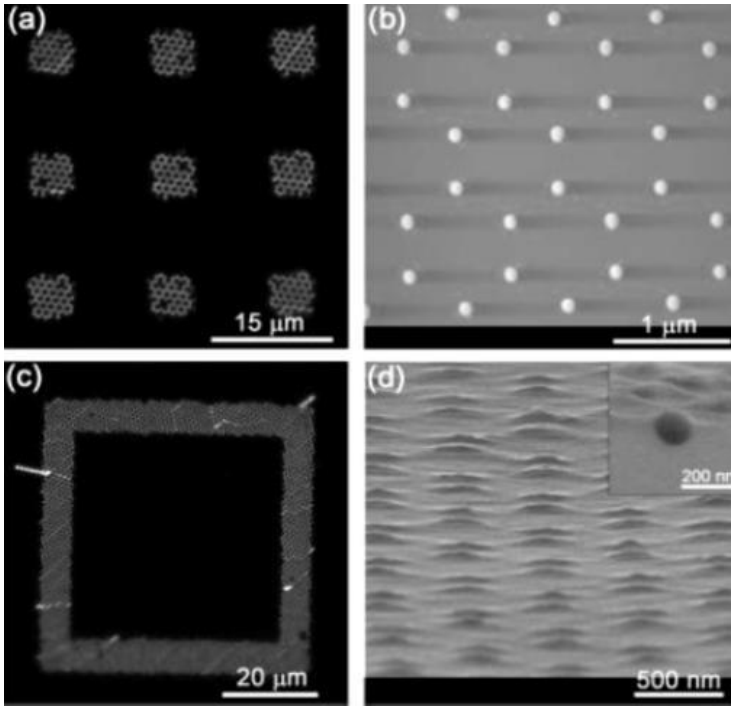

(a) NP structure fabrication by a combination of the nanosphere lithography and laser-induced transfer. (b) Dark-field microscope image and SEM of gold NPs fabricated by single laser pulses on a receiver substrate.

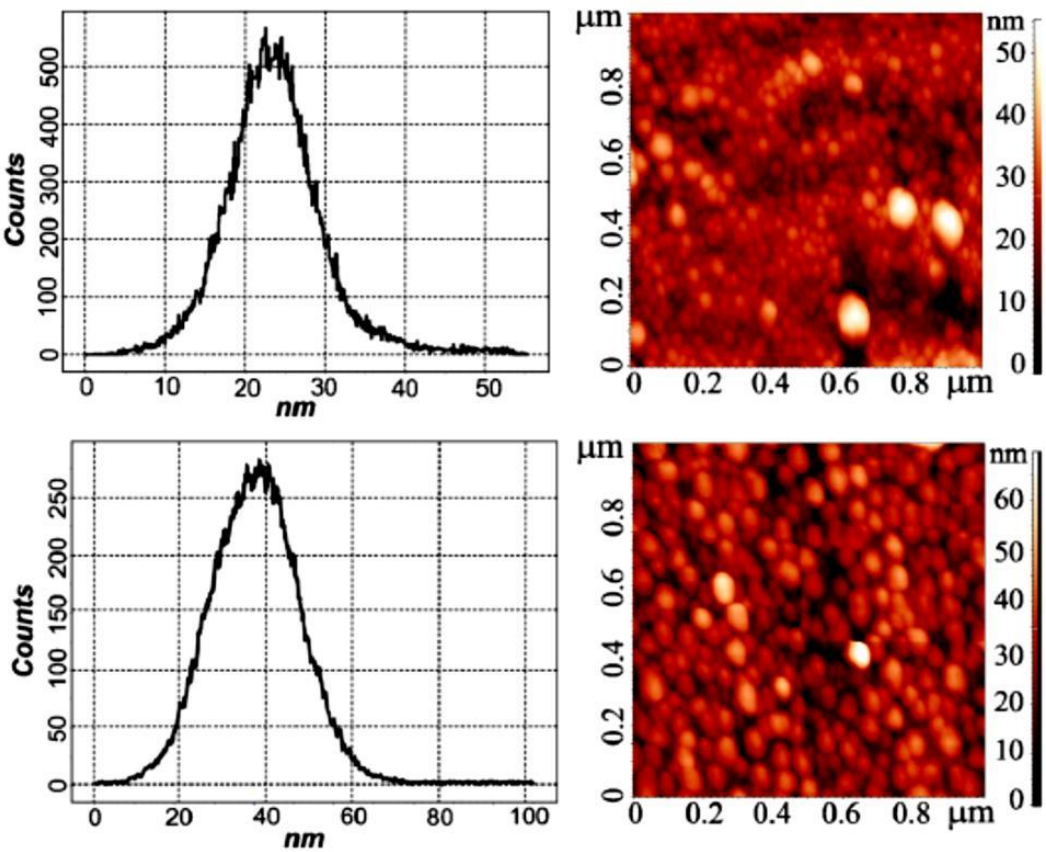

The averaged Ag NP size fabricated under the 45 fs pulse shot was about 20 to 25 nm and those fabricated by 300 ps was about 40 to 50 nm.

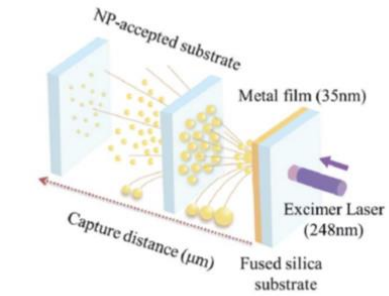

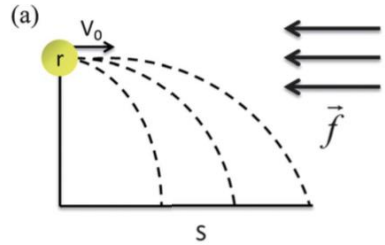

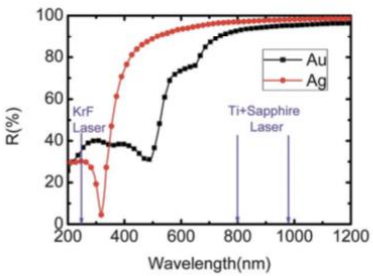

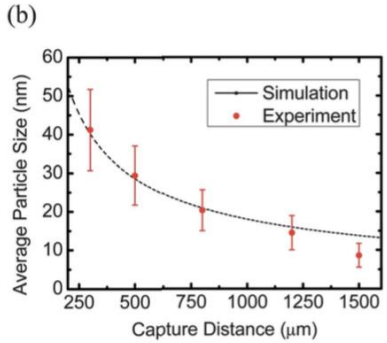

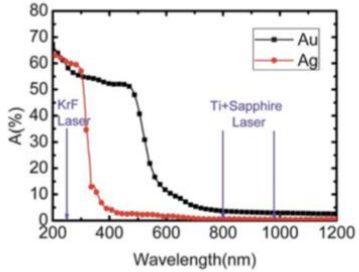

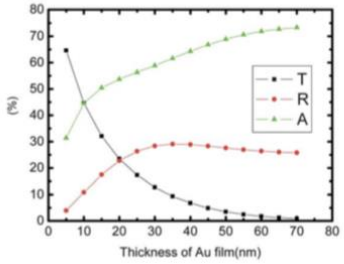

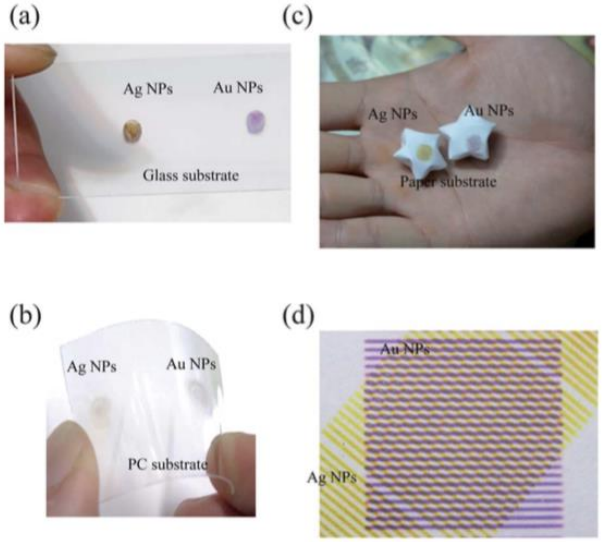

Therefore, the air drag force acting on the NPs in the ambient air was

$$f = -kr^{\alpha}v^{\beta} \tag{1}$$

where k is a constant, r is the diameter of the NPs, and v is the relative velocity of the NPs in air (760 torr).[29,30]

The air drag force on a nanoscale particle moving in a gaseous medium had been reported previously from related theoretical calculations.[31] We proposed that the air drag force was proportional to the volume and the velocity of the NPs; therefore, it was reasonable to assume values of α and β of 3 and 1, respectively. For uniformly accelerated motion,

$$s = v_0 t + \frac{1}{2}at^2 \tag{2}$$

where s is the travelling distance of the NPs. Because the motion of our NPs was a varied accelerated motion, we assumed that the acceleration in a very small velocity change in each moment was constant:

$$\mathrm{d}s = \frac{(v-\mathrm{d}v)^2 - v^2}{2a} = \frac{v^2 - 2v\mathrm{d}v + (\mathrm{d}v)^2 - v^2}{2a} \xrightarrow{\text{ignore}(\mathrm{d}v)^2} \mathrm{d}s = -\frac{v\mathrm{d}v}{a}$$

furthermore, we proposed that each metal NP was a sphere having a mass density ρ and a mass m. Therefore, the kinetic energy was described as

$$E_k = \frac{1}{2}mv^2 = \frac{1}{2}\frac{4}{3}\pi r^3 \rho v_0{}^2 \tag{3}$$

substituting $F = ma$ into eqn (1), we obtain

$$s = \int_0^{v_0} \frac{4\pi\rho}{3k}\mathrm{d}v = \frac{4\pi\rho}{3k}\int_0^{v_0}\mathrm{d}v = \frac{4\pi\rho}{3k}v_0 = \frac{4\pi\rho}{3k}\left(\frac{3E_k}{2\pi\rho r^3}\right)^{\frac{1}{2}}$$
$$= \frac{4\pi\rho}{3k}\left(\frac{3E_k}{2\pi\rho}\right)^{\frac{1}{2}} r^{-\frac{3}{2}} \tag{4}$$

from these equations, we find that s is proportional to $r^{-(3/2)}$. Fig. 5b (dashed line) presents a plot of the calculated average particle size with respect to the jet distance. The experimental data (red dots) fitted the calculated curve quite well.

國家同步輻射研究中心
National Synchrotron Radiation Research Center

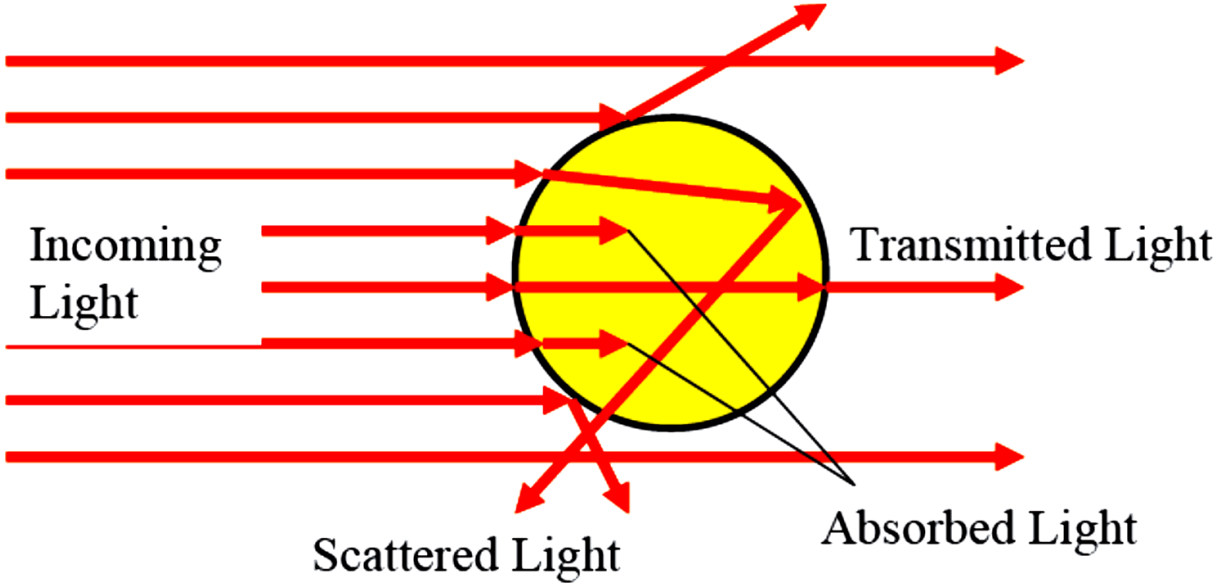

The theoretical principles that describe the metal NCs interaction with light are covered by Mie, Maxwell–Garnett and Drude models.

The extinction spectra (extinction = scattering + absorption) of spherical particles of arbitrary size.

Physical and chemical properties of metal NCs

Surface plasmon resonance (SPR)

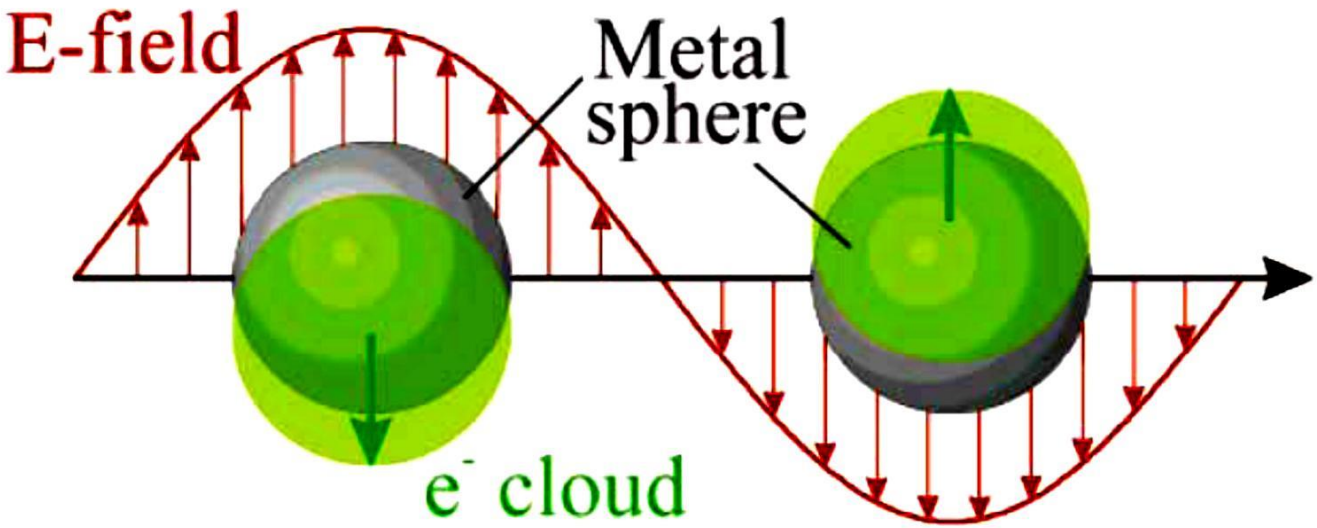

Schematic diagram of plasmon oscillation for a sphere, showing the displacement of the conduction electron charge cloud relative to the nuclei.

The strong interactions of metallic NCs with incident light, i.e., with the oscillating electric field, originate from the excitation of collective oscillations of conduction electrons within these particles. The collective oscillation of the electrons is called the dipole plasmon resonance of the particle.

Particle-particle coupling

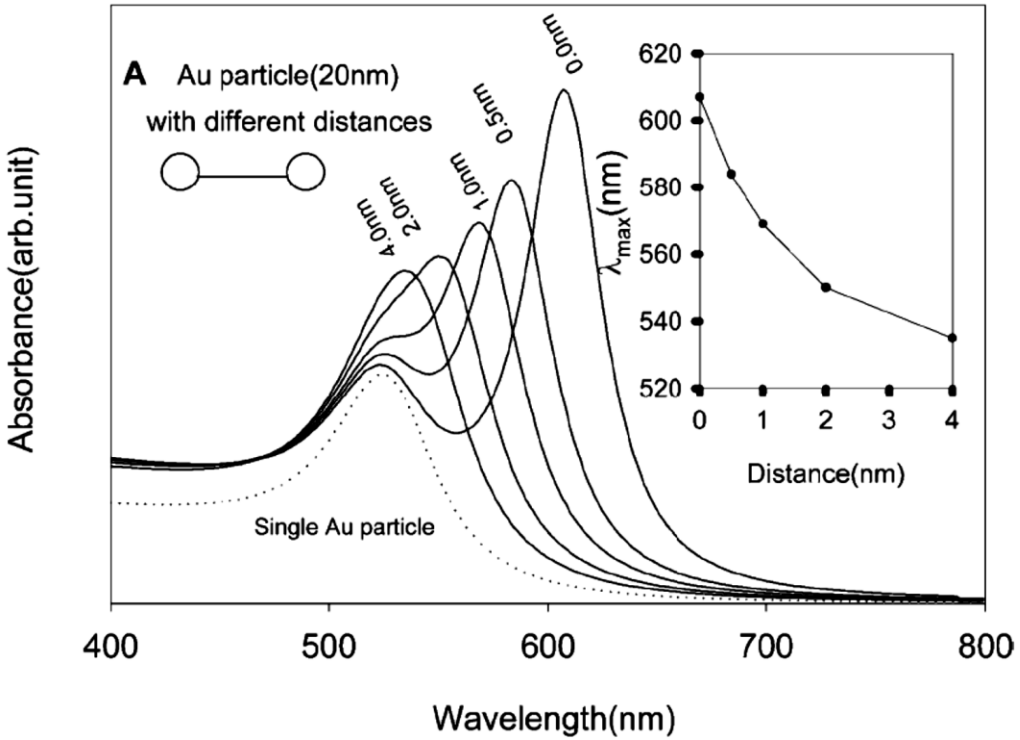

The close contact of metal NCs leads to the appearance of an SPR band attributed to the coupled plasmon absorbances of the NCs. This property has been predicted theoretically.

Chemical affinity

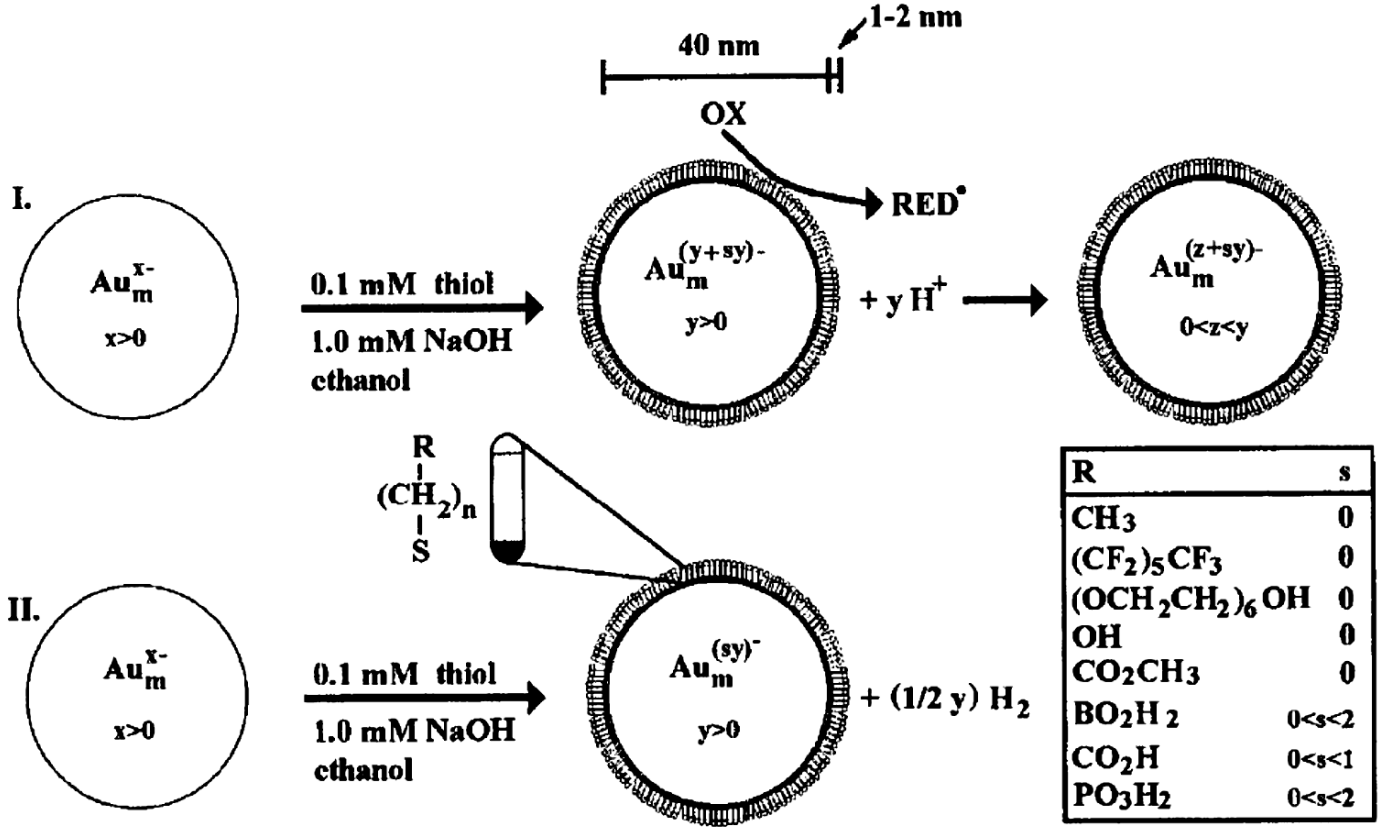

R	s
CH_3	0
$(CF_2)_5CF_3$	0
$(OCH_2CH_2)_6OH$	0
OH	0
CO_2CH_3	0
BO_2H_2	0<s<2
CO_2H	0<s<1
PO_3H_2	0<s<2

Gold-thiol chemistry: The modulation of SPR for surface-modified Au nanostructures should be dominated by the dielectric constant of the absorbed layers instead of the bulk solvent medium. As a result, Au nanostructures provide a highly sensitive means of detecting changes that occur in the region extremely close to the gold-solution interface.

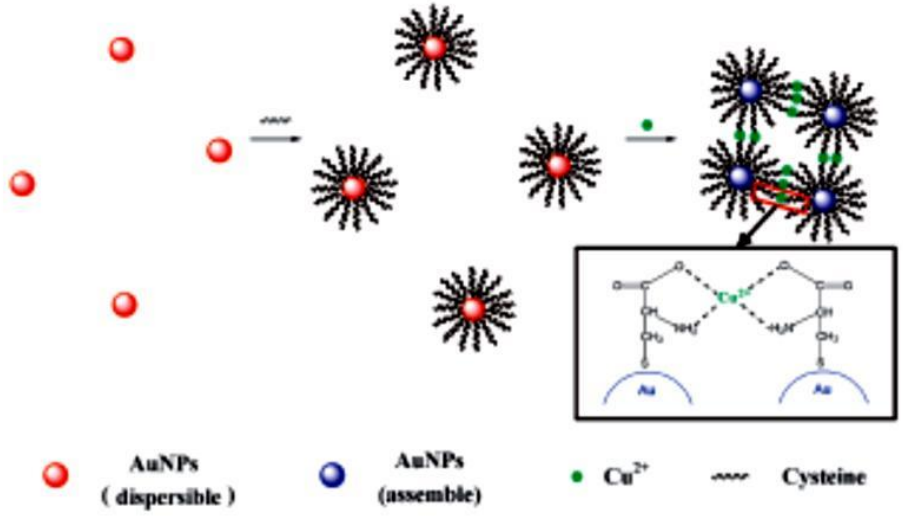

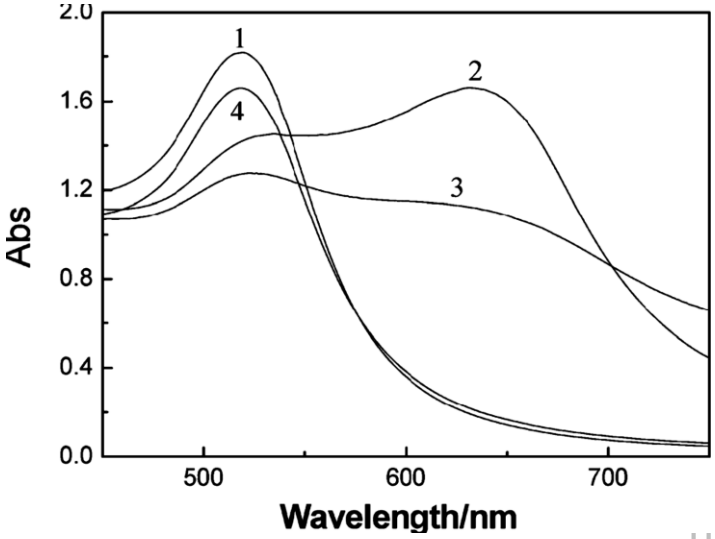

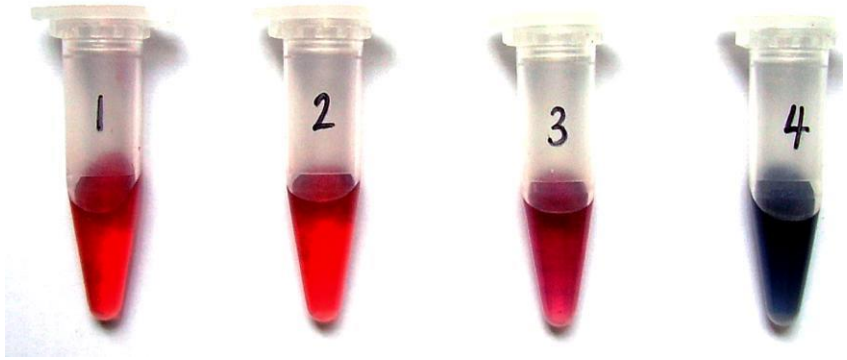

Absorption spectra of AuNPs (1) in the absence of cysteine, (2) in the presence of $1*10^{-5}$M cysteine and 1mM Cu^{2+}, (3) in the presence of $1*10^{-6}$M cysteine and 1mM Cu^{2+}, and (4) in the presence of $1*10^{-7}$M cysteine and 1mM Cu^{2+}.

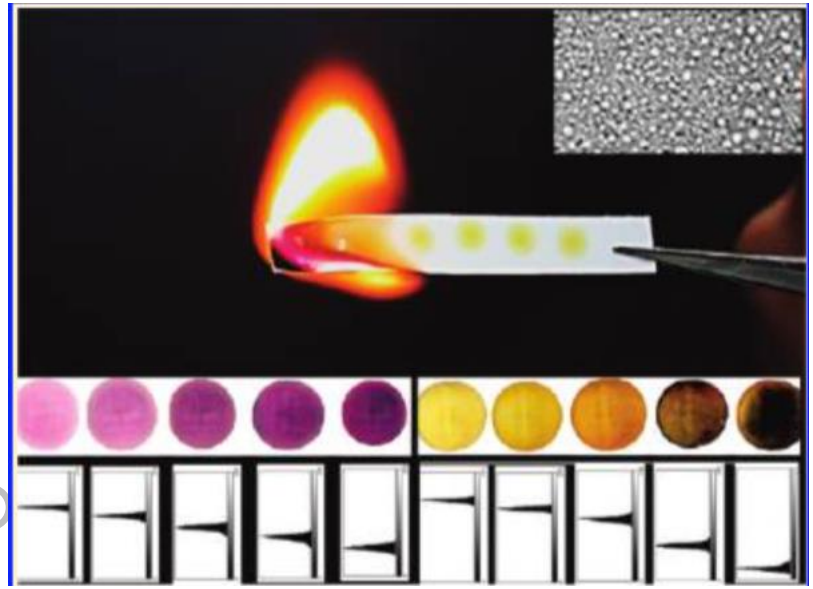

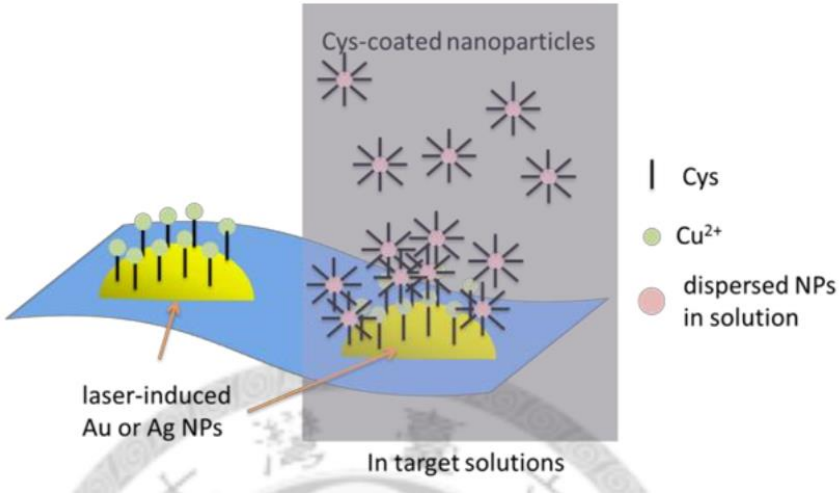

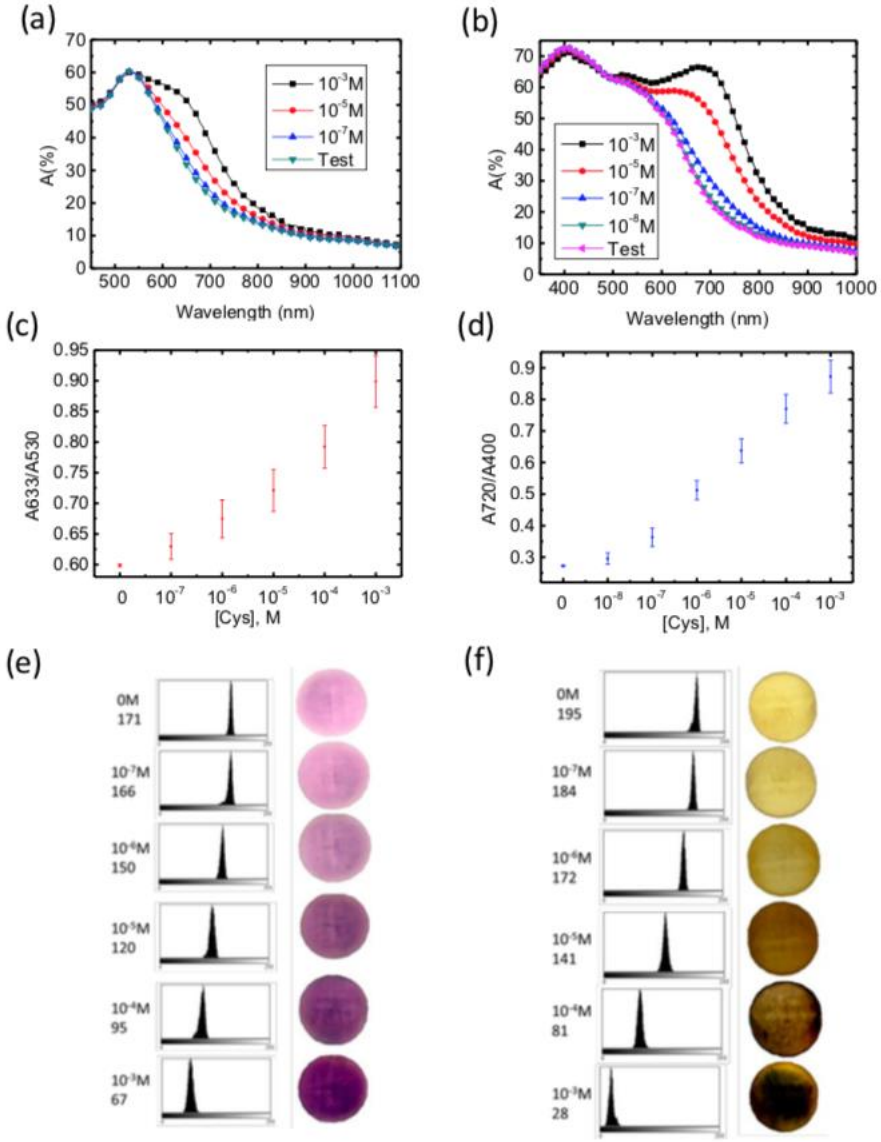

國家同步輻射研究中心
National Synchrotron Radiation Research Center

Quantum size effect

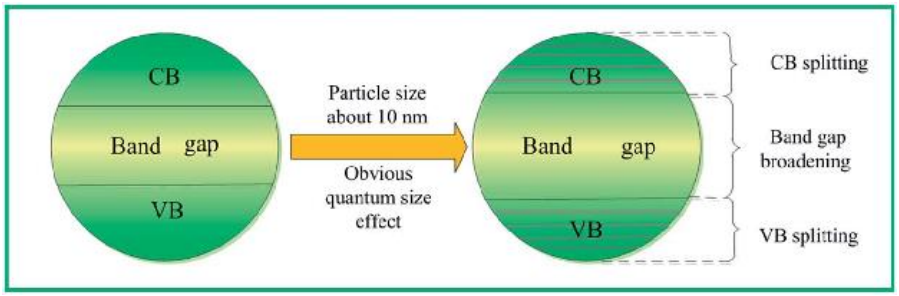

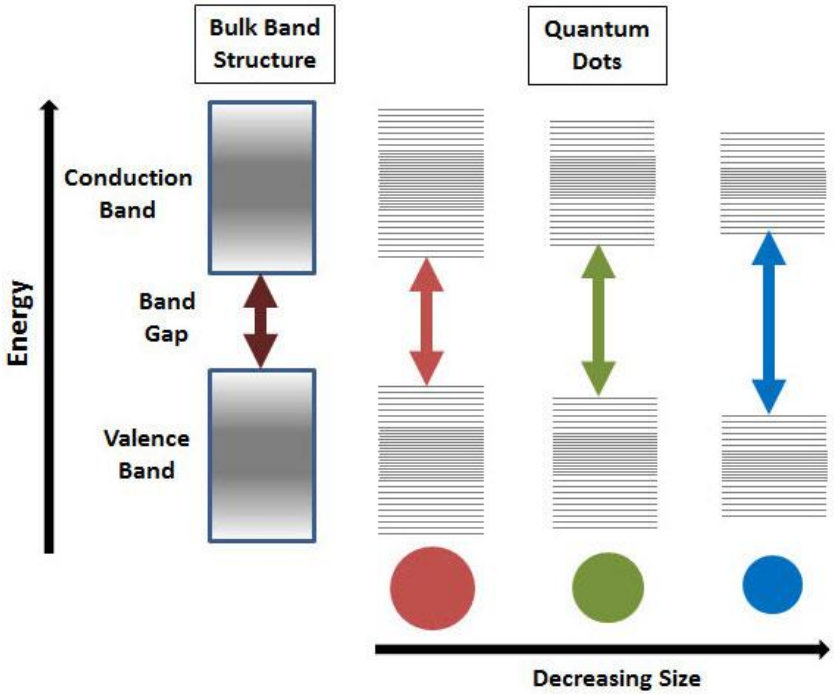

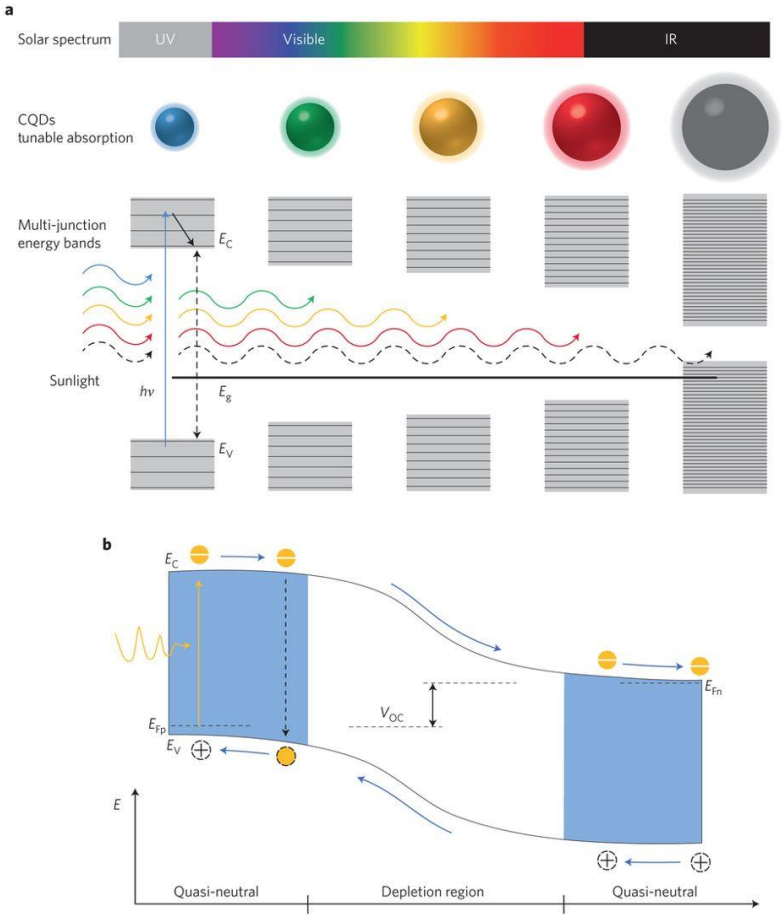

國家同步輻射研究中心
National Synchrotron Radiation Research Center

Nature Materials **volume13**, pages233–240 (2014)

Catalytic properties

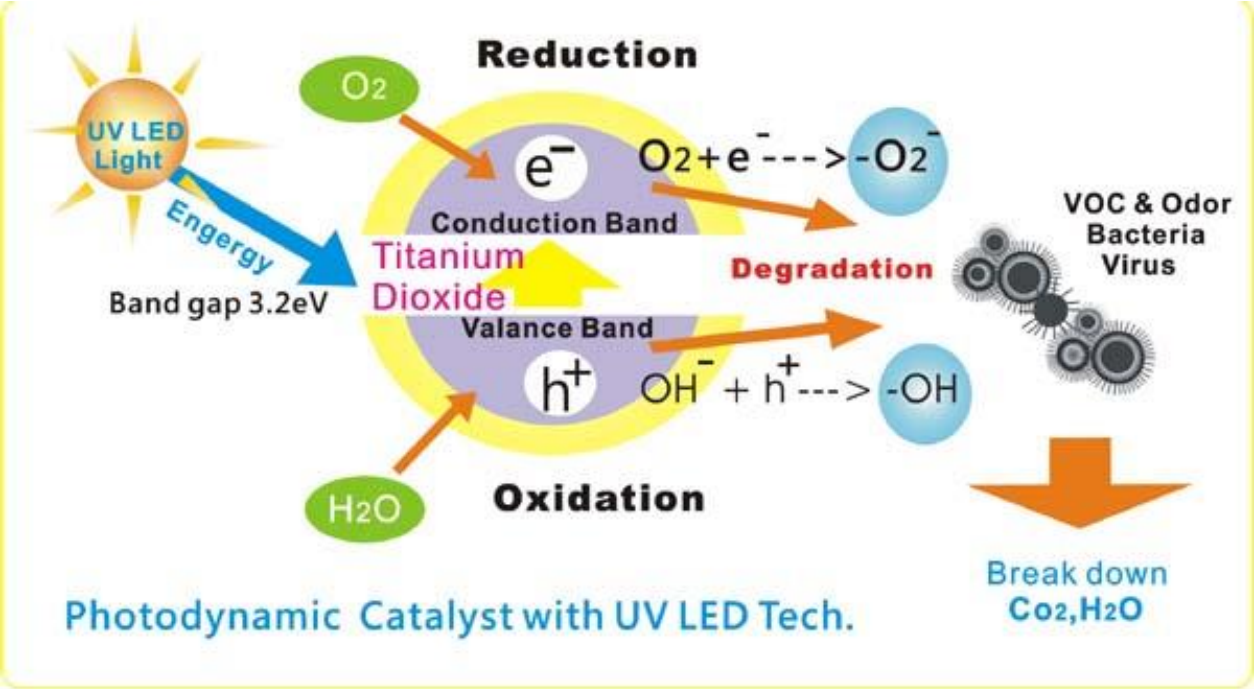

Au NCs supported on Co_3O_4, Fe_2O_3, or TiO_2 were highly active catalysts, under high dispersion, for CO and H_2 oxidation, NO reduction, water-gas shift reaction, CO_2 hydrogenation, and catalytic combustion of methanol was a surprise, and was considered important by the chemical community.

國家同步輻射研究中心
National Synchrotron Radiation Research Center

Surface Antireflection

Micro-scale texturing techniques

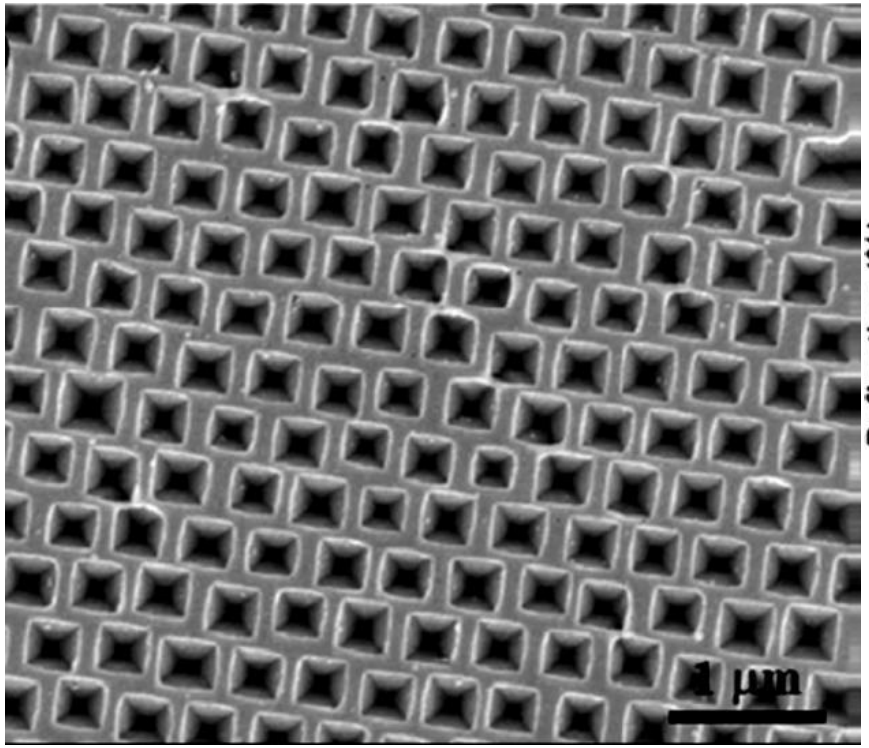

Replicated inverted pyramid arrays in silicon.

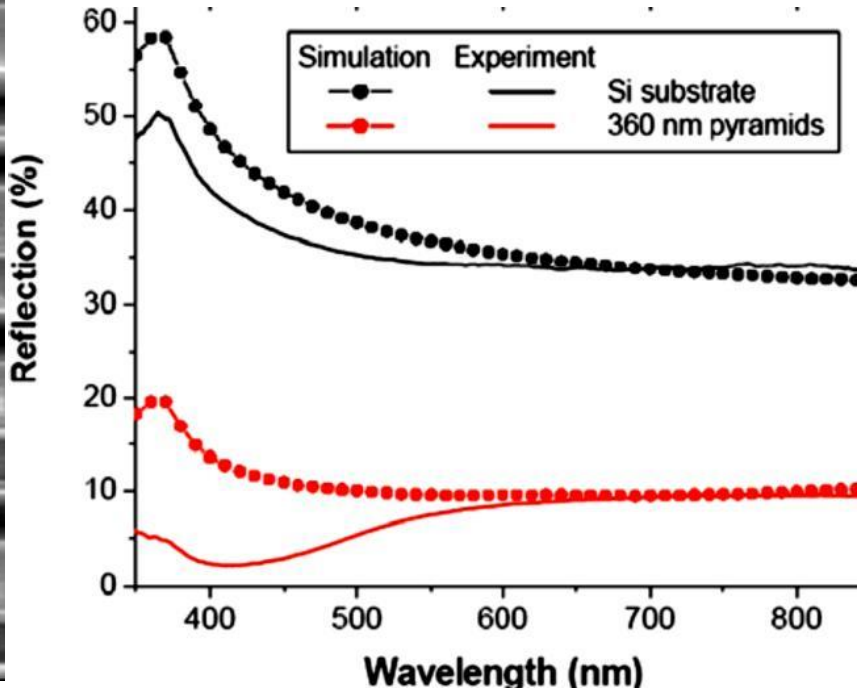

Experimental (solid) and simulated (dotted) optical reflectivity at normal incidence.

Most of optical devices on thin layer of a dielectric as a antireflective coating to reduce the reflection of light from the front surface of the cell.

國家同步輻射研究中心
National Synchrotron Radiation Research Center

Sub-wavelength antireflective texturing techniques

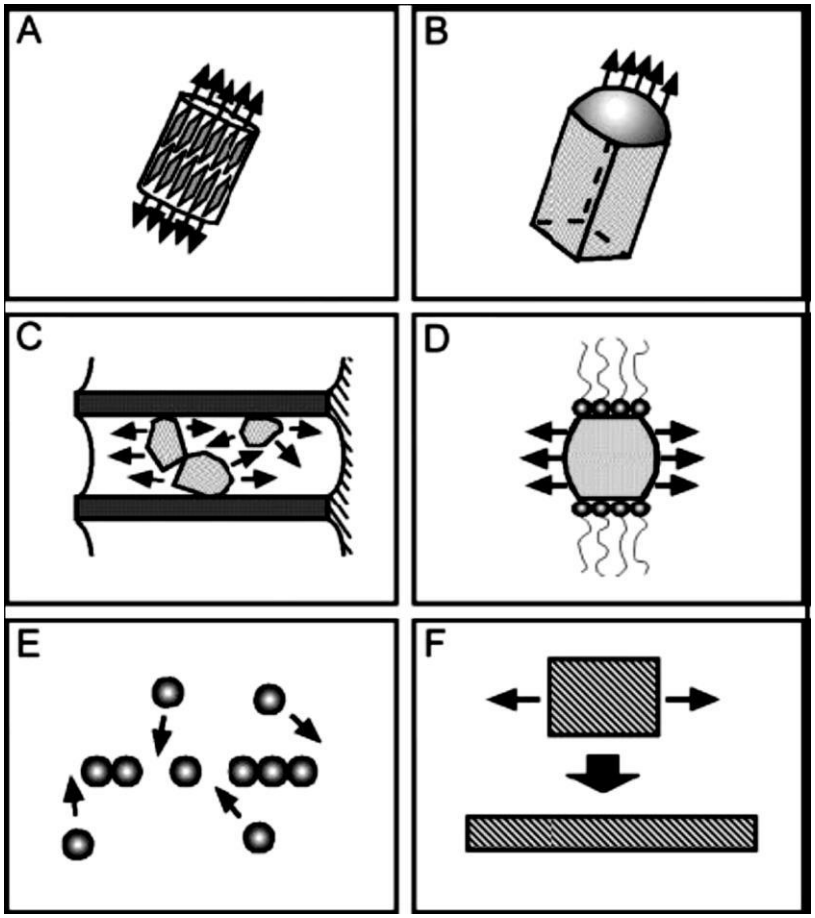

Numerous methods have been developed to fabricate Si nanostructures using top-down or bottom-up approaches

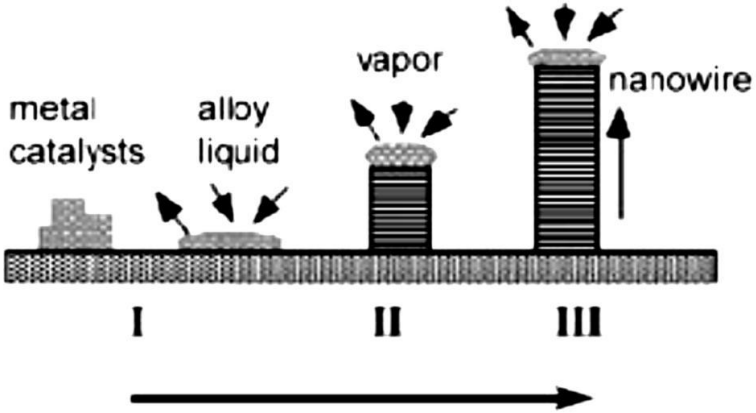

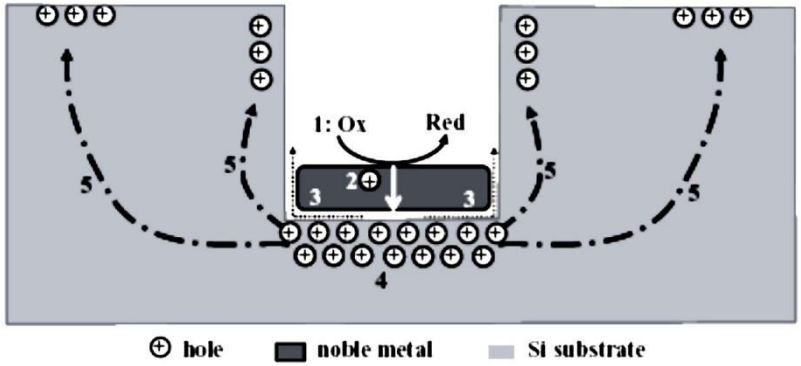

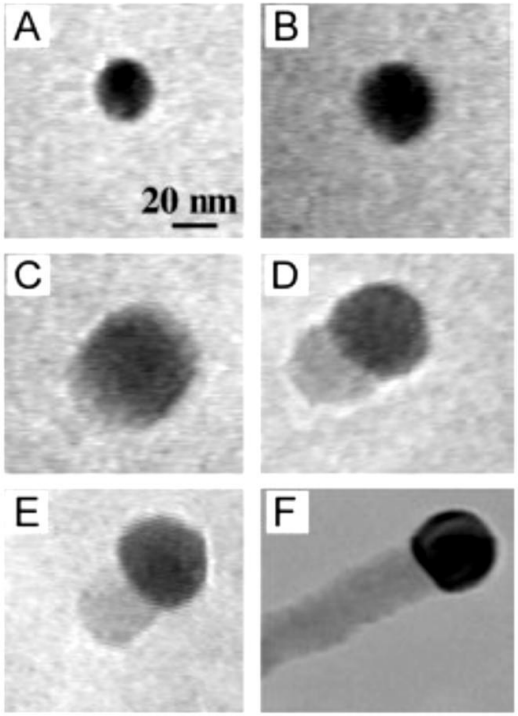

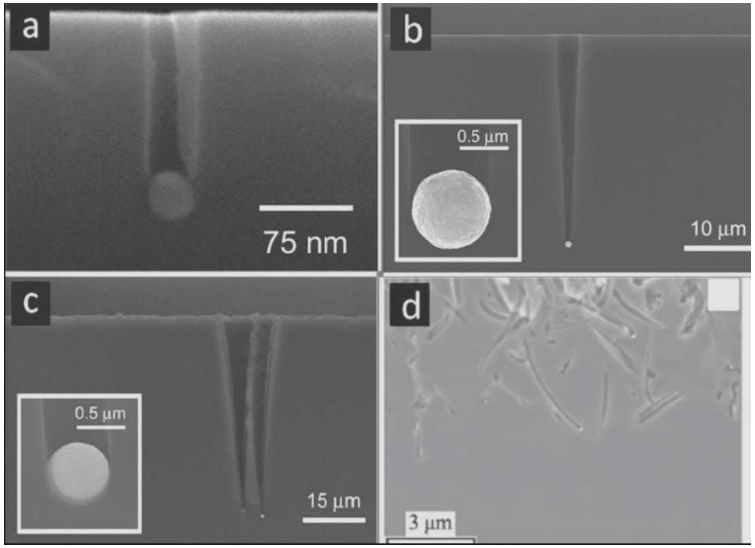

Vapor-liquid-solid (VLS) growth, reactive ion etching (RIE), electrochemical etching, or metal-assisted chemical etching, all of which aim to control various parameters of the Si structures.

One-dimensional nanostructure optical

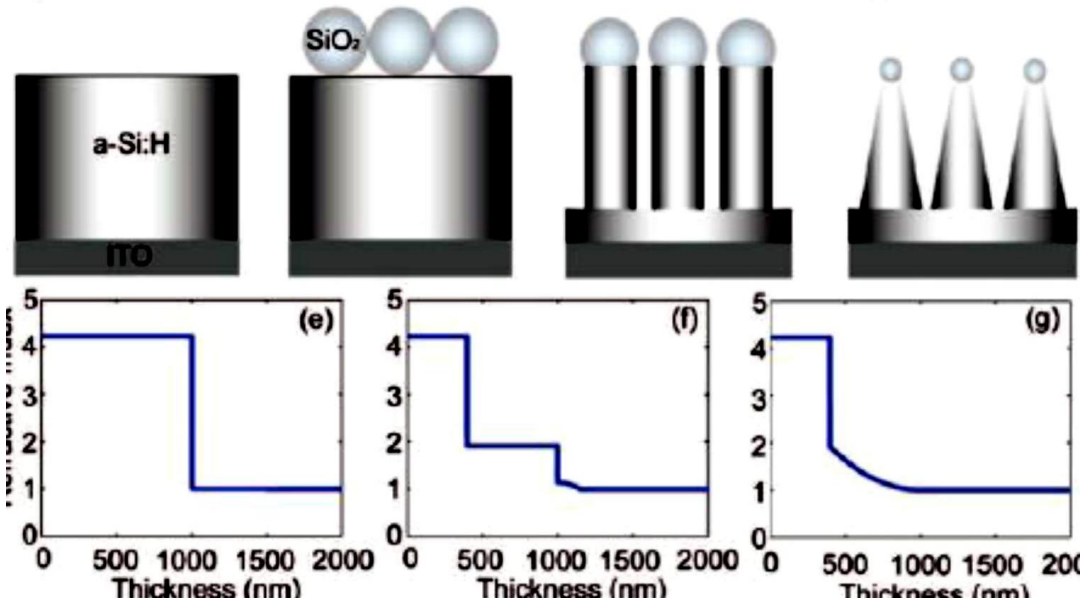

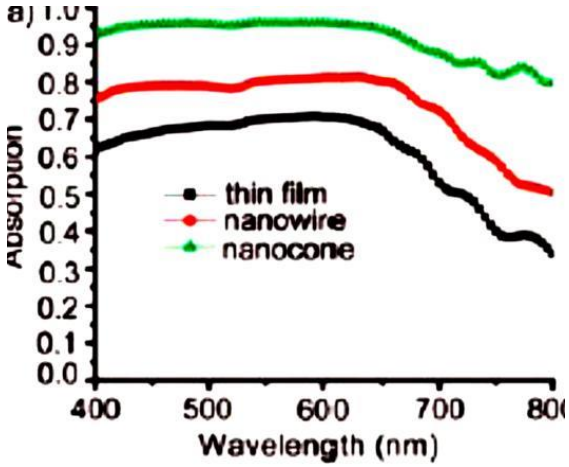

The enhancement effect is particularly strong for Si surface nanostructure arrays, which provide nearly perfect impedance matching between Si and air through a gradual reduction of the effective refractive index.

Tunneling effect

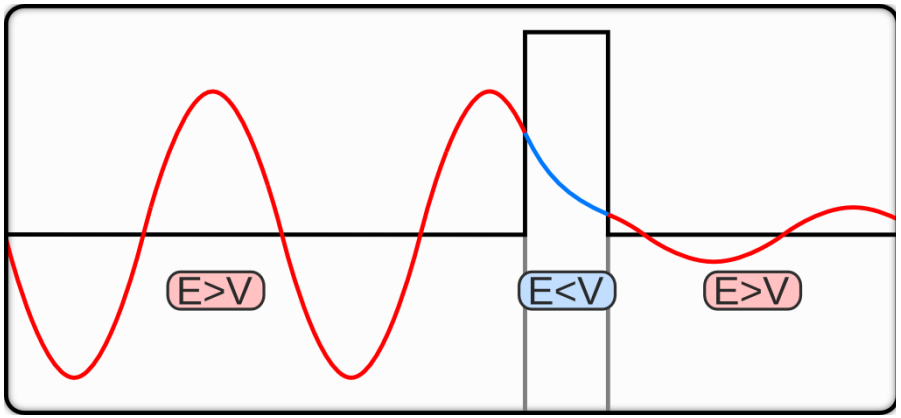

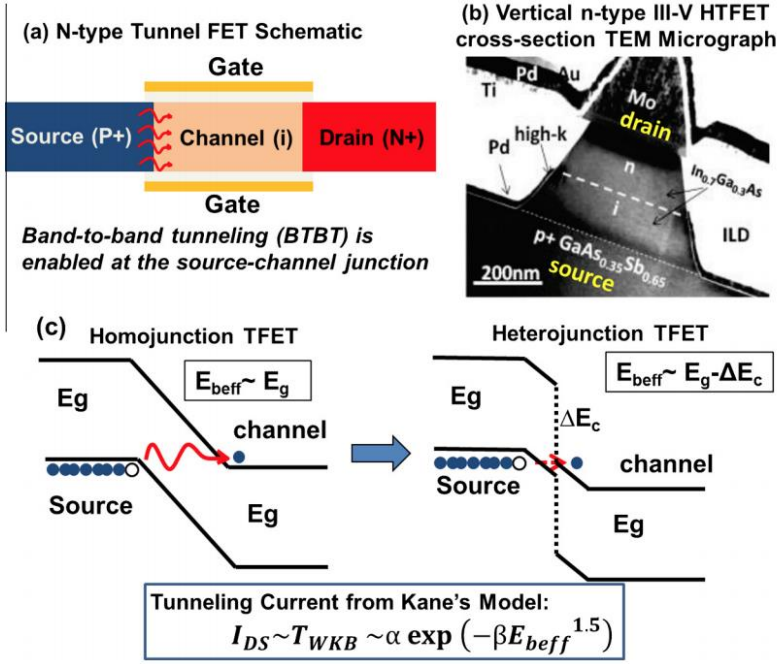

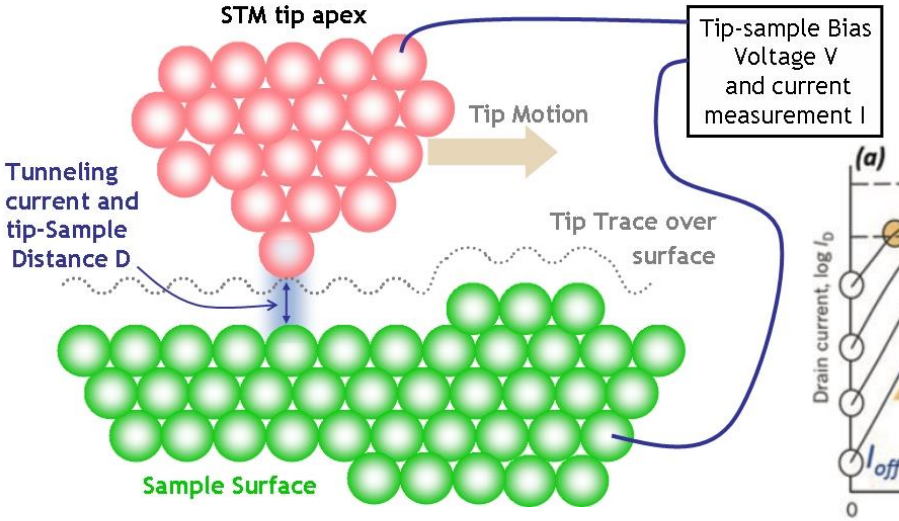

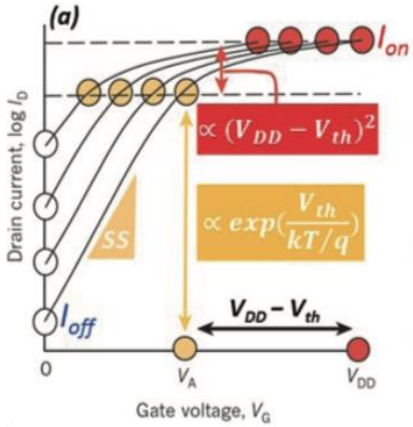

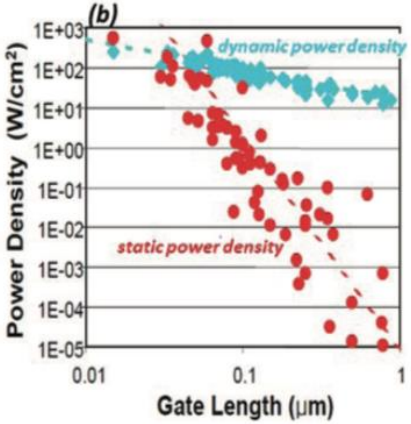

國家同步輻射研究中心
National Synchrotron Radiation Research Center

One-dimensional nanostructure field emission properties

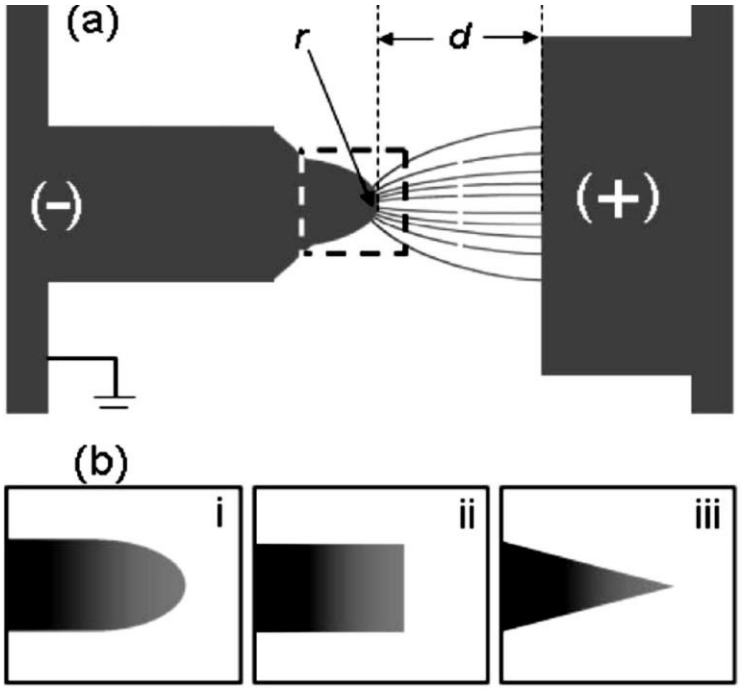

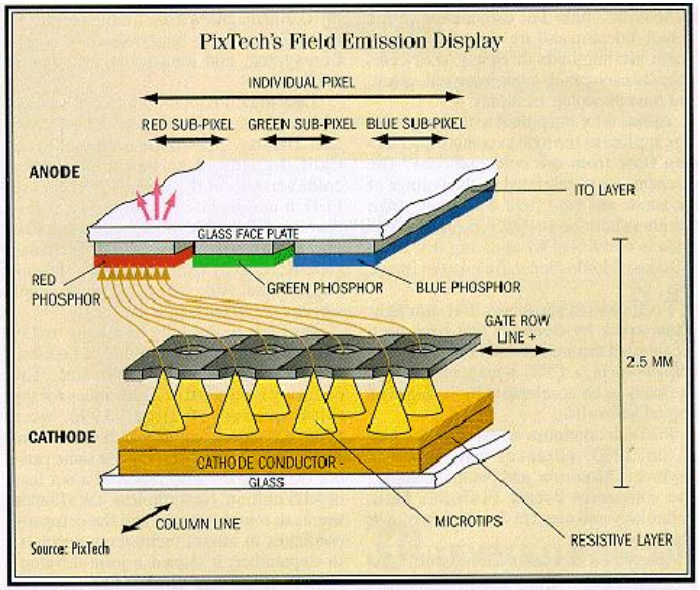

PixTech uses a Spindt-type conical cathode structure. The molybdenum cathodes are about 1.2 μm tall. There are hundreds of such cathodes for each pixel, containing red, green, and blue phosphor elements.

Field-emission, is one of the main features of nanomaterials and nanostructures, and is of great commercial interest in displays and other electronic devices.

2D Materials--Device

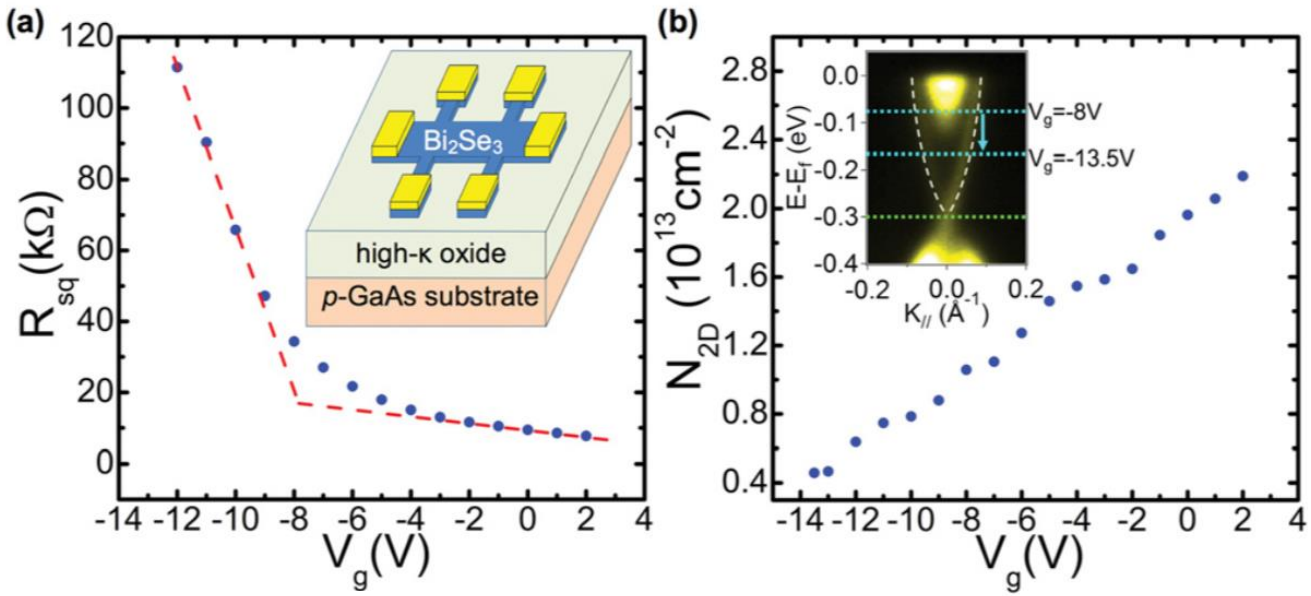

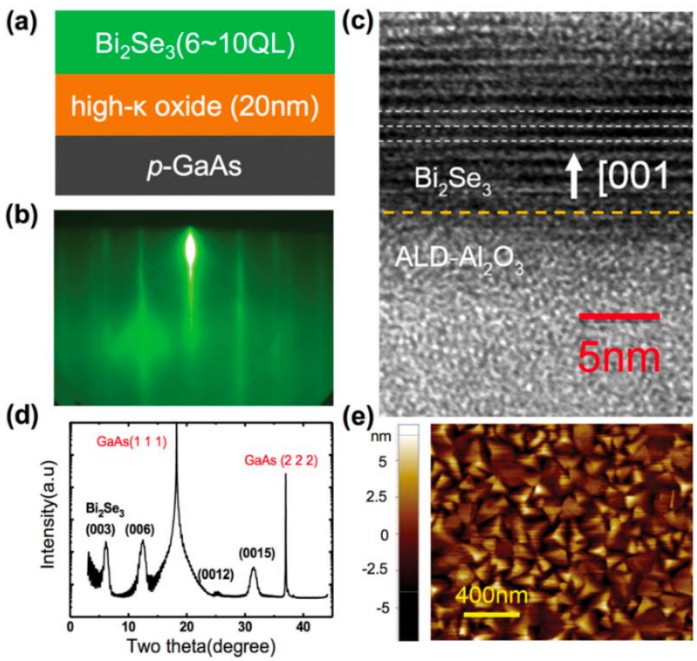

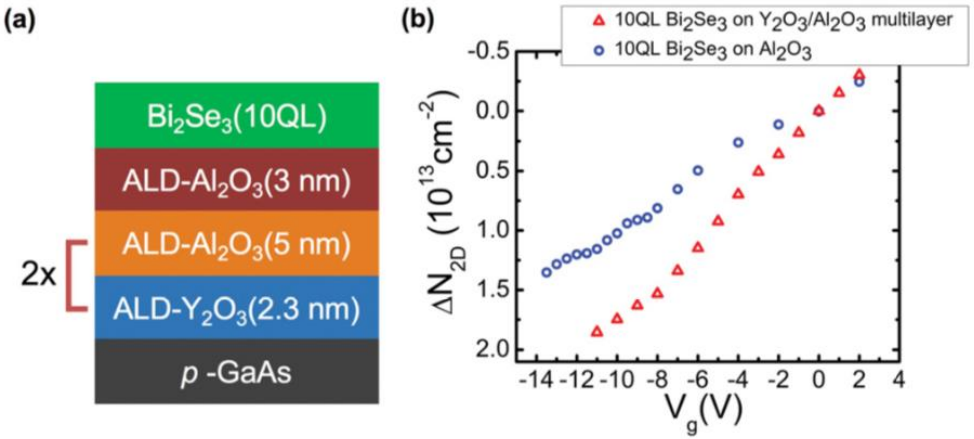

Appl. Phys. Lett. **108**, 202403 (2016)

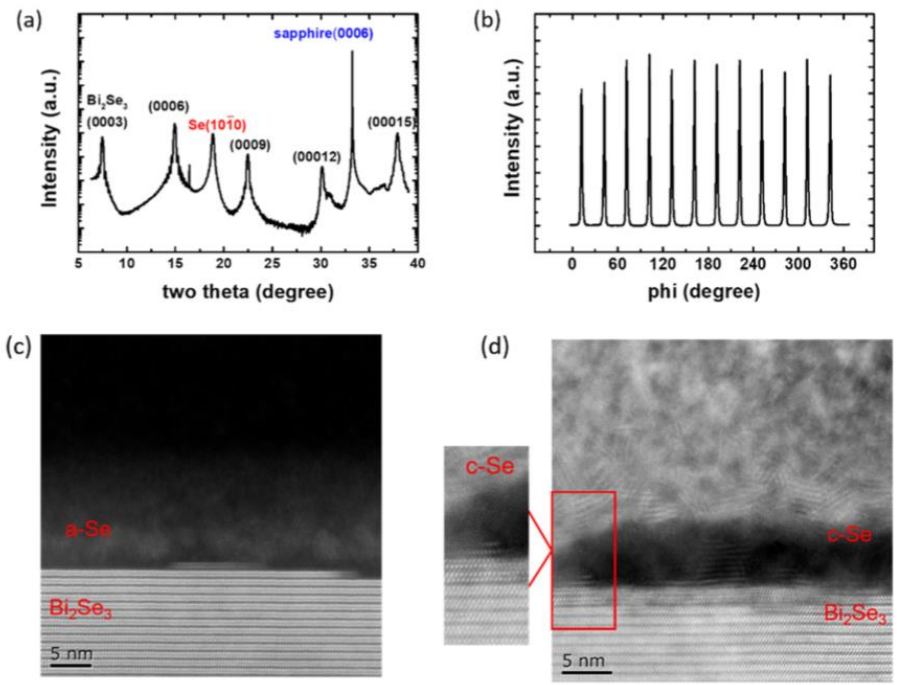

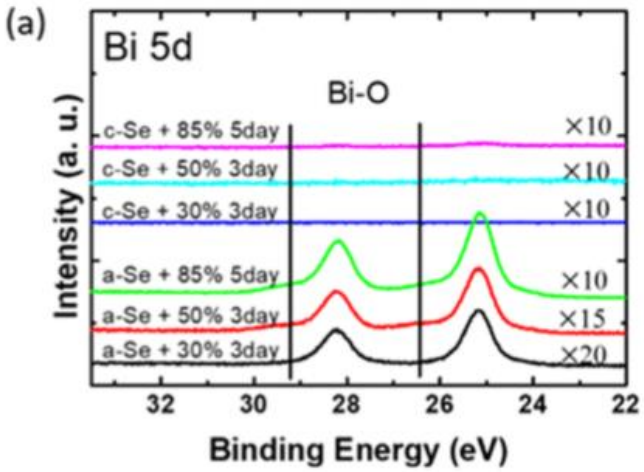

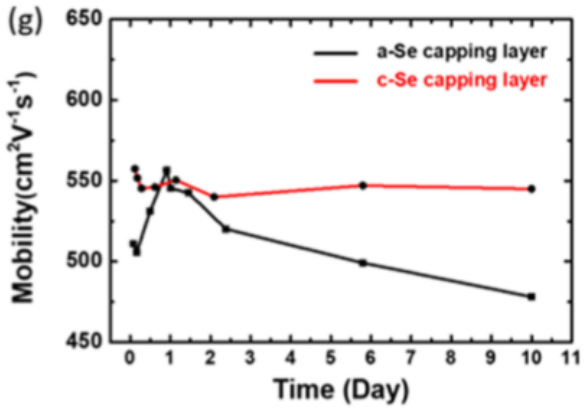

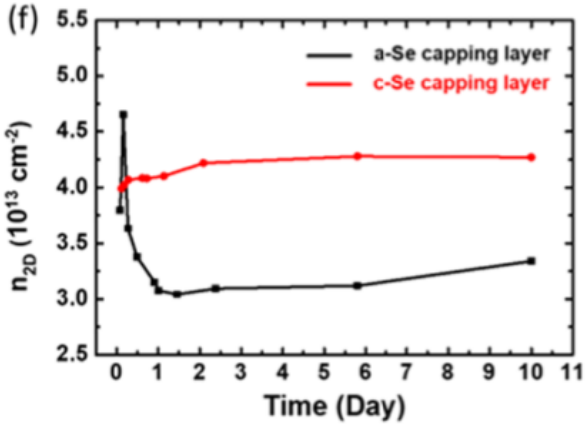

國家同步輻射研究中心
National Synchrotron Radiation Research Center

APL Mater. **6**, 066108 (2018)

Outline

- Advantage of materials in nanometer dimensions
- Nanomaterial analysis technology

Annalysis-Workfunction

Kelvin Probe

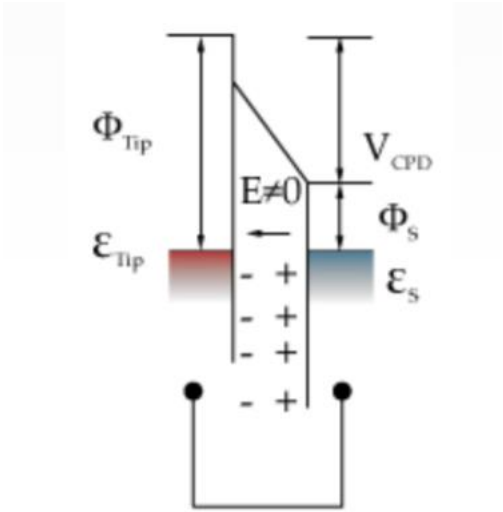

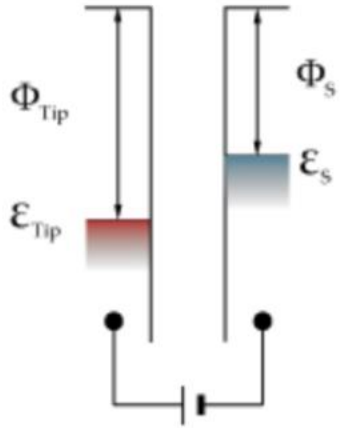

$V_b = - V_{CPD}$

Non-contact, non-destructive vibrating *capacitor* device used to measure the *work function* of conducting materials or *surface potential* of semiconducting or insulating surfaces.

- The technique is extremely sensitive to the topmost layers of atoms or molecules, work function resolution of 1 - 3 meV.
- Unique 'off-null' measurement system also maintains average tip-sample separation to within 1 m, tip to sample tracking

Vibrate the tip, AC Signal Produced

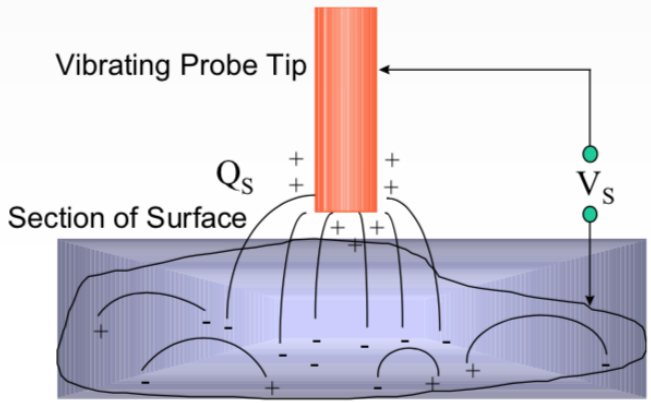

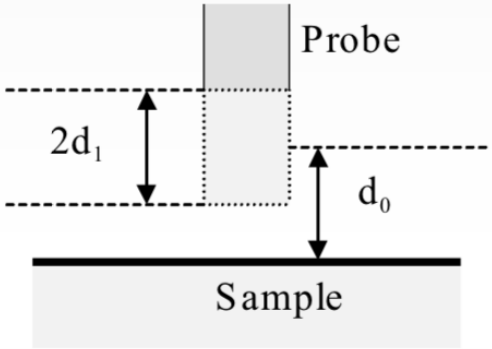

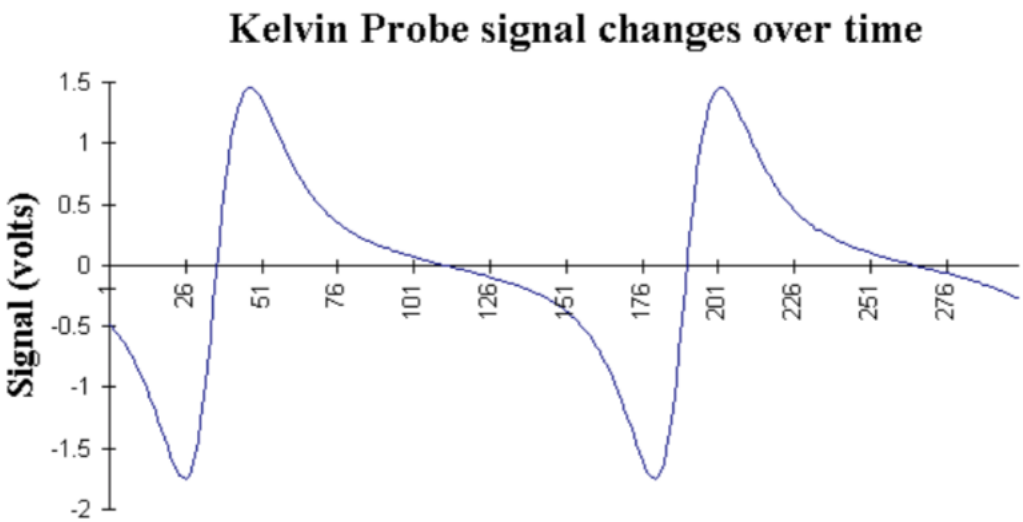

Scanning Kelvin Probe 1993

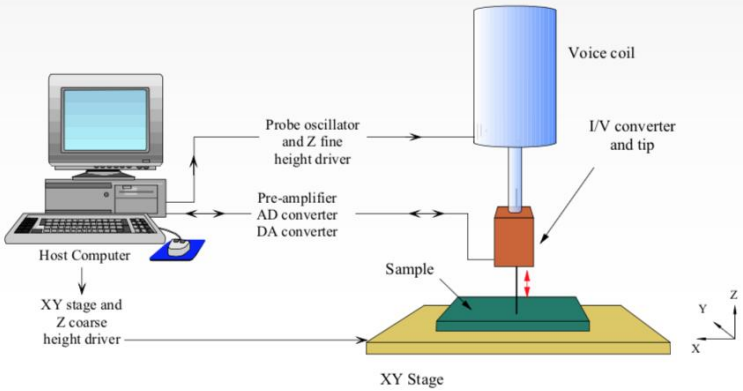

PC houses the digital oscillator (which powers the voice coil actuator), data acquisition system and motorised (x,y,z) stage controller. The signal is derived from a low-noise, high-gain current to voltage (I/V) converter mounted close to the tip.

I.D. Baikie et al Rev. Sci. Instrum. 70, 1842 (1999), Rev. Sci. Instrum 69, 3902 (1998).

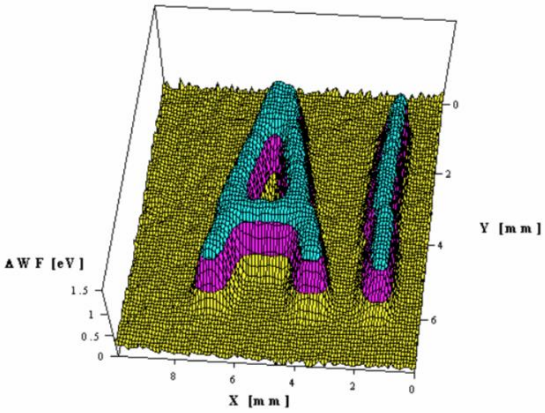

KPTechnology

國家同步輻射研究中心
National Synchrotron Radiation Research Center

Gold / Aluminium Reference Sample

Tip Size: 2mm
Scanning Area: 10x16mm
Operator: I. Baikie

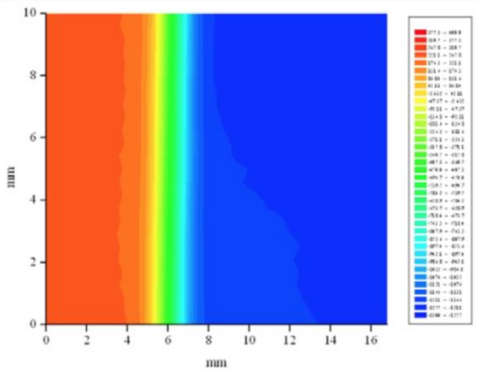

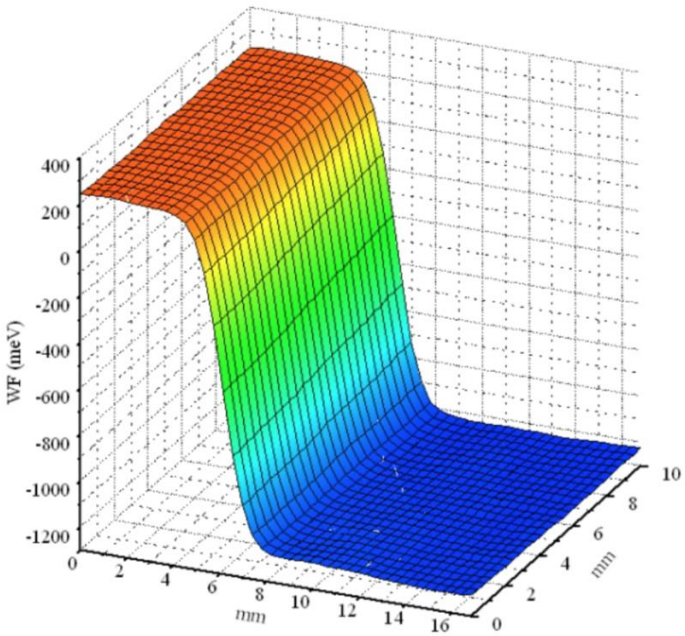

KPTechnology

國家同步輻射研究中心
National Synchrotron Radiation Research Center

掃描式光電子能譜顯微術

(Scanning Photoelectron Microscopy; SPEM)

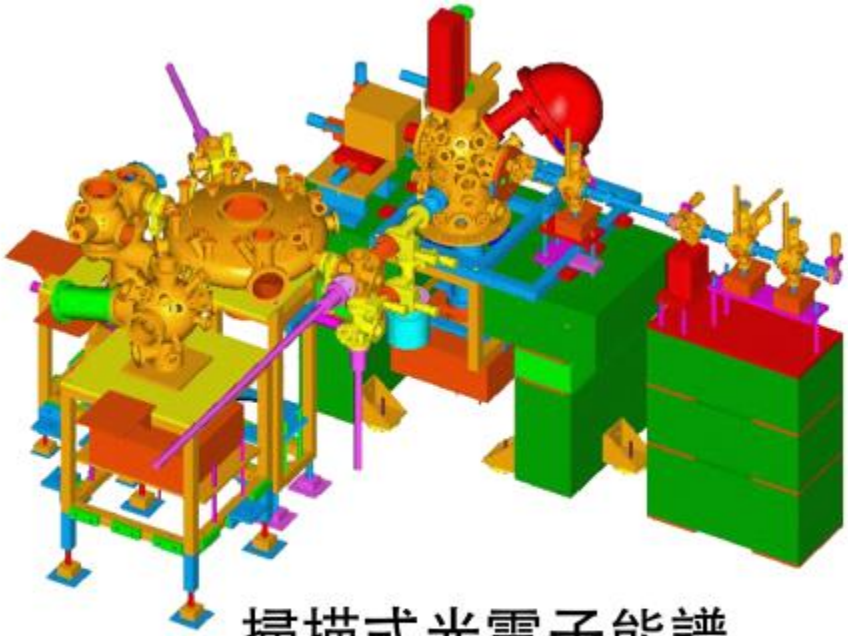

掃描式光電子能譜
顯微實驗站

大綱：

一. 為何發展光電子能譜顯微術？

二. 何謂光電子能譜術？

三. 如何顯微？

四. 舉例說明。

五. 其餘新型態顯微術簡介。

為何發展光電子能譜顯微術？

小尺度結構分析：STM，TEM，SEM…等

小尺度成份分析：

SPEM

二、何謂光電子能譜術？

光電子能譜術（Photoemission Spectroscopy）

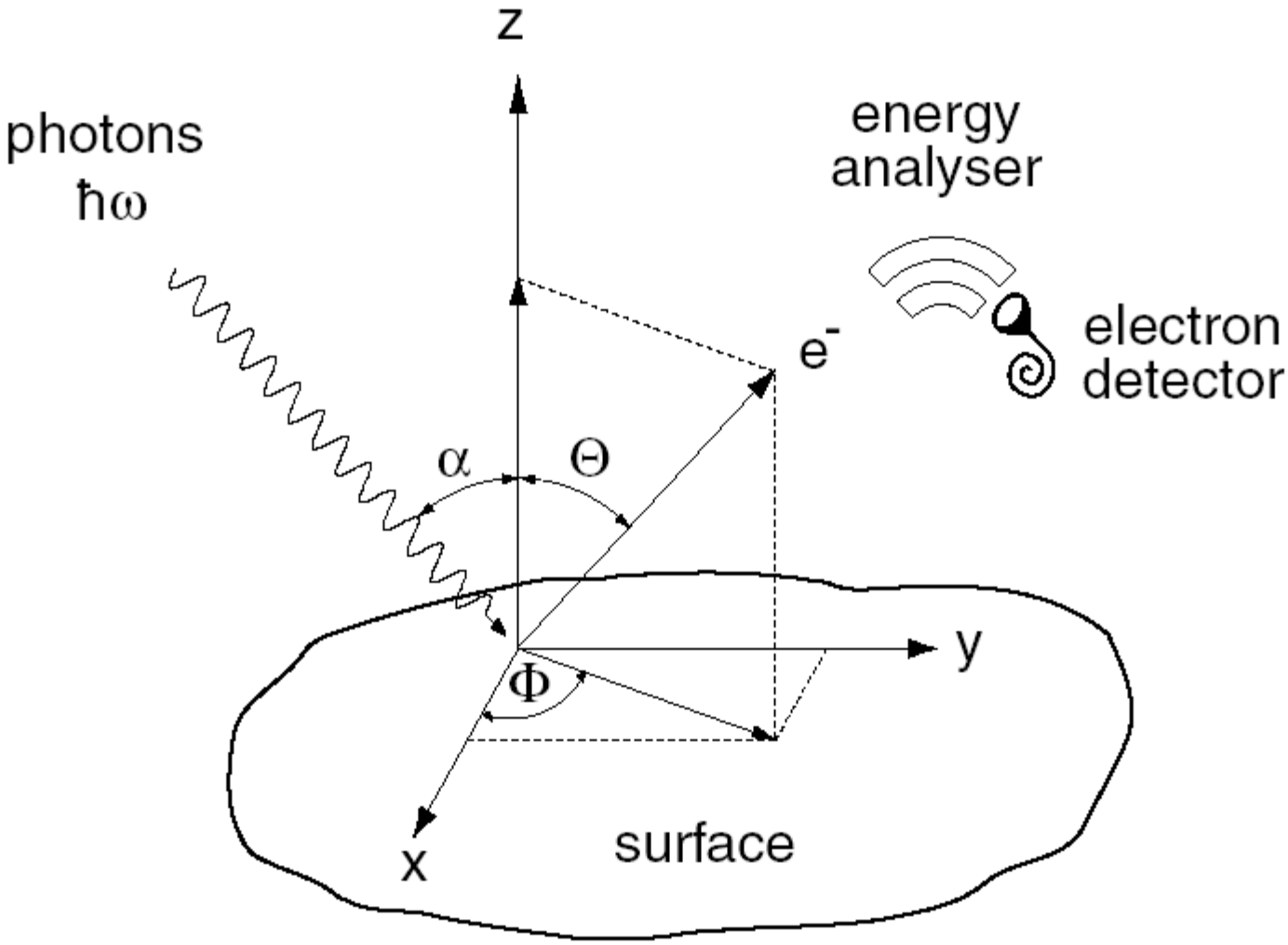

典型 ESCA 能譜

BE = hv- KE-eΦ

BE: 束縛能

hv:入射光能量

KE:電子動能

eΦ:功函數

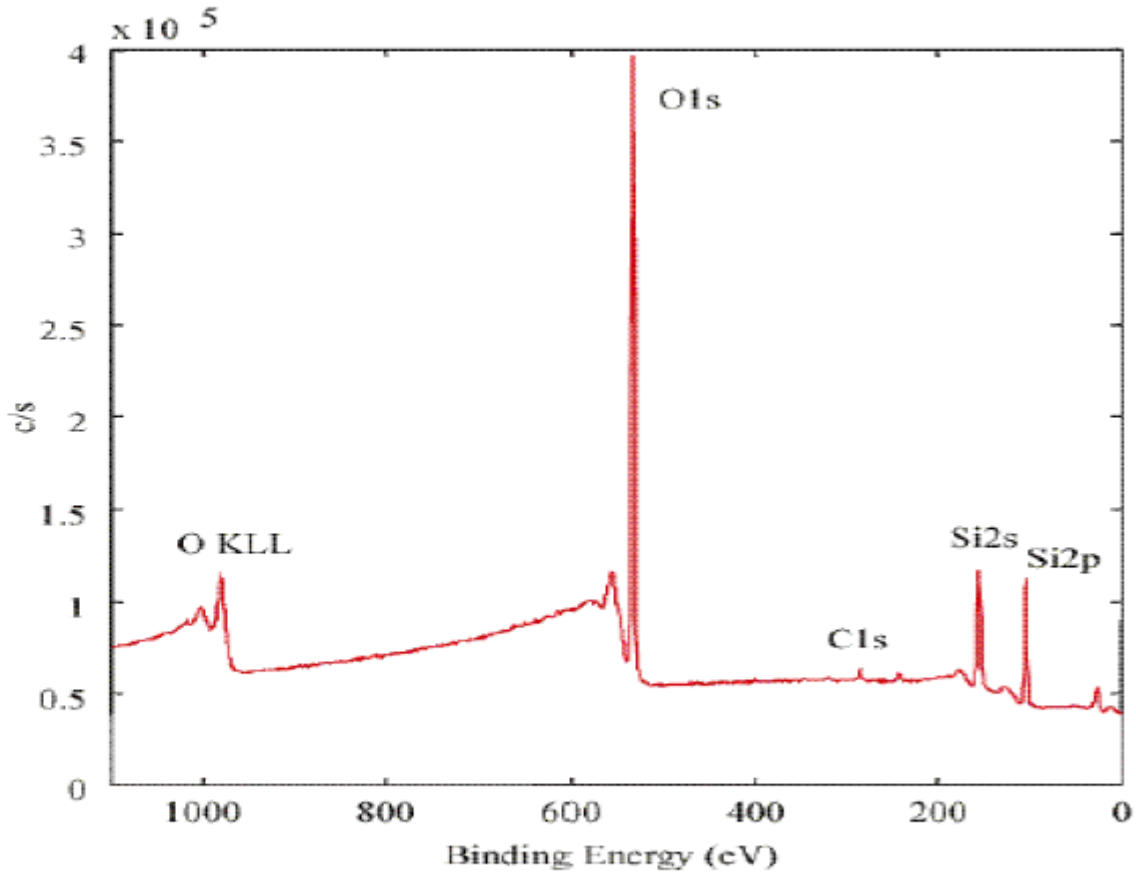

Survey Spectrum of Silicon Wafer

光電子發射之特性：

1.非破壞性

2.表面分析技術

3.具化學鍵結分辨能力

Universal Curve

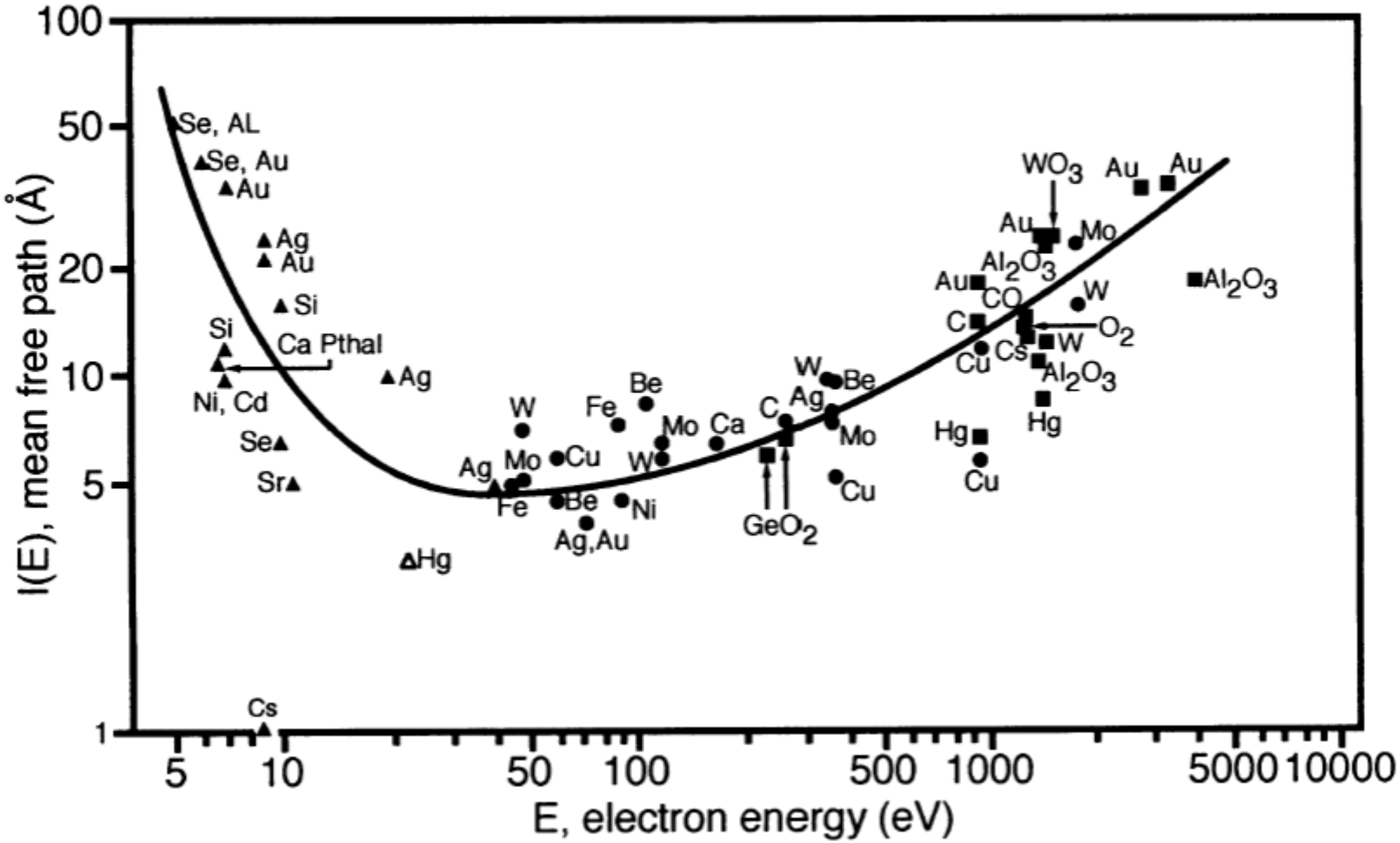

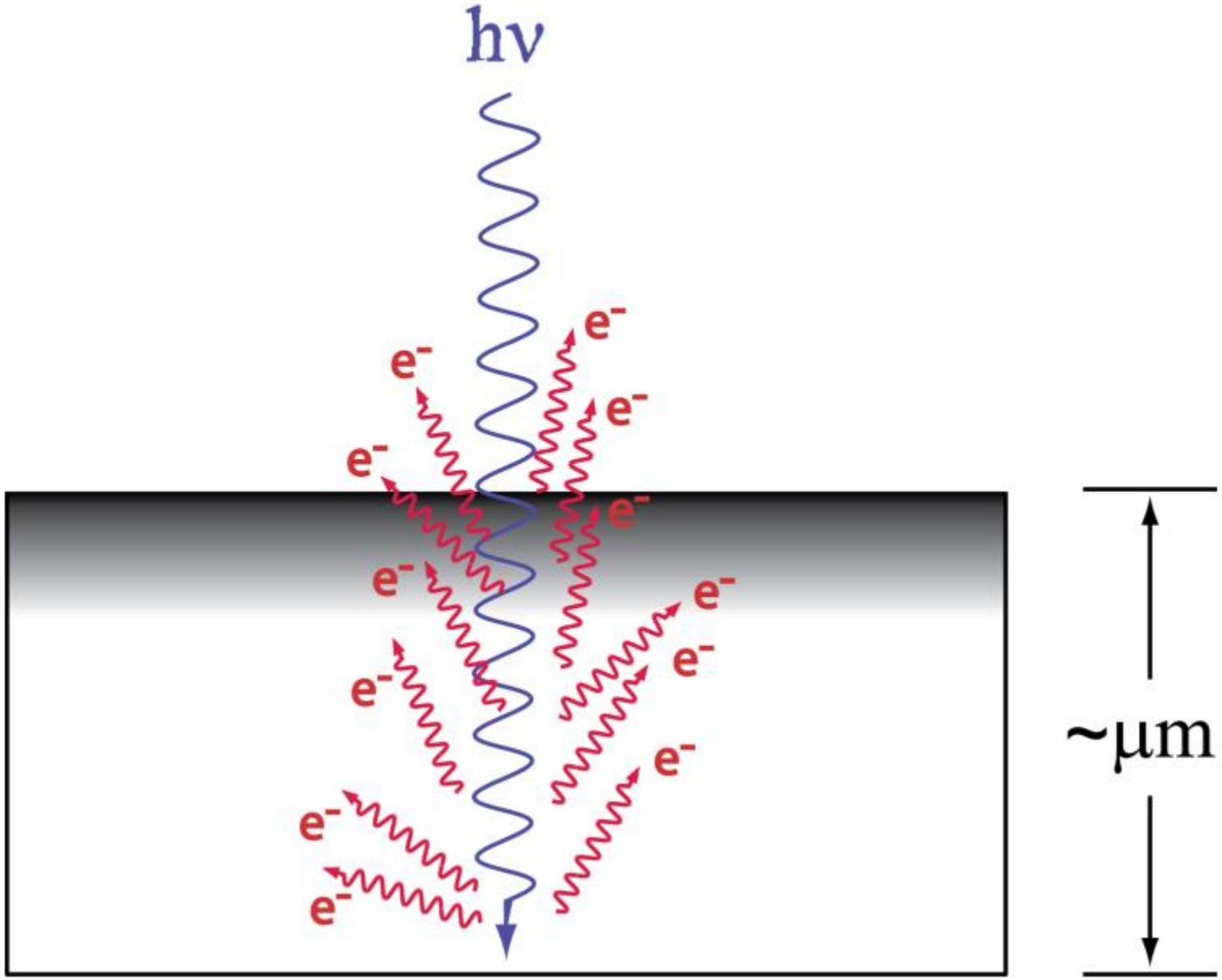
hν
e⁻
e⁻
e⁻
e⁻
e⁻
e⁻
e⁻
e⁻
e⁻
e⁻
e⁻
e⁻
~μm

化學位移(Chemical Shifts)

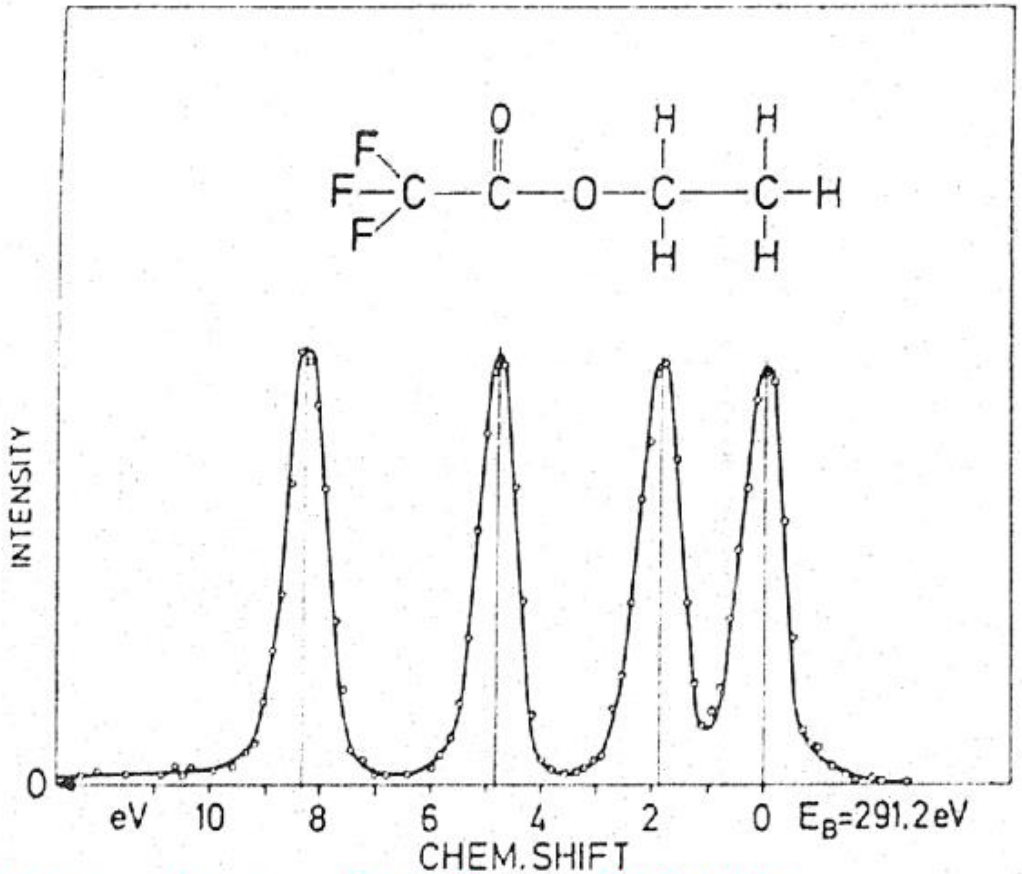

J. Electron. Spectrosc. Relat. Phenom., **2**(1974)405
Rev. Mod. Phys., **54**(1982)709

Provides information about

- Kind of atom
- Number of atoms
- Chemical shift

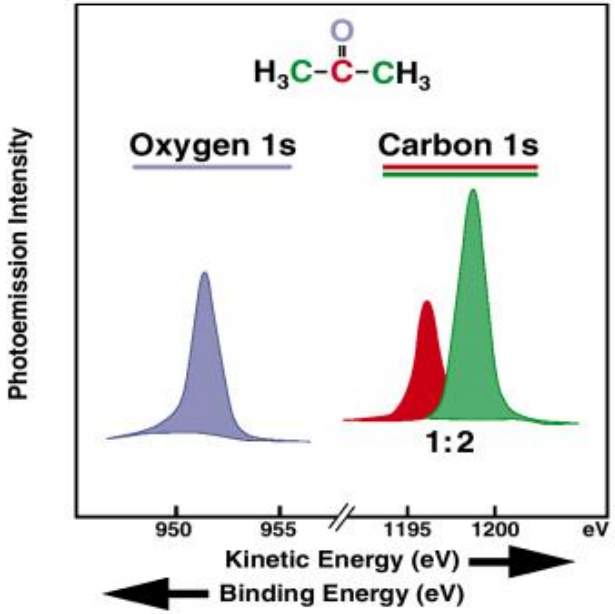

6 Å SiO_2 grown on Si(100)

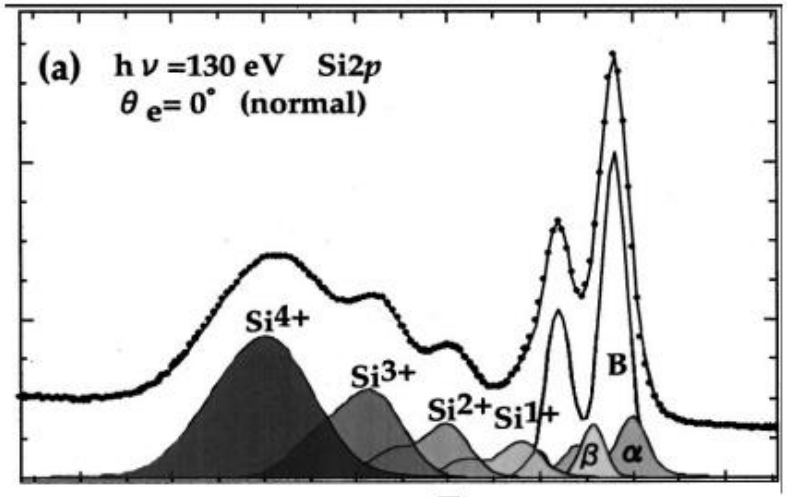

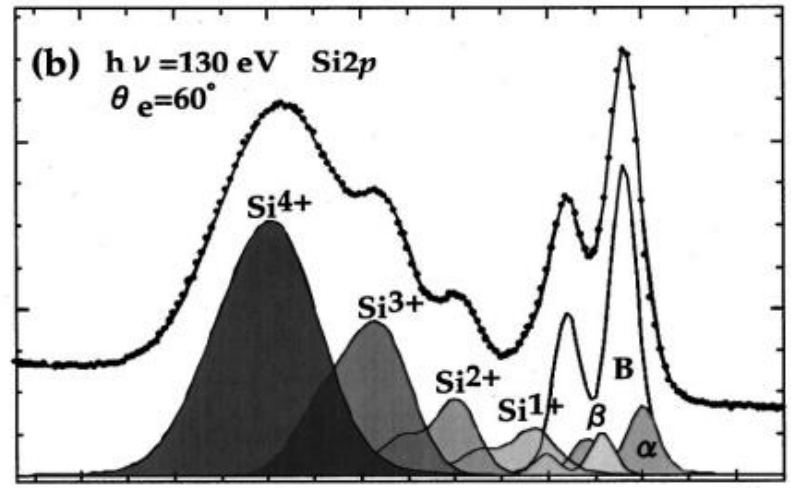

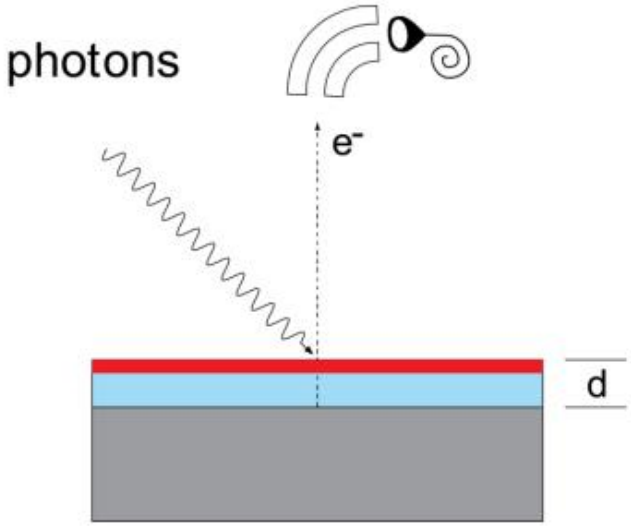

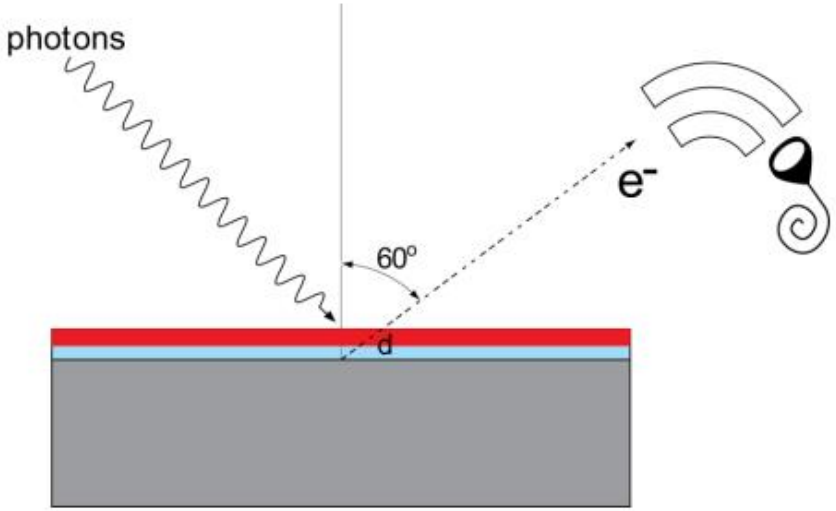

Scanning Tunneling Microscope (STM)
Scanning Probe Microscope (SPM)

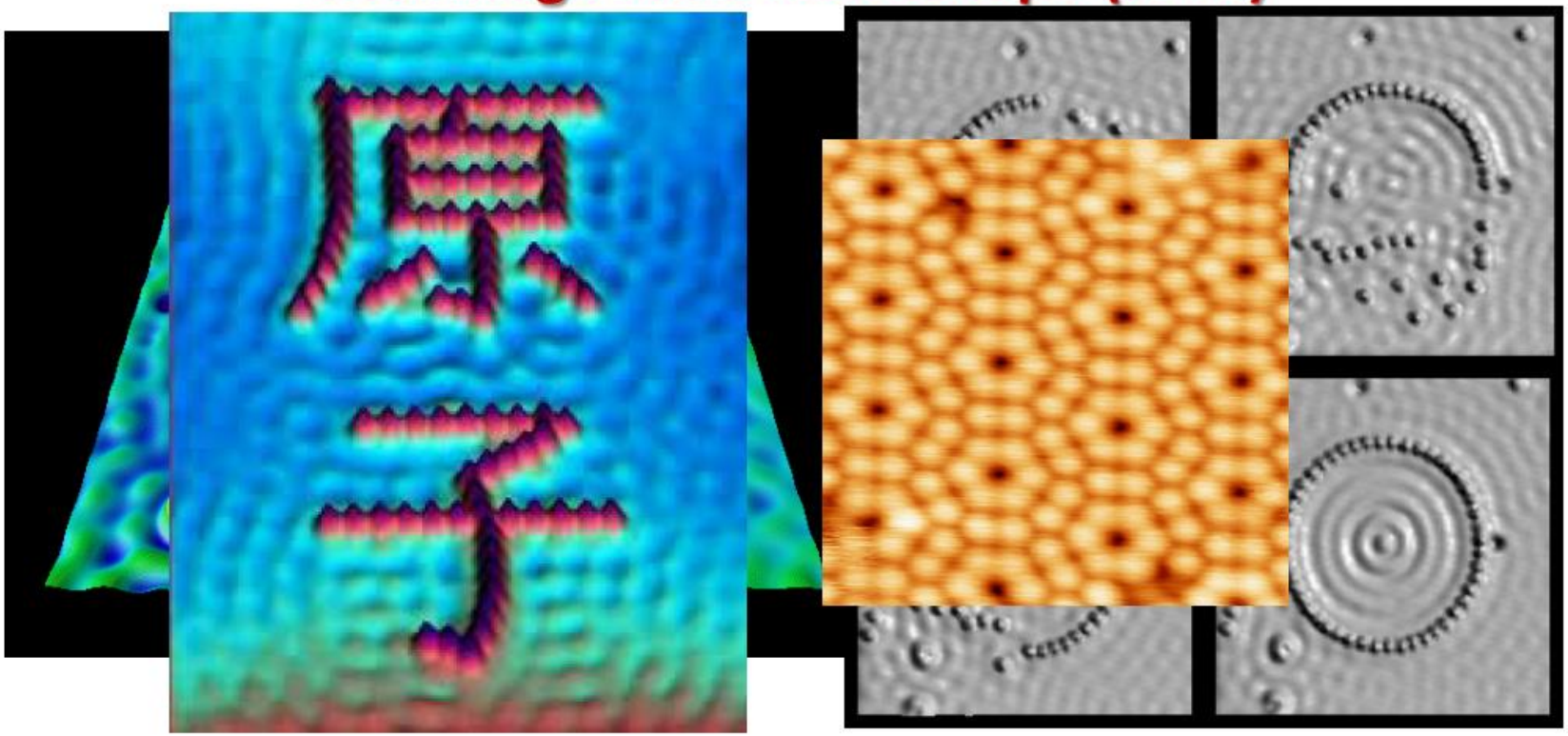

Almost every analytical technique can benefit from spatial resolution!

But how to achieve that?

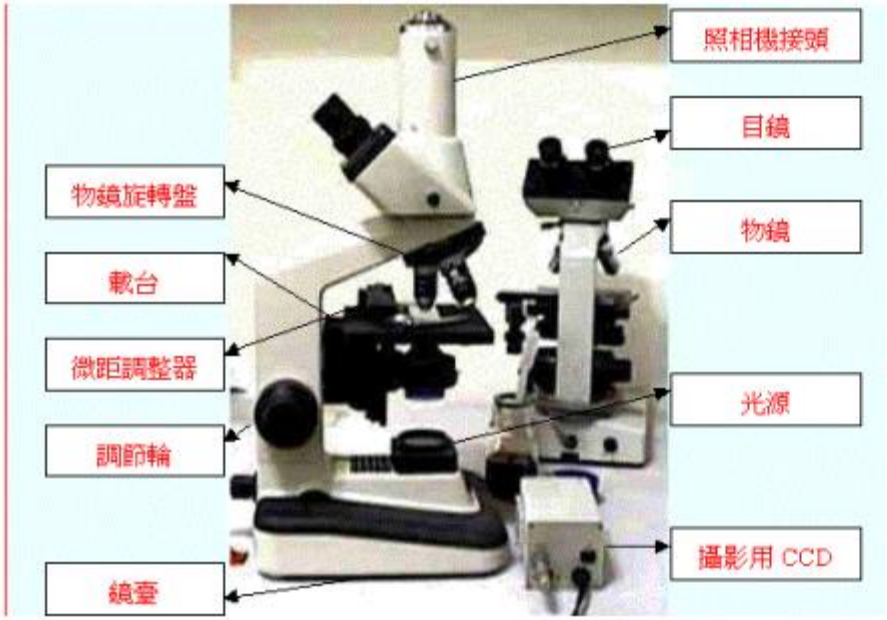

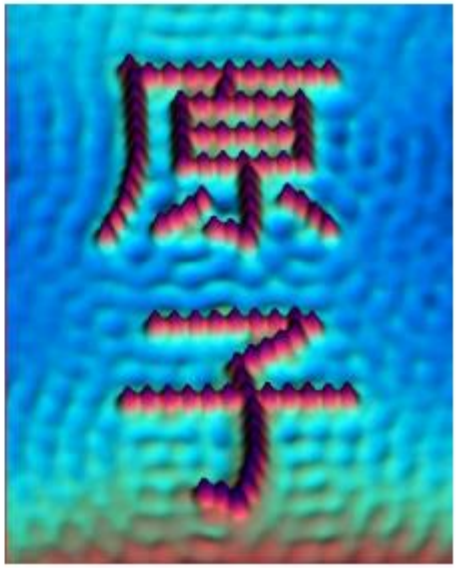

Does this work?

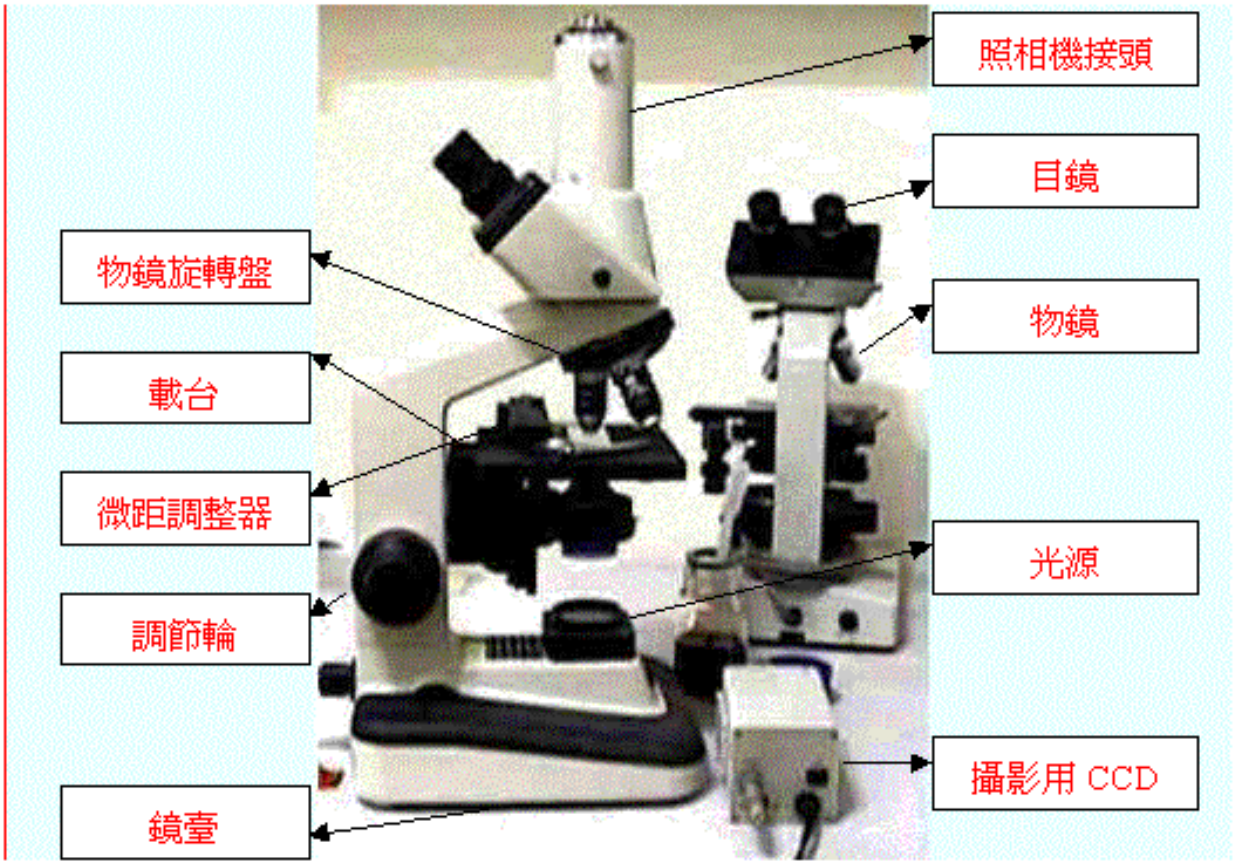

Fresnel Zone Plate (波帶環片)

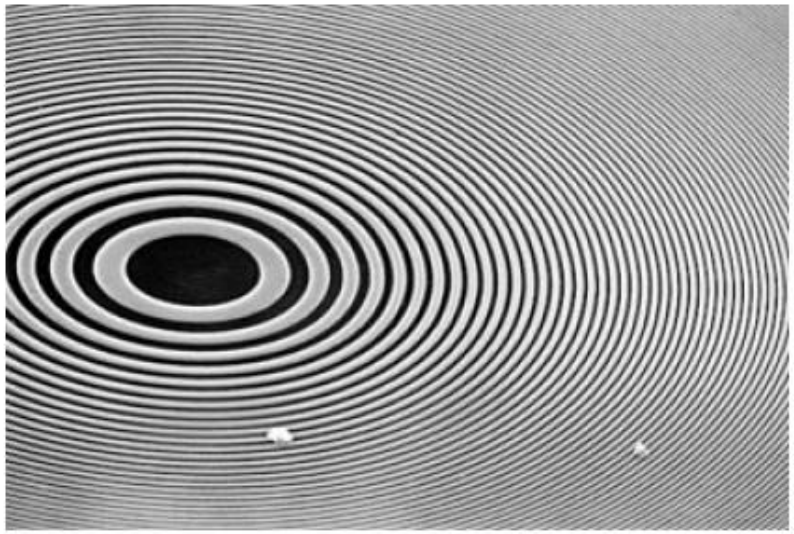

view in beam direction

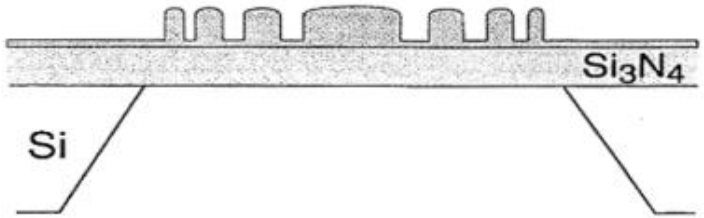

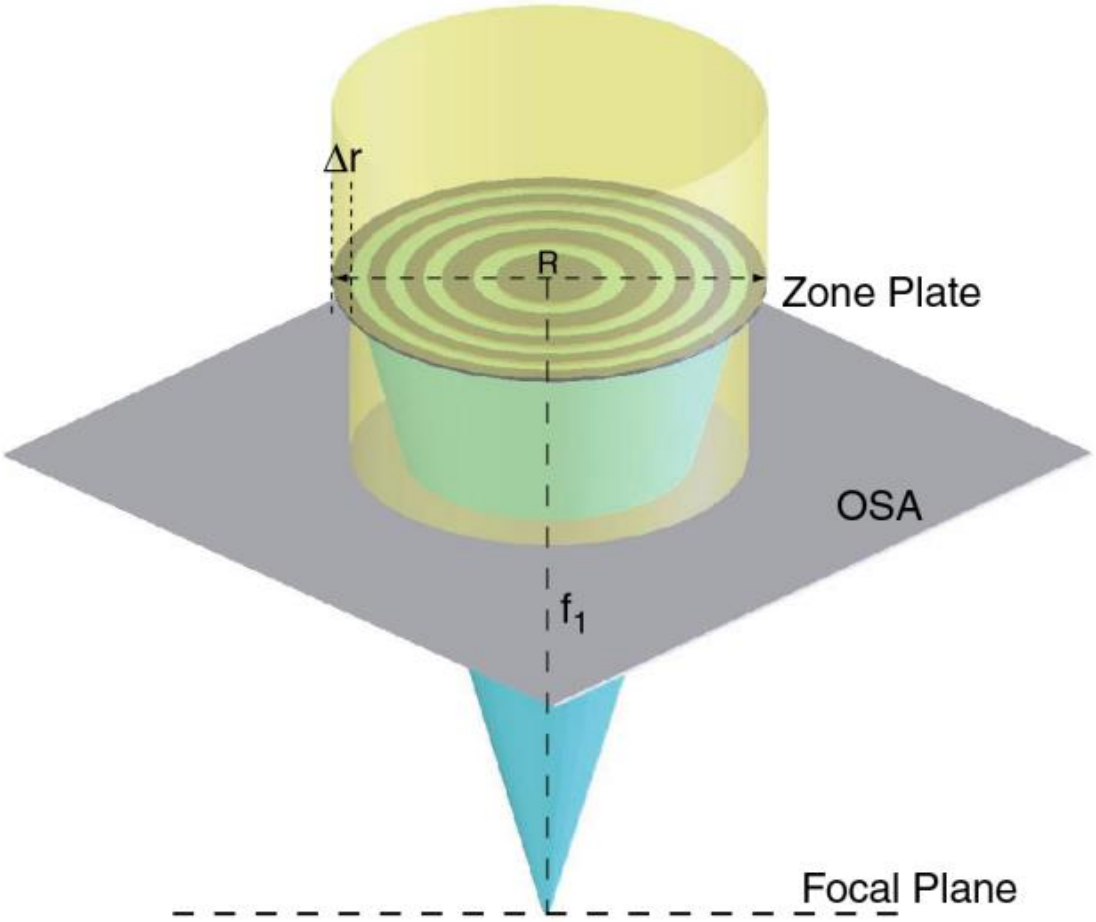

Spatial Resolution = 1.22 × Δr

Focal Length = R × Δr / λ

Diffraction Efficiency = 5-20%

For Example:

200 μm = R, 100 nm = Δr

280 eV = P.E.

focal length = 4.5 mm

OSA-sample distance = 1.1 mm

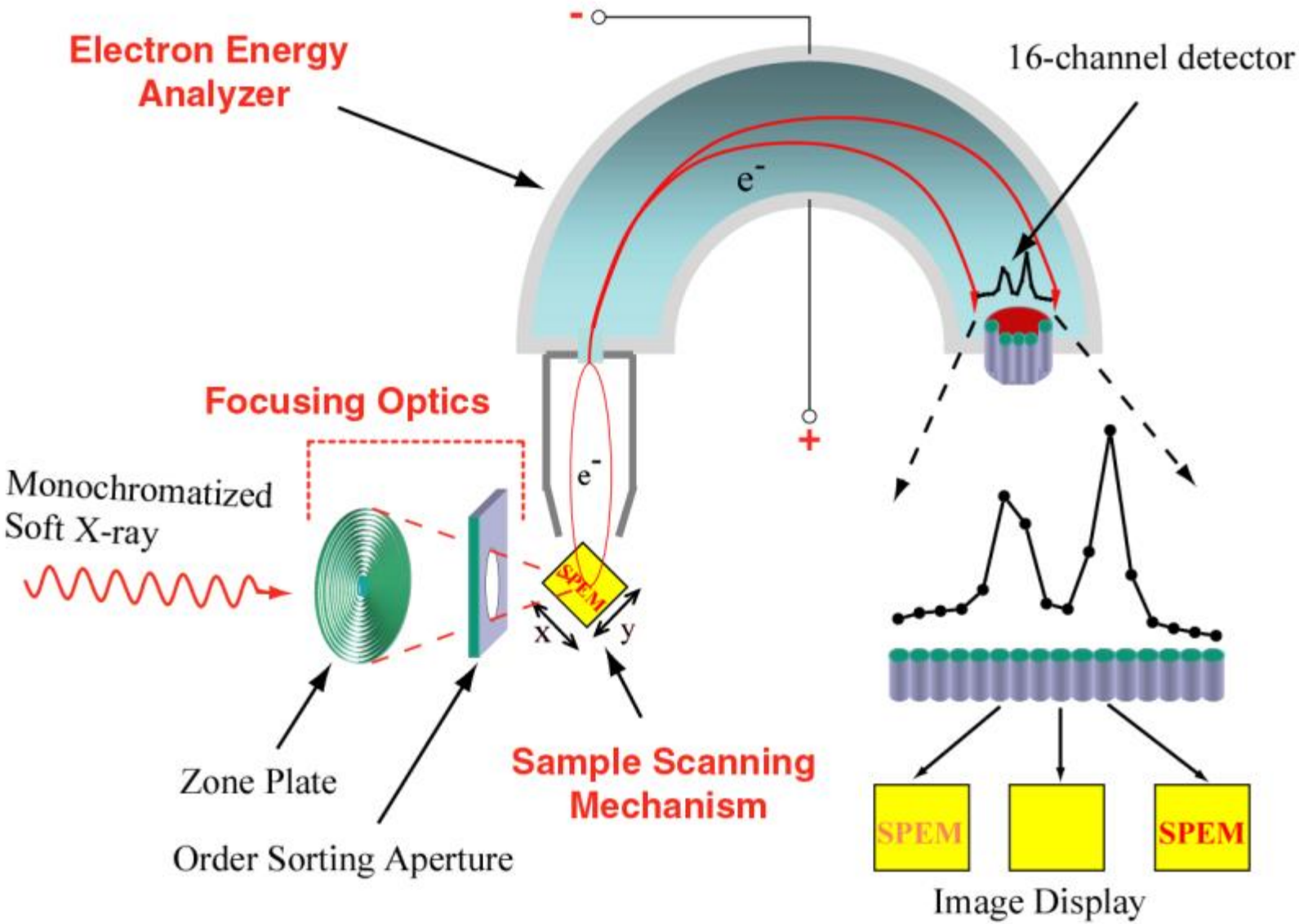
Electron Energy Analyzer
16-channel detector
-
+
e-
e-
Focusing Optics
Monochromatized Soft X-ray
SPEM
x
y
Zone Plate
Order Sorting Aperture
Sample Scanning Mechanism
SPEM
SPEM
Image Display

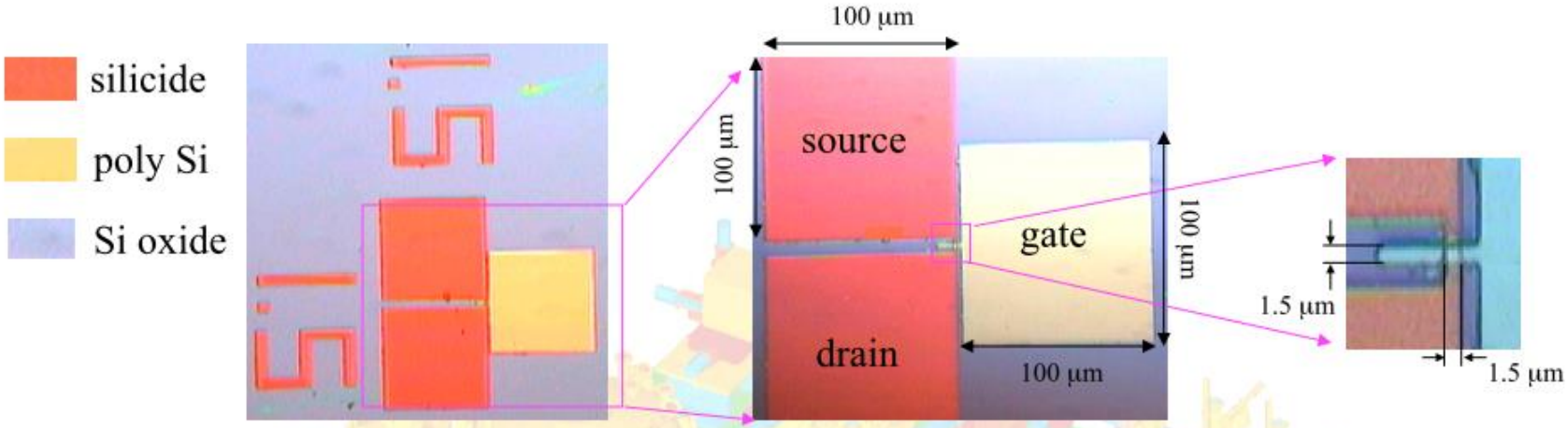

Si 2p SPEM image of FET

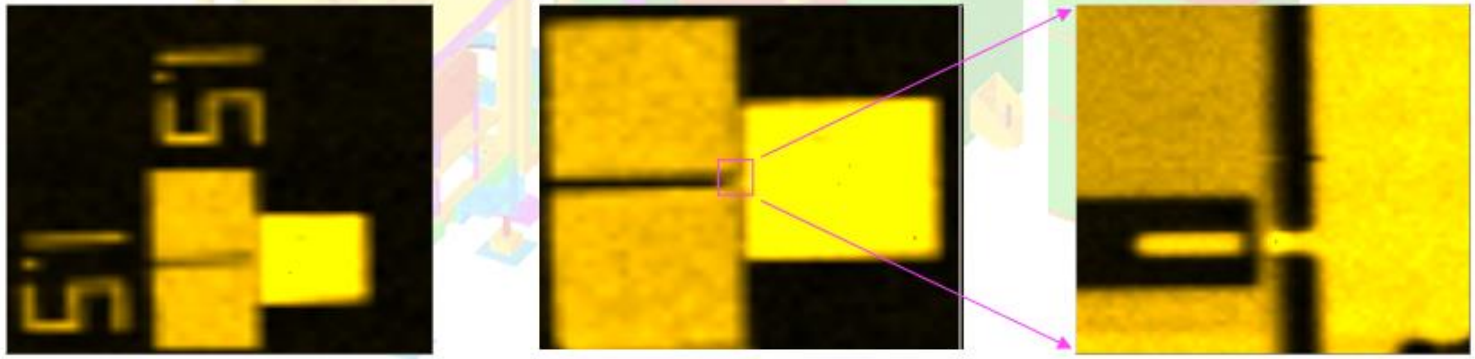

440μm × 440μm, 11μm/pixel　　240μm × 240μm, 6μm/pixel　　20μm × 20μm, 0.5μm/pixel

Yes, good image is beautiful!

BUT, most of the time,

IMAGES SUGGEST,

SPECTRA TELL

Parallel Imaging for Chemical State Mapping (PICSM)

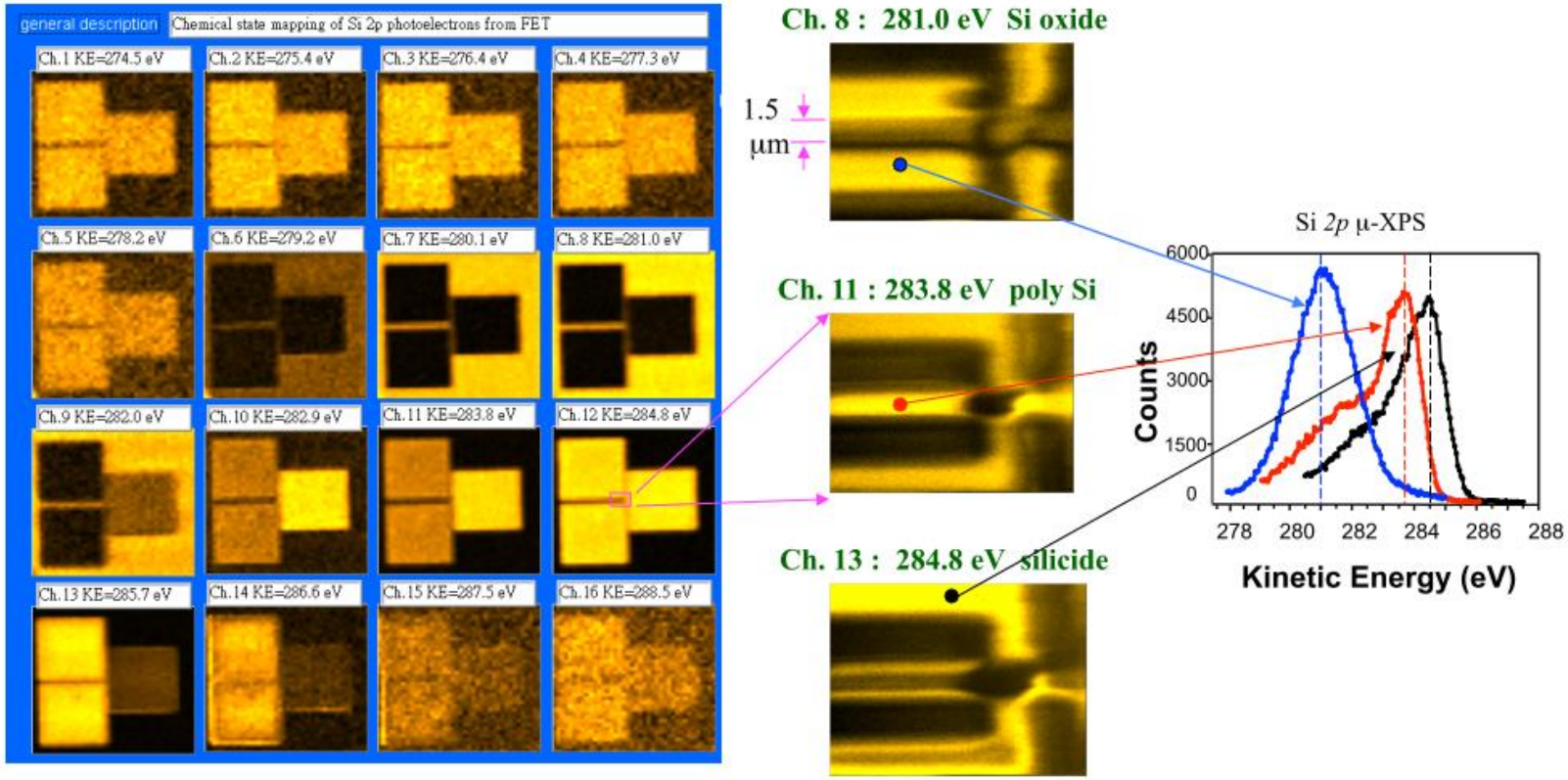

MOSFET 240 μm × 240 μm

12 μm × 12 μm, 0.1 μm/pixel

SPEM 實驗站

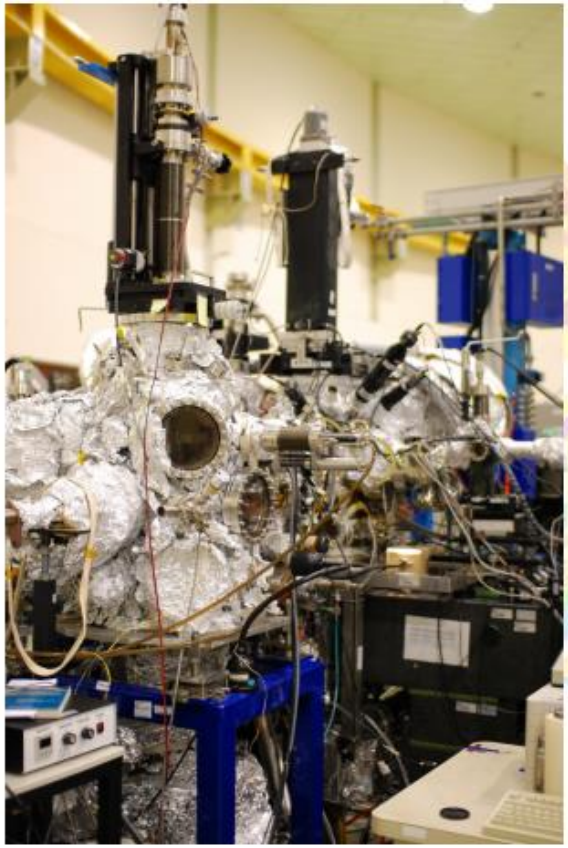

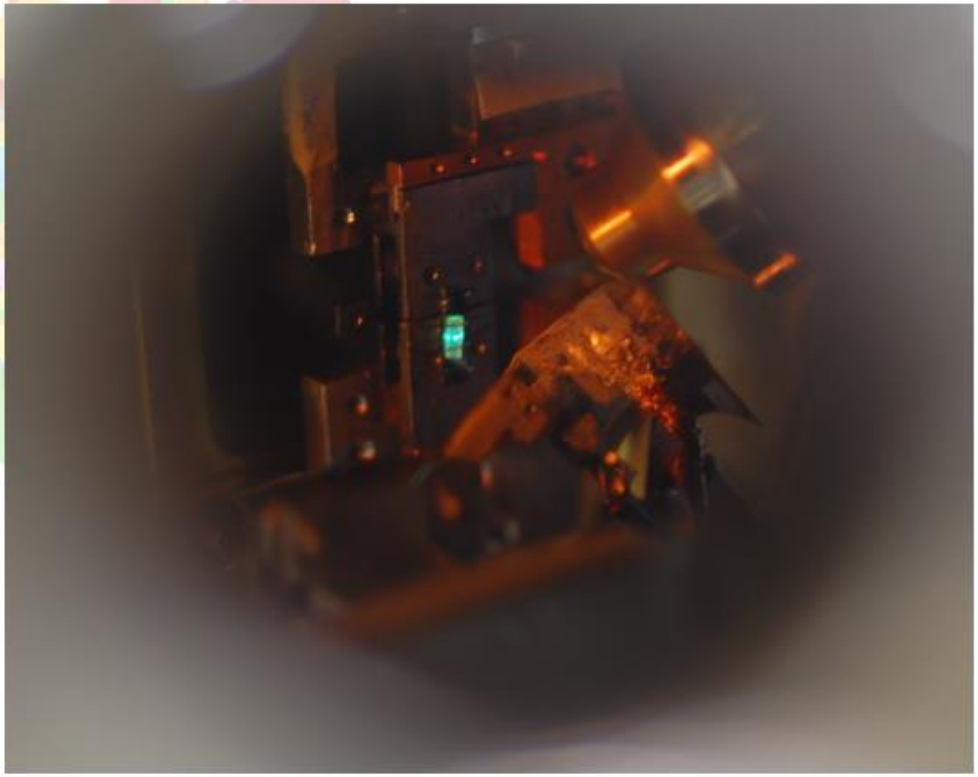

Is silicon dioxide essential to make graphene visible?

Let's Talk About Graphene

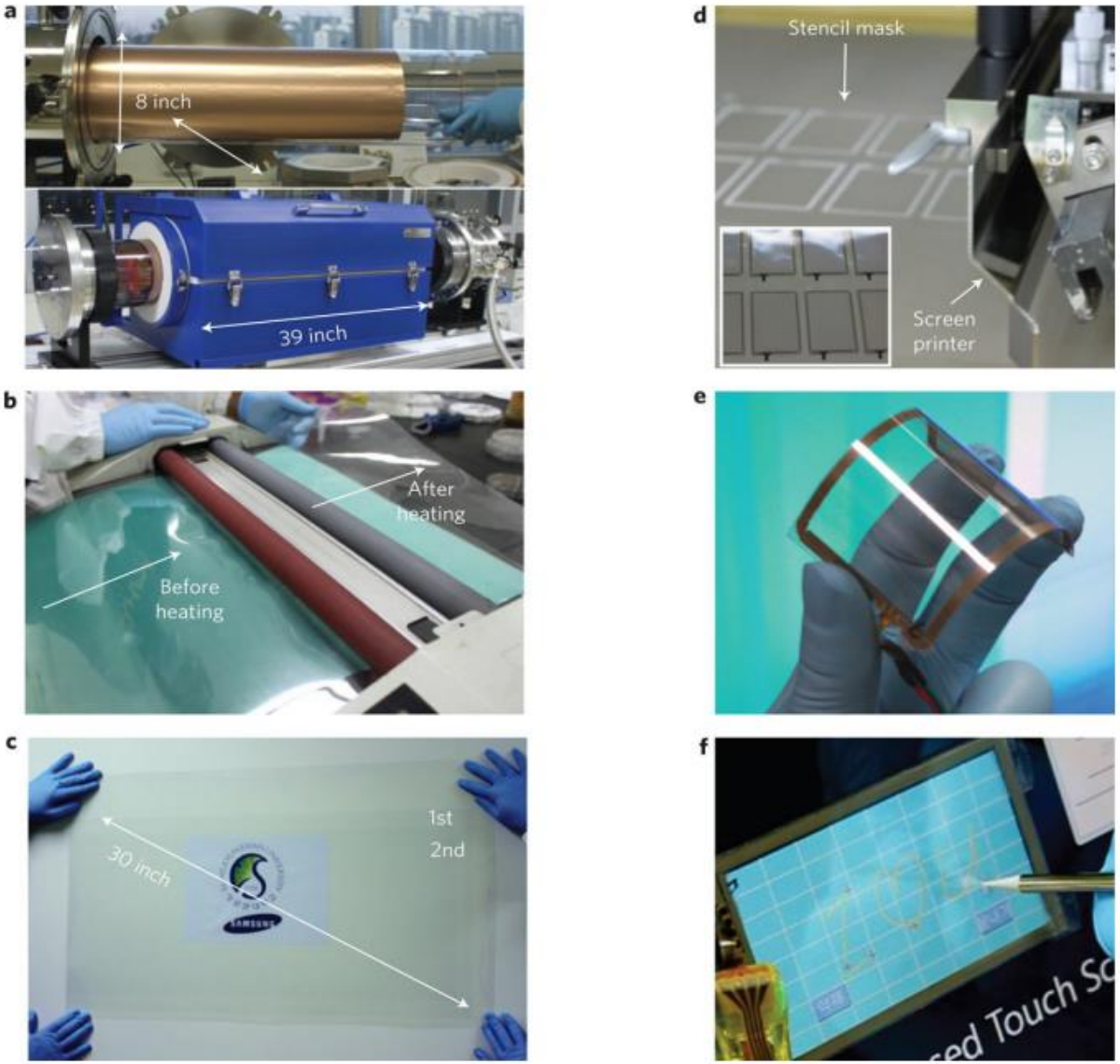

S. Bae et al., *Nat. Nanotech.*, **5**, 574 (2010)

IOP Publishing
Nanotechnology 21 (2010) 175201 (6pp)

Large-scale patterned multi-layer graphene films as transparent conducting electrodes for GaN light-emitting diodes

Gunho Jo[1], Minhyeok Choe[1], Chu-Young Cho[1], Jin Ho Kim[3], Woojin Park[1], Sangchul Lee[2], Woong-Ki Hong[1,4], Tae-Wook Kim[1,5], Seong-Ju Park[1,2], Byung Hee Hong[3], Yung Ho Kahng[1,6] and Takhee Lee[1,2,6]

[1] Department of Materials Science and Engineering, Gwangju Institute of Science and Technology, Gwangju 500-712, Korea
[2] Department of Nanobio Materials and Electronics, Gwangju Institute of Science and Technology, Gwangju 500-712, Korea
[3] Department of Chemistry and SKKU Advanced Institute of Nanotechnology, Sungkyunkwan University, Suwon 440-746, Korea

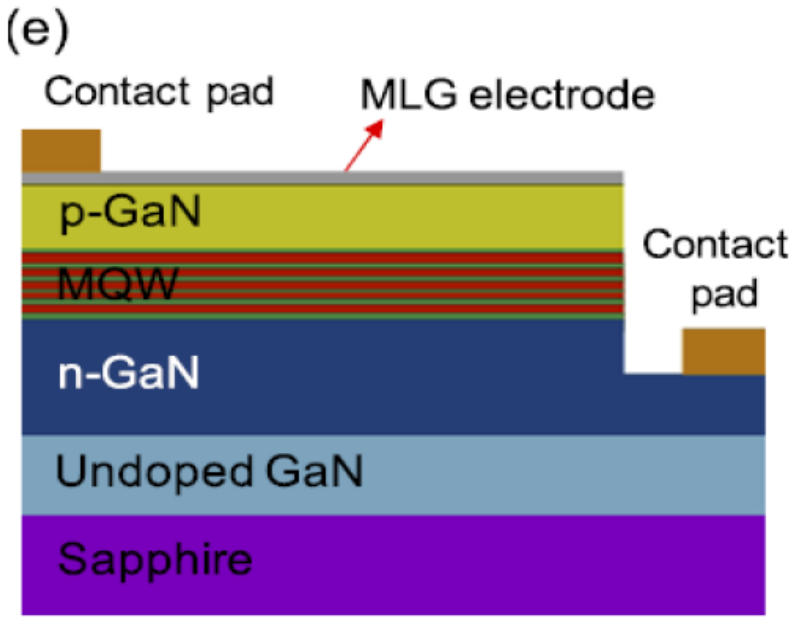

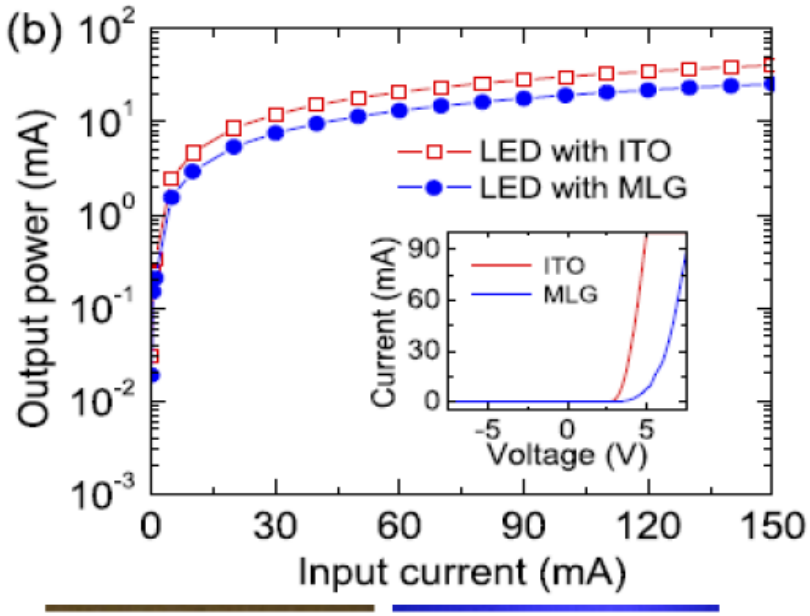

新型態同步輻射顯微術簡介

Spatially resolved ARPES

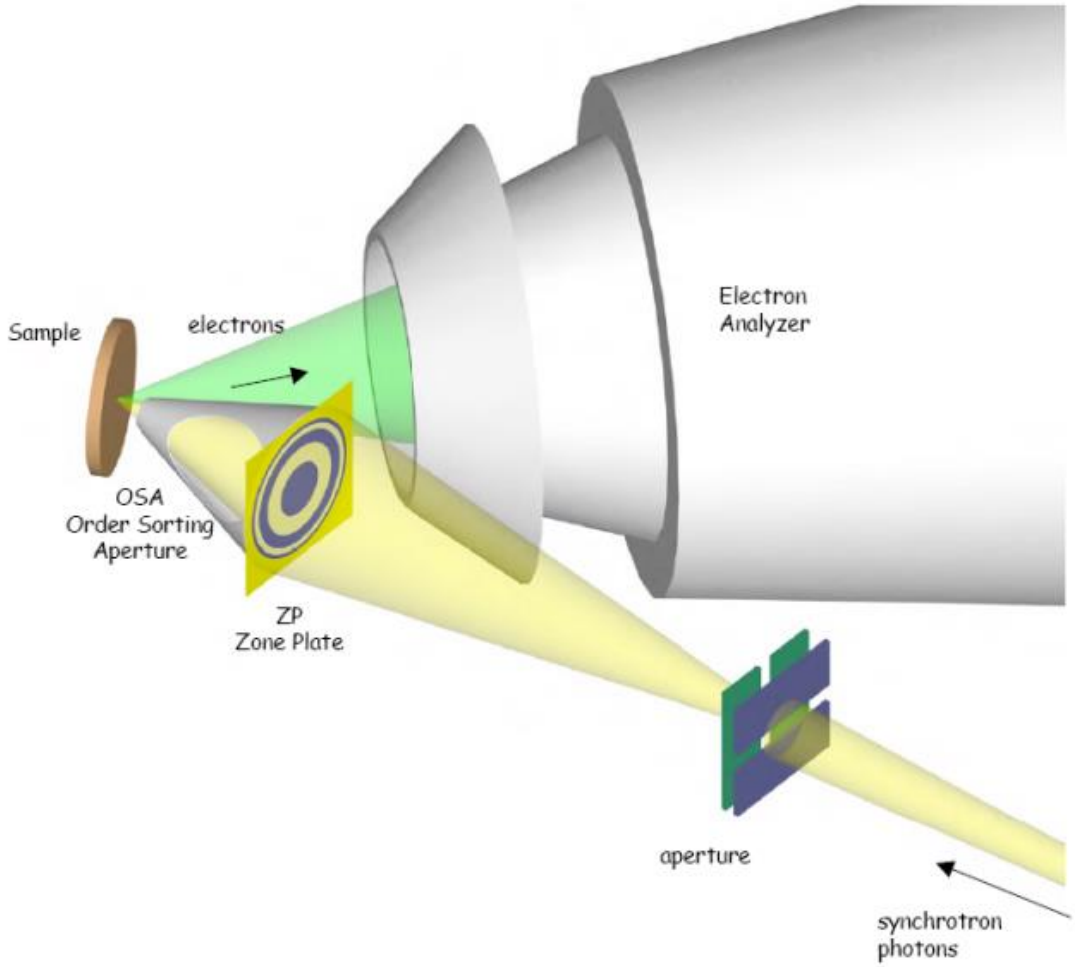

conventional ARPES on a large, pure single crystal

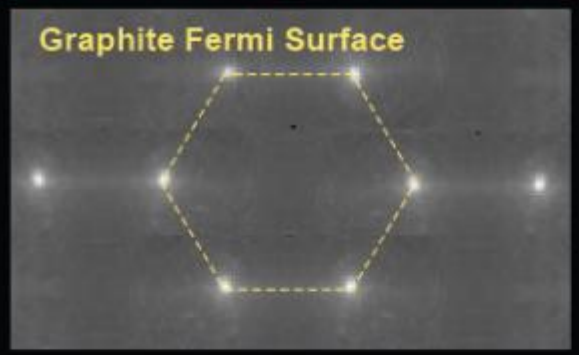

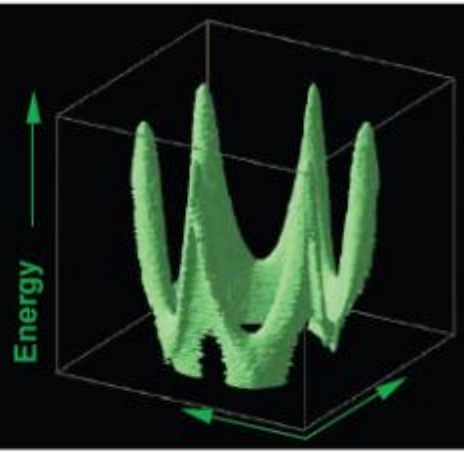

conventional ARPES of polycrystalline graphite

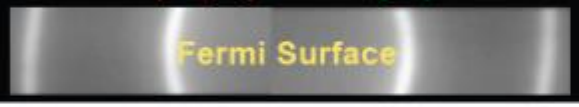

most of the momentum information is lost
as our spot size is much larger than the grain size.

nanoARPES of polycrystalline graphite

we can recover all the momentum
information by sampling one grain at a time

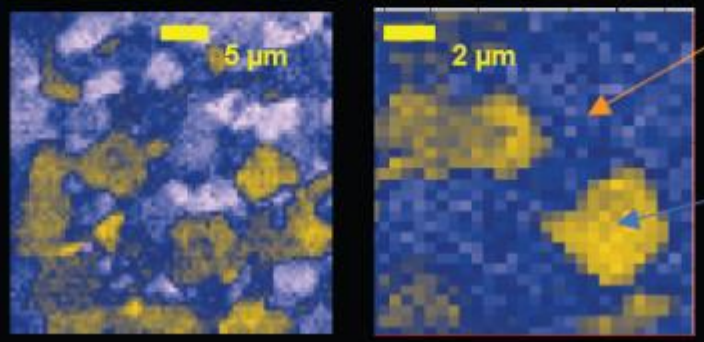

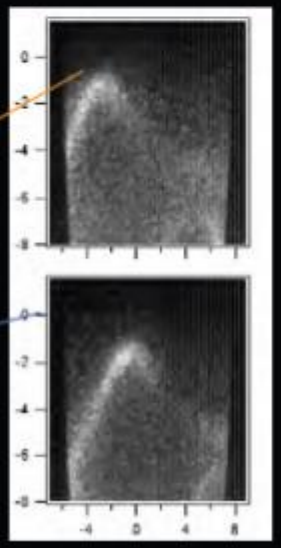

掃描式穿透光吸收能譜顯微術

(Scanning Transmission X-Ray Microscope; STXM)

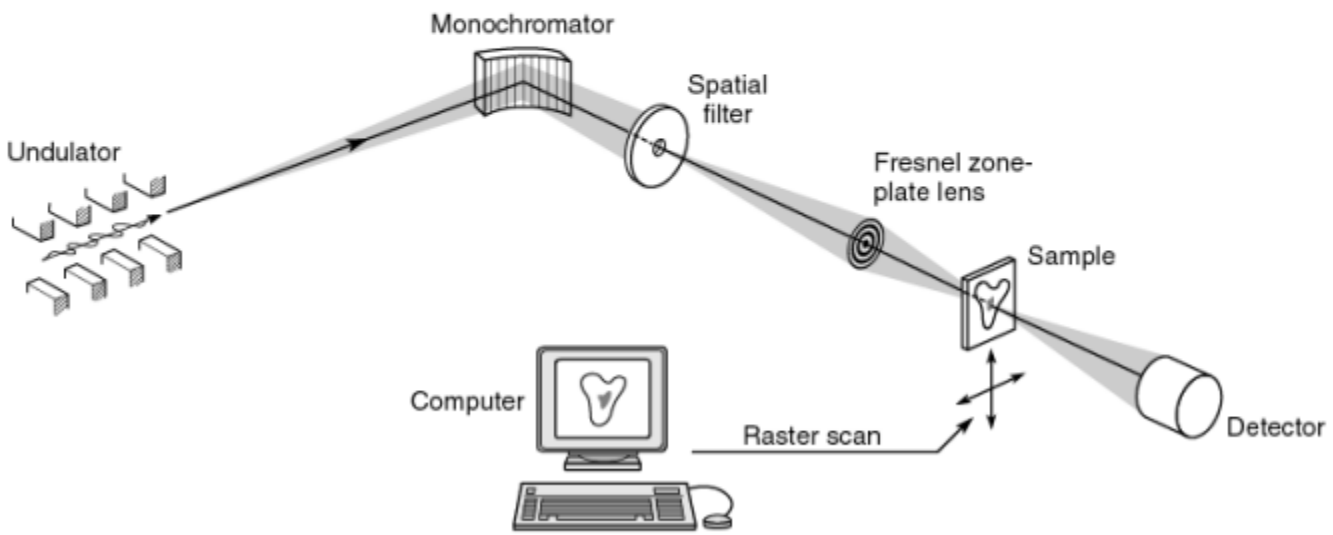

STXM specifications:

- spatial resolution: 25~50 nm
- energy resolution< 0.1 eV
- sample : 01.-1 micron
- He/inert gas atmosphere or vacuum environment
- solid/liquid/gas sample

Applications:

- **Magnetism**
- **Soft Matter**
- **Earth/Environmental Science**
- **Polymer Science**
- **Materials Science**
- **Catalyst**

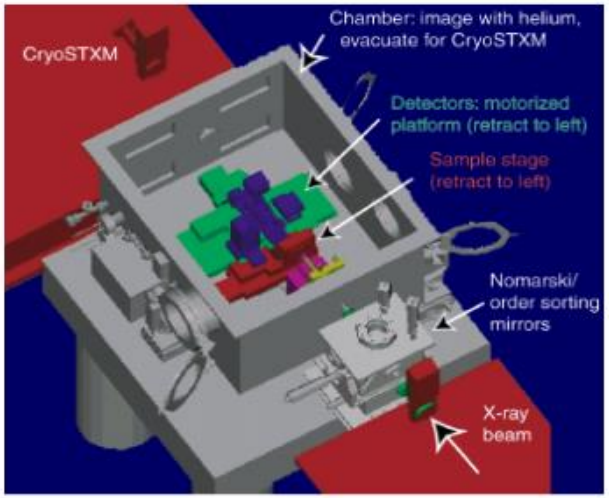

XAS

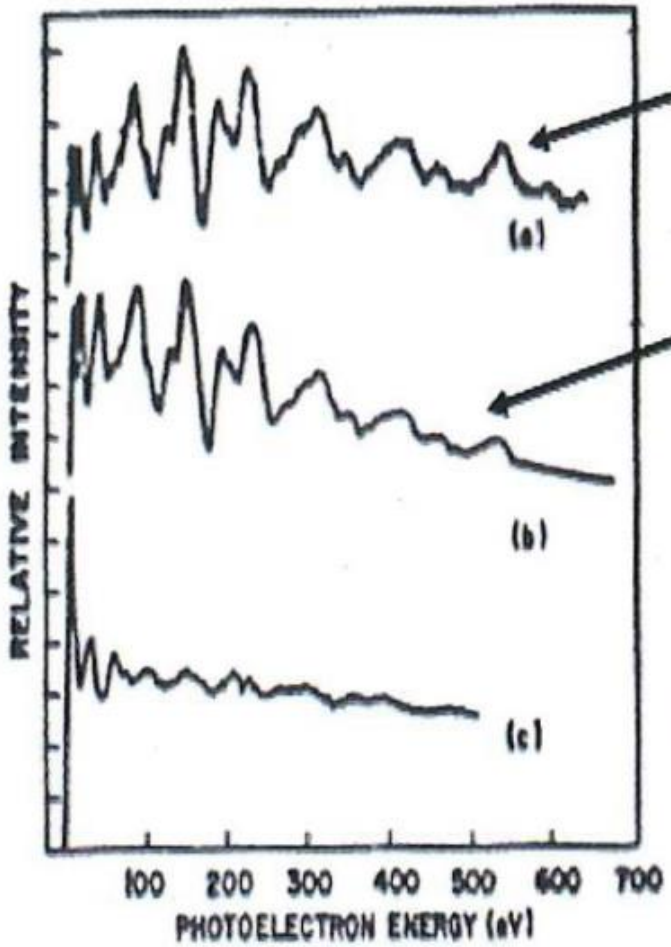

~ 10 days using rotating anode X-Ray tube

Cu EXAFS

~ 20 minutes using synch. rad. from SPEAR bending magnet

Ratio of intensity; SR/X-Ray Tube ~100,000

Extended X-ray Absorption Fine Structure for Cu (a) and (b), by Peter Eisenberger and Brian Kincaid, taken in 1974 at the Stanford Synchrotron Radiation Project. (c) is EXAFS from a thin Nb3Ge superconducting thin film.

典型的 X 光吸收光譜實驗配置圖

(虛線表示實驗站的輻射屏蔽屋)

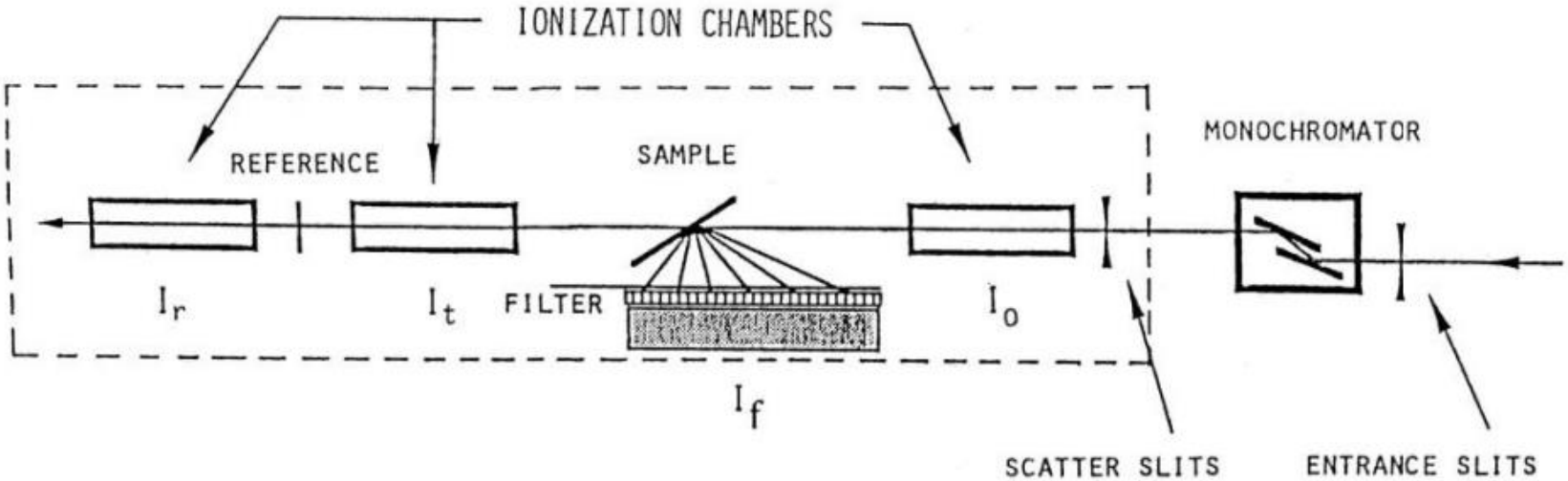

穿透法之樣品吸收係數為 $Ln(I_0/I_t)$

螢光法或電子產率法為 I_f/I_0 或 I_e/I_0

參考標準品之吸收係數為 $Ln(I_t/I_r)$

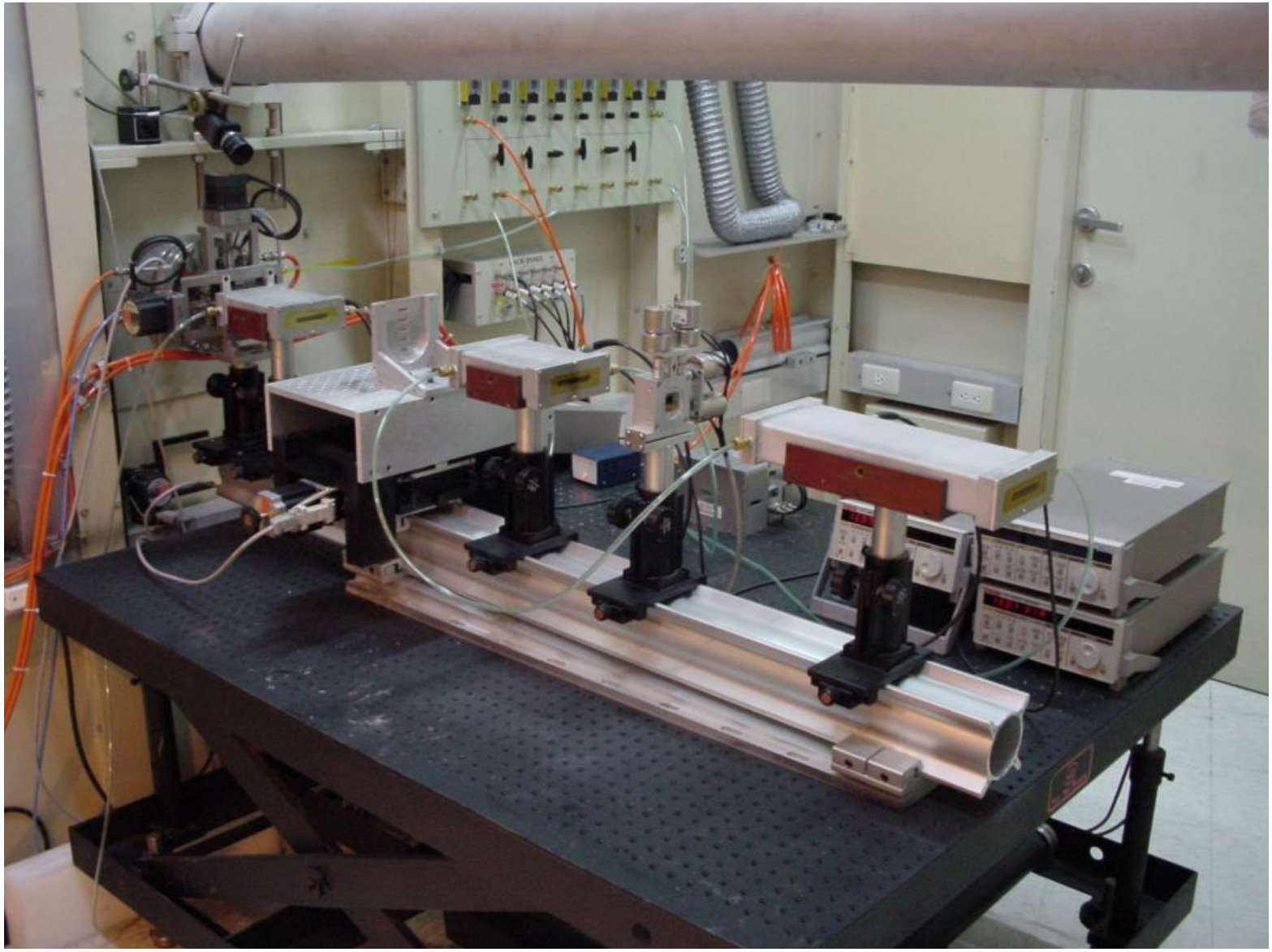

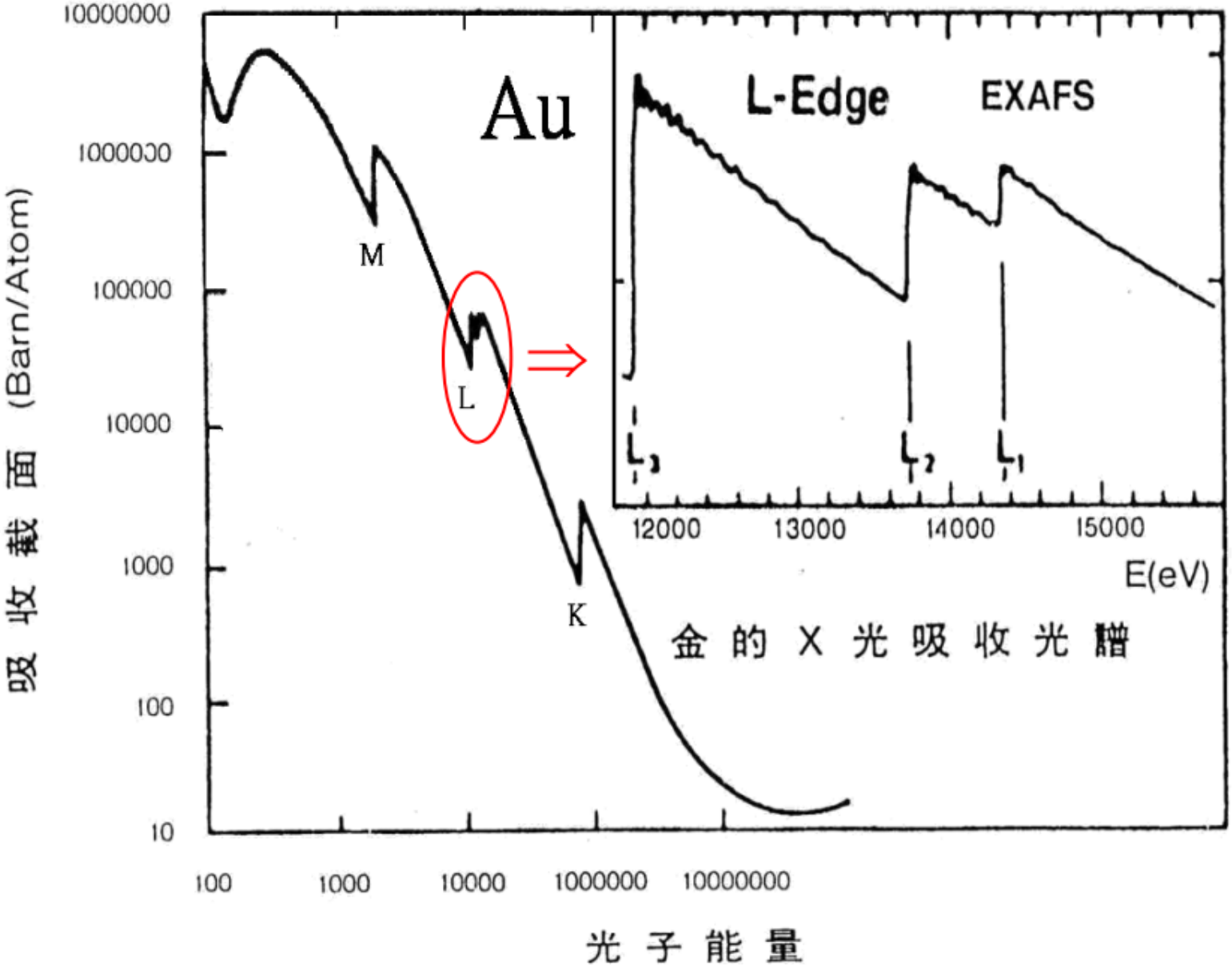
Au
L-Edge
EXAFS
M
L
K
L3
L2
L1
12000
13000
14000
15000
E(eV)
10000000
1000000
100000
10000
1000
100
10
100
1000
10000
1000000
10000000
吸收截面 (Barn/Atom)
光子能量

金的X光吸收光譜

Absorption edges

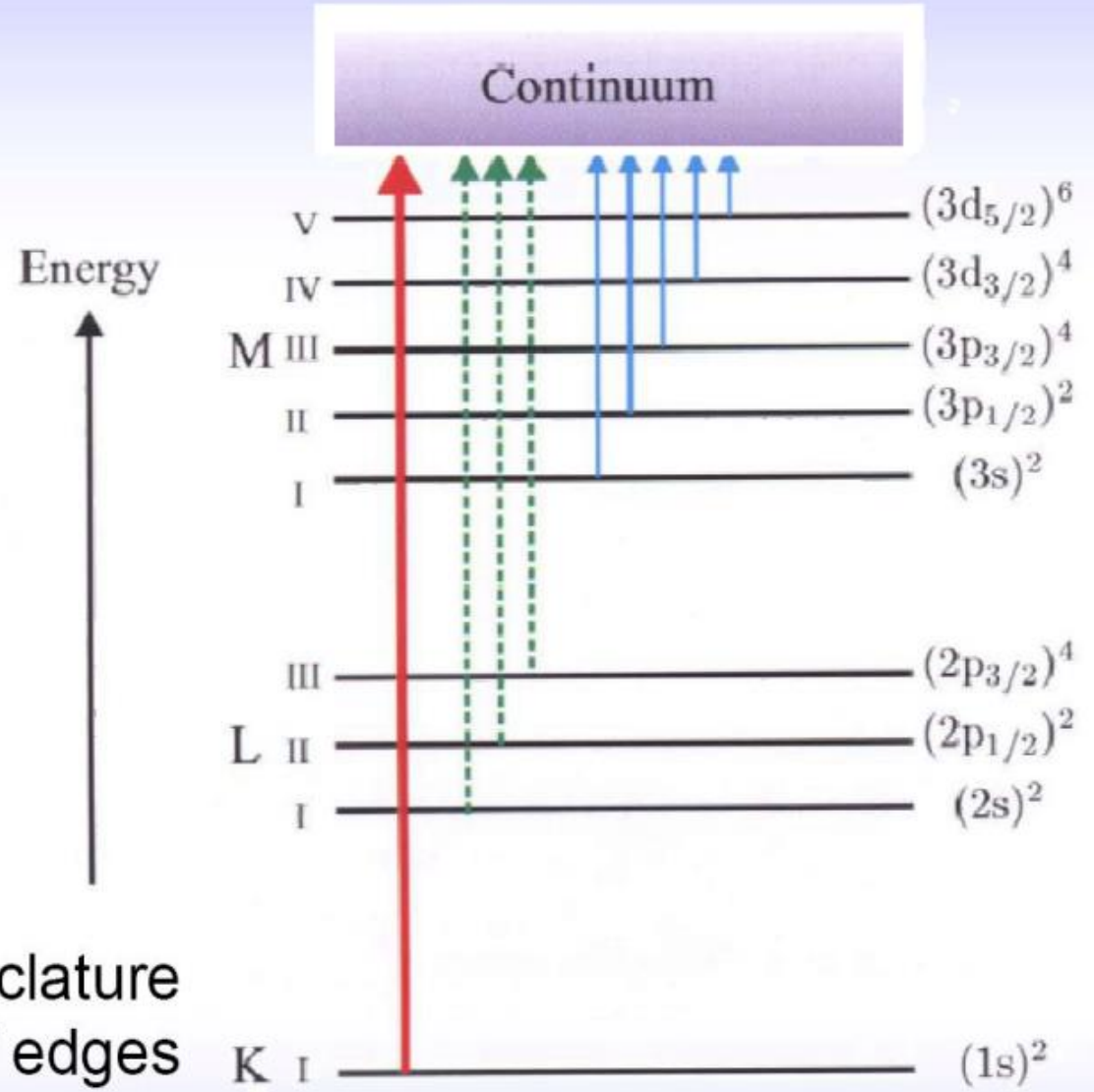

electron states

nomenclature of edges

X 光吸收近邊緣結構 (XANES) ====>

吸收原子的電子性質(如:氧化價數以及 *d*-軌域之電子填滿程度)

吸收原子所處之晶位對稱性

延伸 X 光吸收精細結構 (EXAFS) ====>

吸收原子周圍之局部幾何結構(如:周圍原子種類、配位數、原子間距離、排列之雜亂度)

EXAFS: Extended X-ray Absorption Fine Structure

XANES: X-ray Absorption Near-Edge Structure

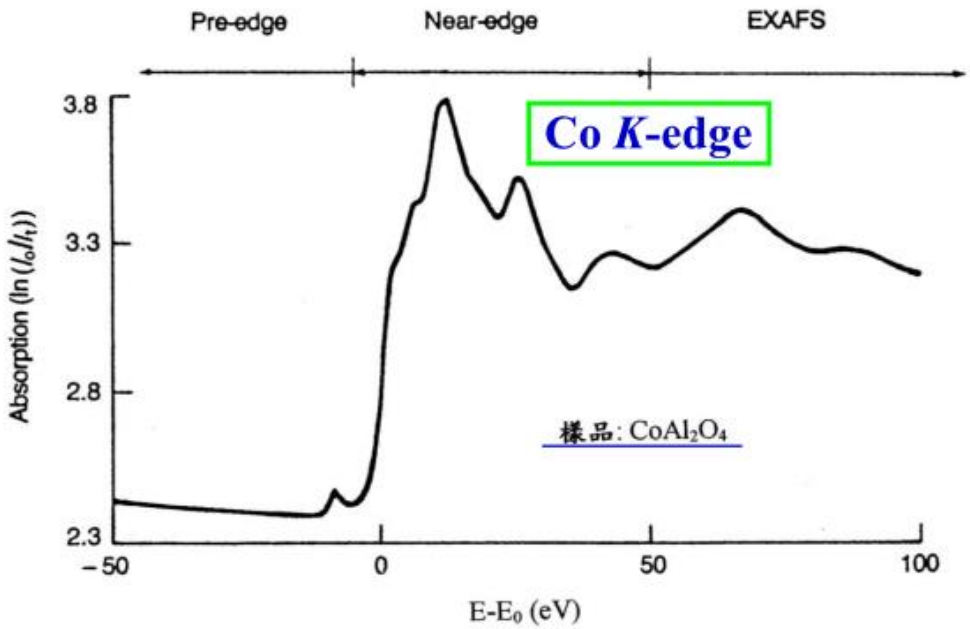

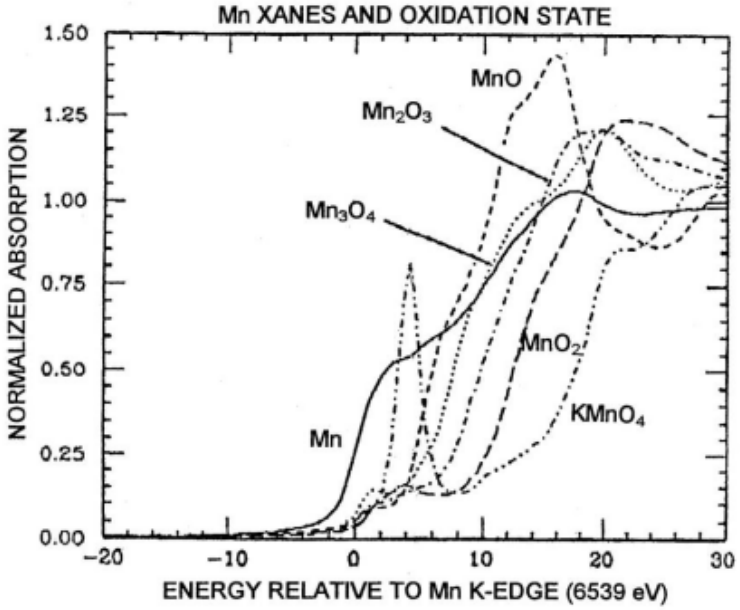

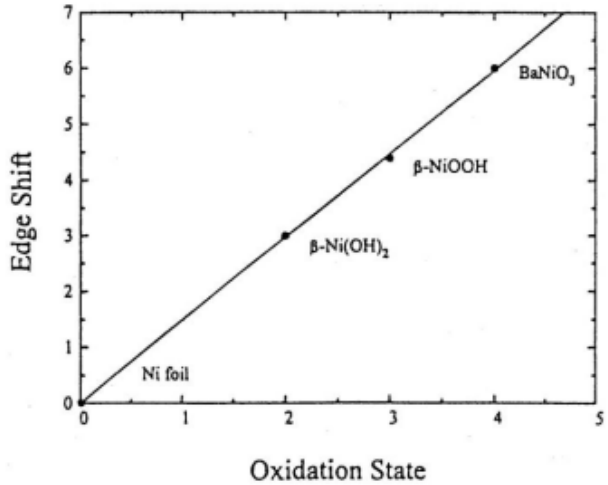

Fig. 3. Plot of the edge shifts in the XANES spectra vs. the increasing oxidation state of nickel.

1. **Absorption edges of many elements show significant energy shifts with <u>oxidation state</u>.**

2. **Why does edge shift with oxidation state?**

- **Electrostatics – harder to remove bound electron.**
- **Higher oxidation states have shorter bonds (in general).**

"White line" intensity reflects the d-orbital occupancy

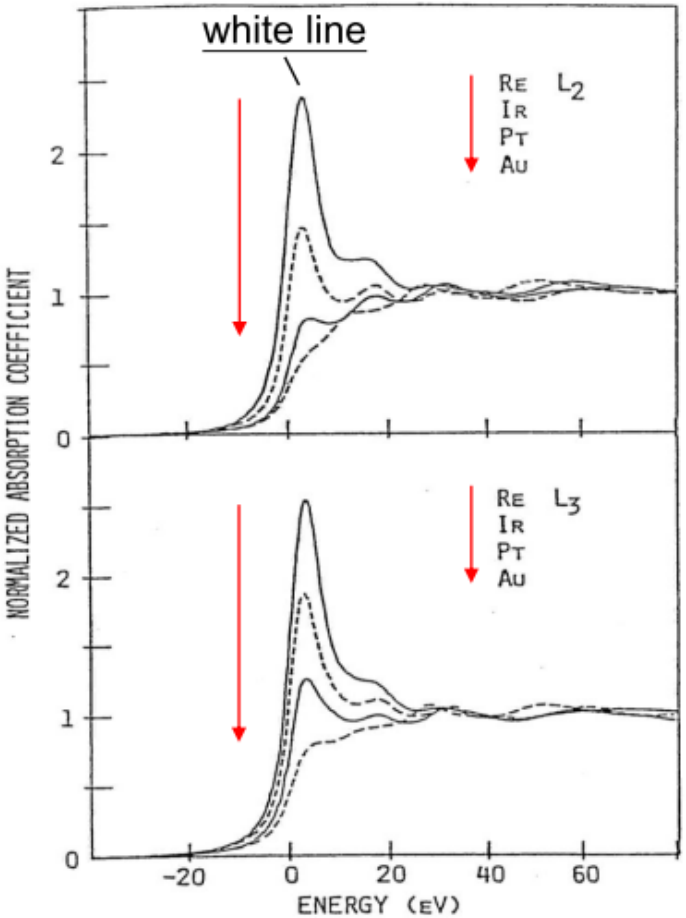

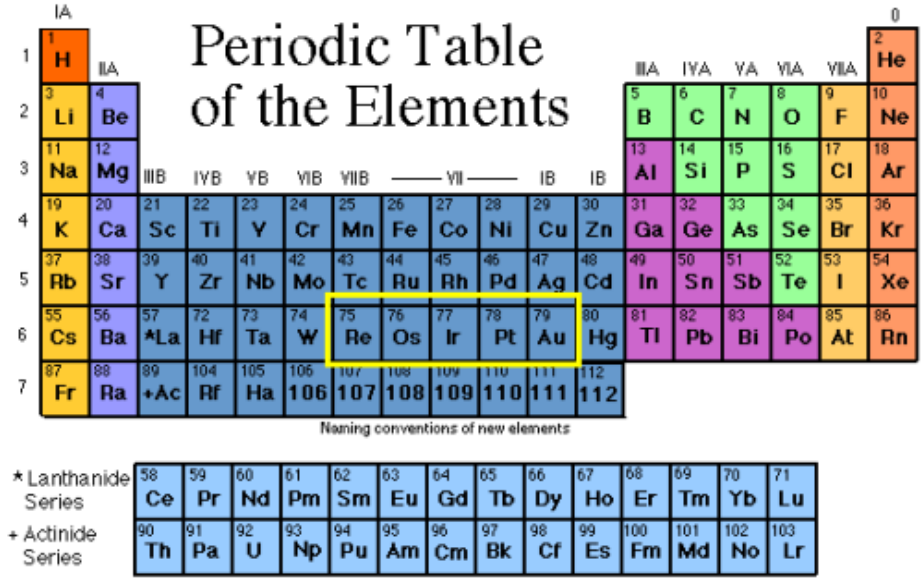

XANES spectra for the $L_{2,3}$-edges of Re, Ir, Pt, and Au. Spectra were normalized to unit edge jump and aligned to the first inflection point.

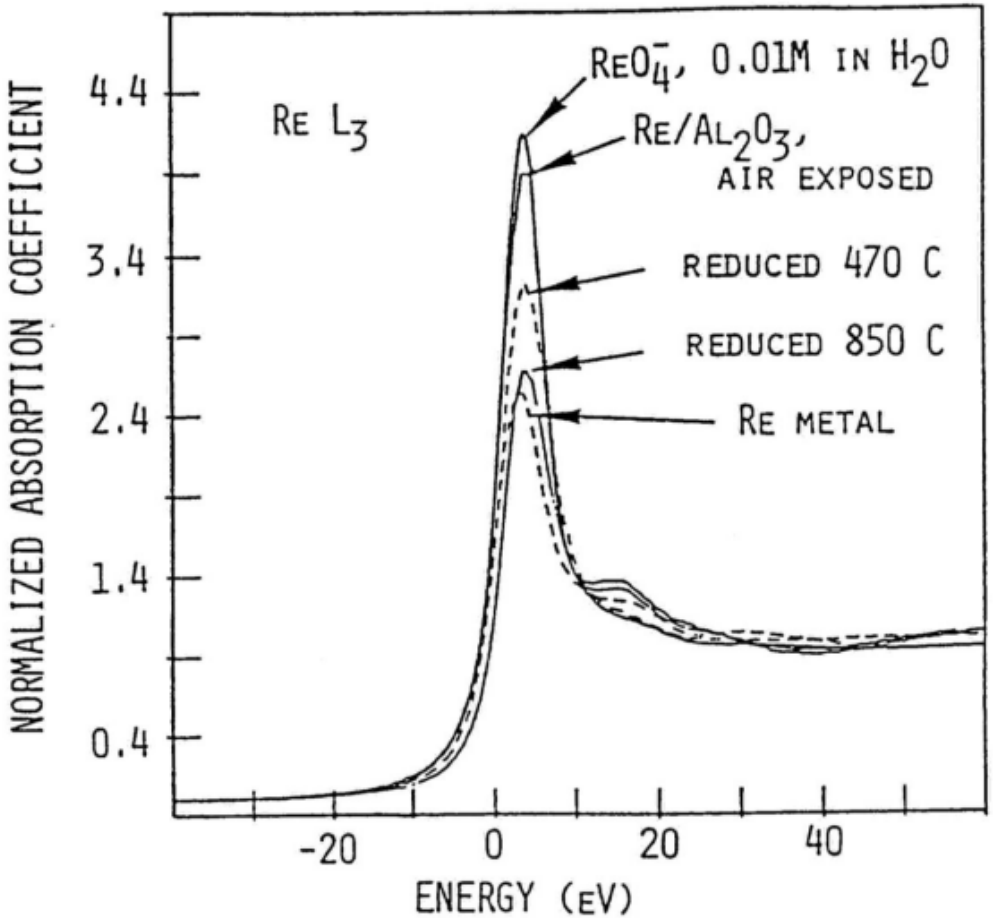

Higher oxidation state

⇓

More empty *d*-orbitals

⇓

More intense white line

Overplot of Re L_3-edges for 1 wt% Re on Al_2O_3 catalyst with Re^{+7} and Re metal reference edges.

Why are we interested in XANES?

Local Coordination Symmetry

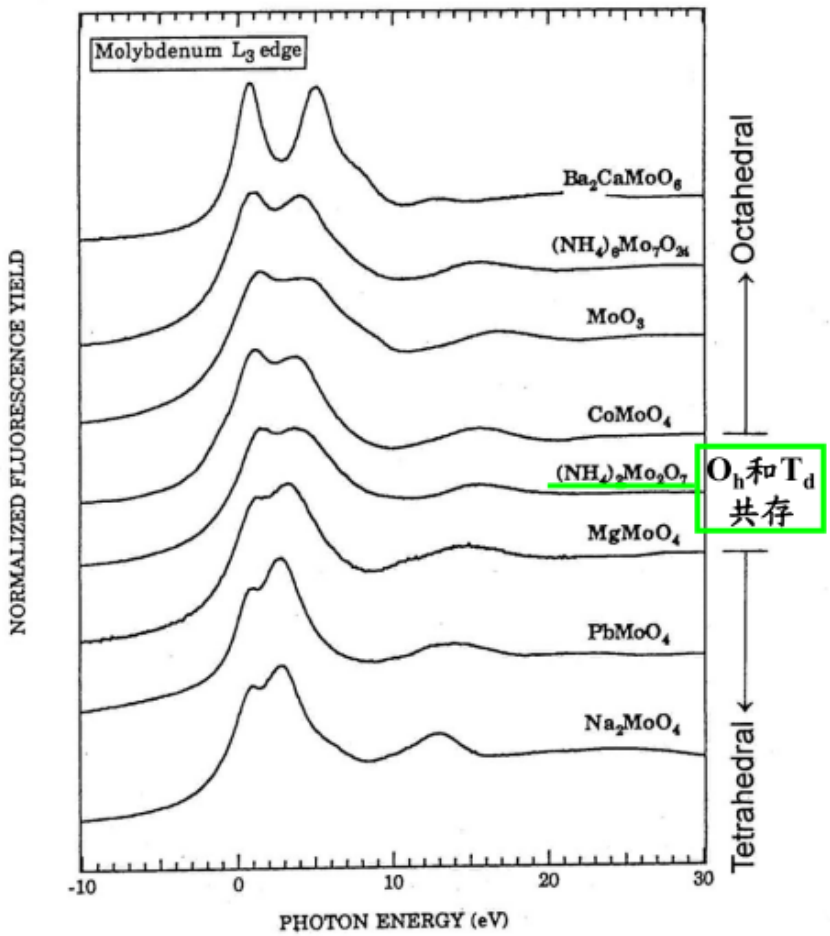

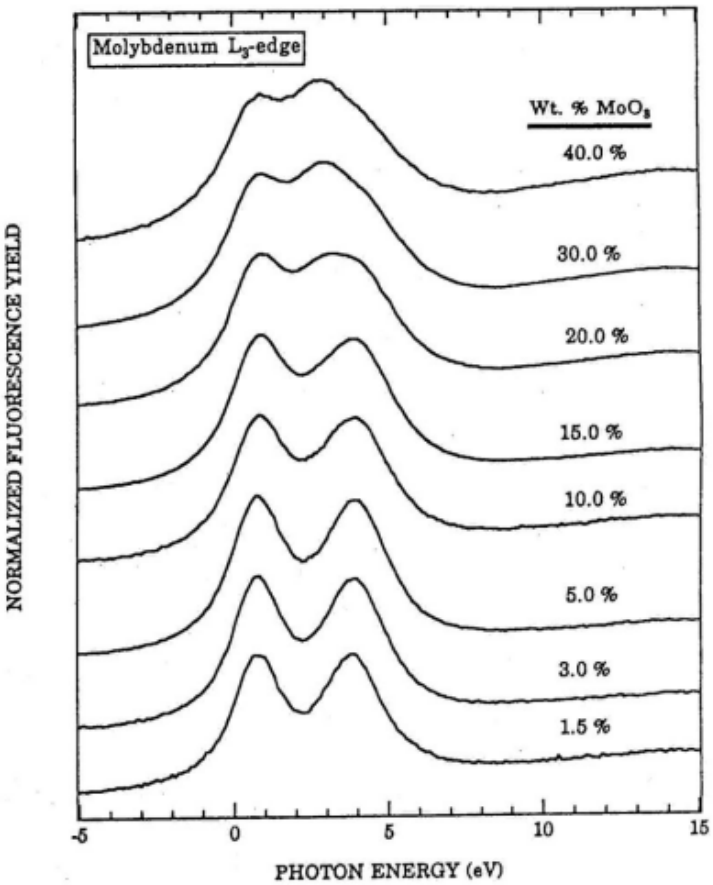

Local Coordination Symmetry

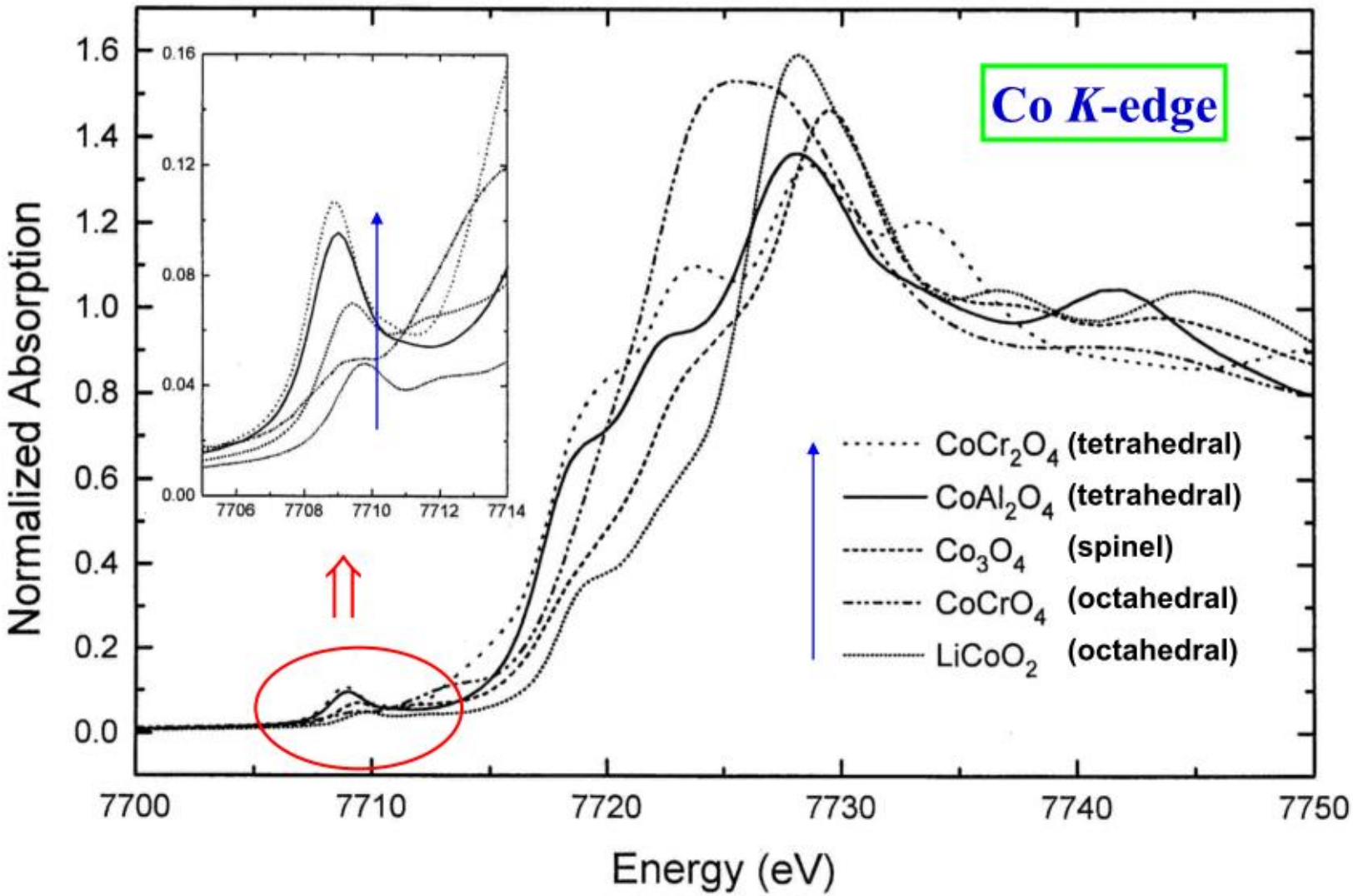

Theory of EXAFS

當中心原子A的內層電子因吸收X光而被游離時，此種**光電子(photo-electron)**將帶著E-E_0的動能遠離原子核，形成一向外行進的**光電子波**，其波長為：

$$\lambda_e = \frac{h}{p} = \frac{h}{[2m(E\text{-}E_0)]^{1/2}}$$

***h*:蒲朗克常數**
***p*:電子動量**
***m*:電子質量**

若吸收原子周圍存在其他原子B時，會將向外行進的光電子波予以**背向散射**，假設A、B兩原子相距R，則向外行進與背向散射的光電子波之間存在$2R$的路程差，此一路程差將使得二者的相位差為：

$$2\pi\left(\frac{2R}{\lambda_e}\right) = 2R\left[\frac{8\pi^2 m(E-E_0)}{h^2}\right]^{1/2} = 2kR$$

其中k稱為**光電子波向量**，常以**Å^{-1}**為單位。

當電子動能的單位為eV時，$k = [0.2625(E-E_0)]^{1/2}$

Theory of EXAFS

向外行進與背向散射的光電子波彼此間的相位差將隨原子間距離及入射能量而變化，進而產生**建設性(同相)**或**破壞性(反相)干涉**，造成在吸收係數上之調諧作用(modulation)，亦即**EXAFS振盪**。

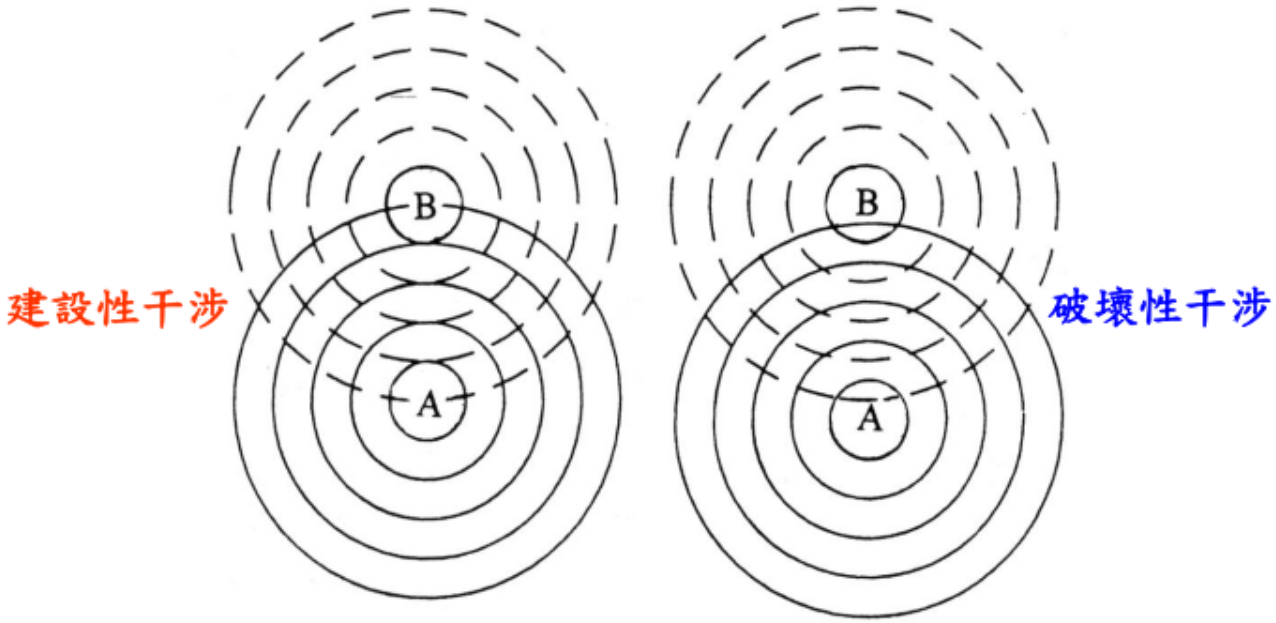

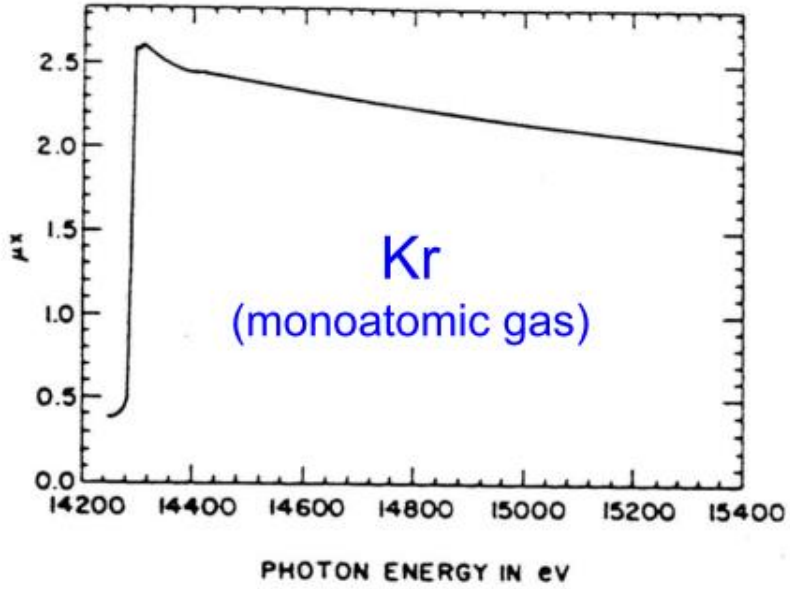
Kr
(monoatomic gas)
μx
2.5
2.0
1.5
1.0
0.5
0.0
14200
14400
14600
14800
15000
15200
15400
PHOTON ENERGY IN eV

(a)

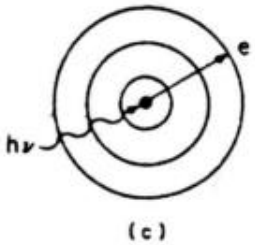
e
hν

(c)

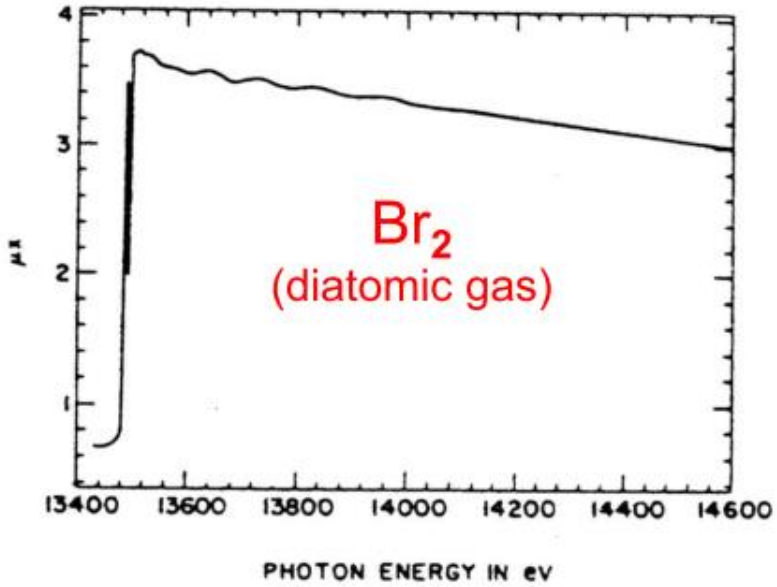
Br_2
(diatomic gas)
μx
4
3
2
1
13400
13600
13800
14000
14200
14400
14600
PHOTON ENERGY IN eV

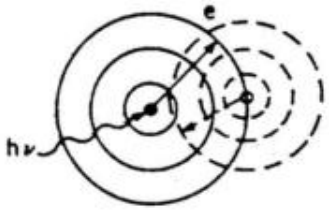
e
hν

(d)

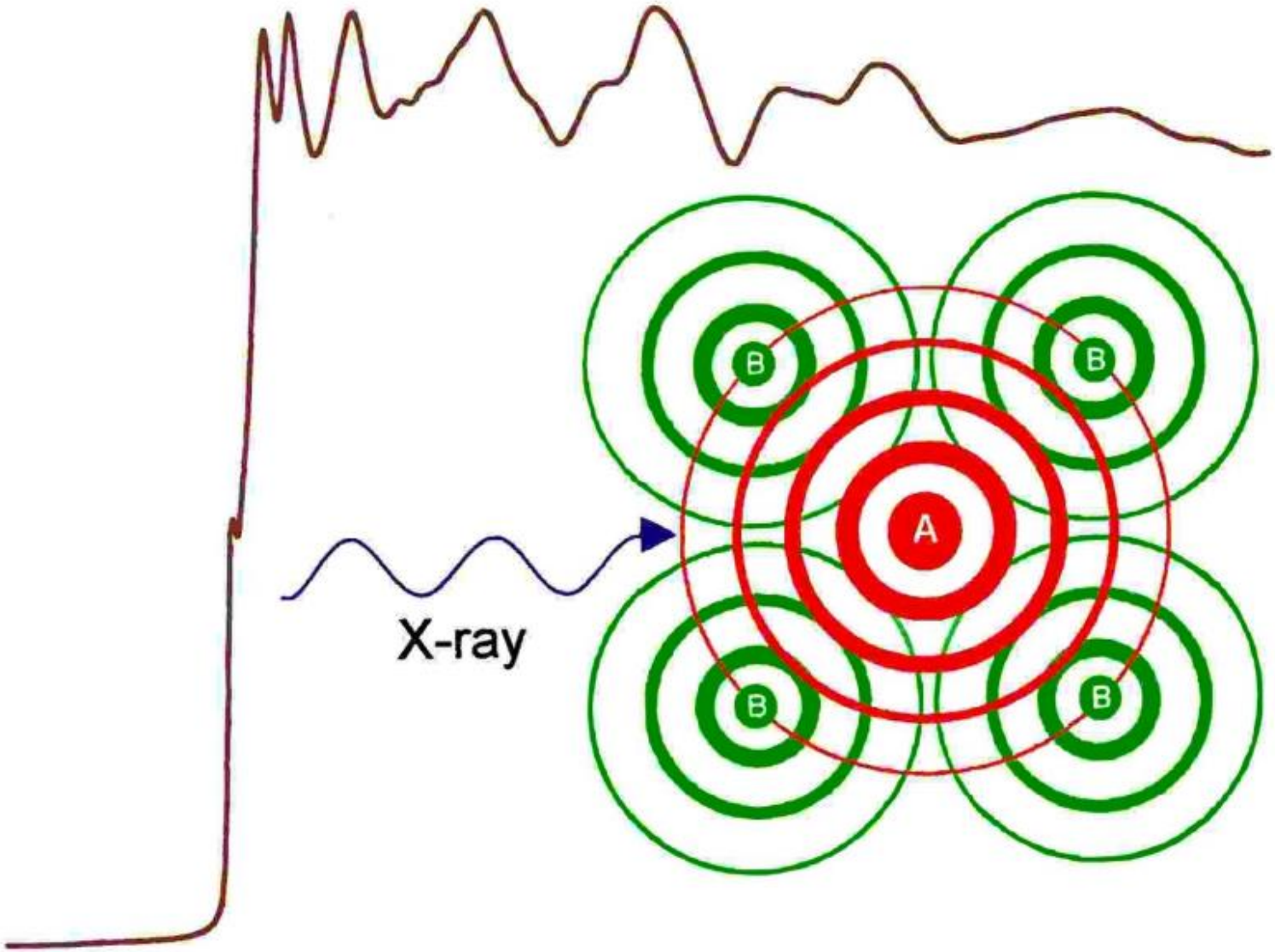
B
B
A
X-ray
B
B

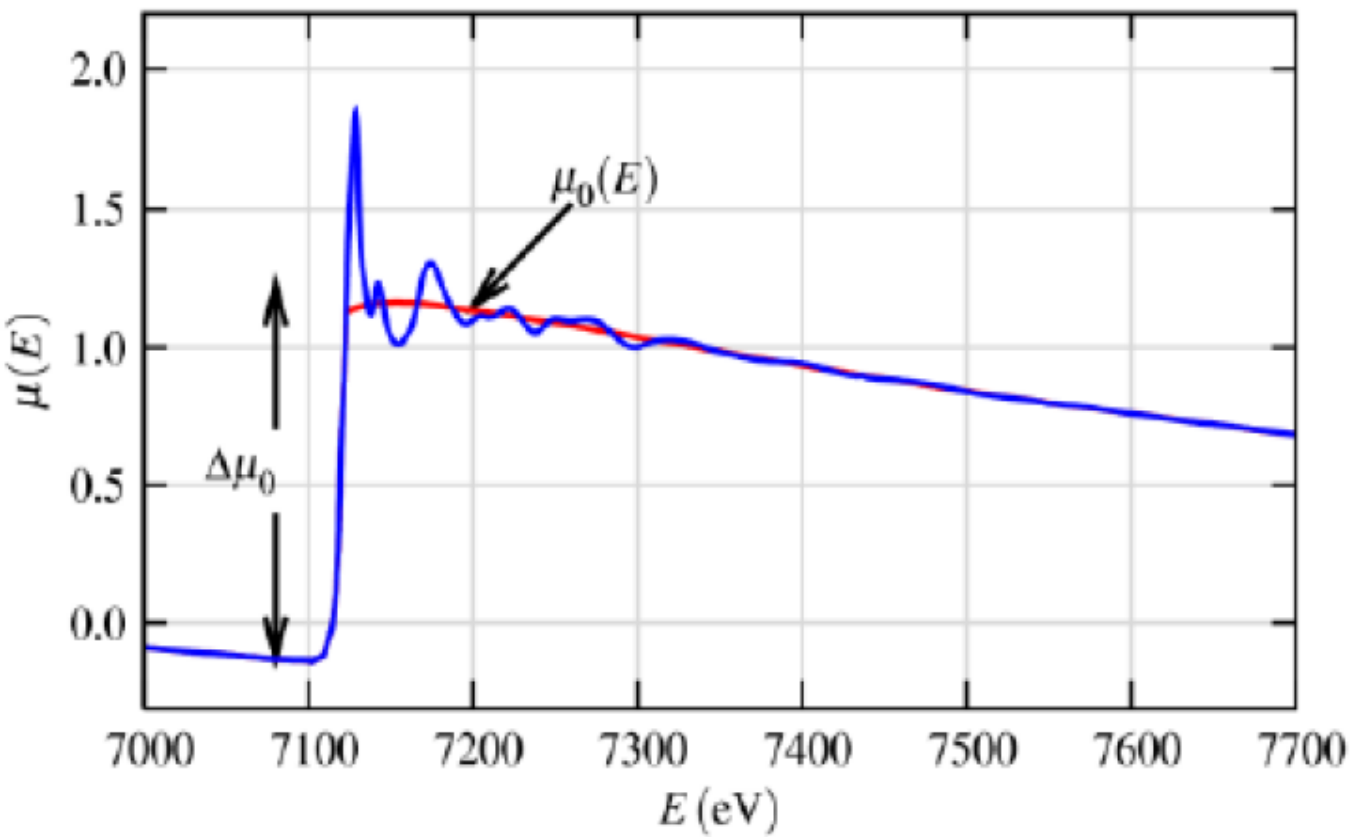

$$\chi(\mathbf{E}) = \frac{\mu(\mathbf{E}) - \mu_0(\mathbf{E})}{\Delta\mu_0(\mathbf{E_0})}$$

$$\mathbf{k} = \sqrt{\frac{2\mathbf{m}(\mathbf{E} - \mathbf{E_0})}{\hbar^2}}$$

EXAFS函數與各結構參數間的關係式

Coordination number

Debye-Waller factor

Phase shift

$$\chi(k) = \sum_j \frac{N_j}{kR_j^2} S_i(k) F_j(k) e^{-2\sigma_j^2 k^2} e^{-2R_j/\lambda(k)} \sin\left[2kR_j + \delta_{ij}(k)\right]$$

Back scattering amplitude

Bond length

Structural Parameters from EXAFS Analysis

Structural parameter	Accuracy	Observable spectral features
bond length (interatomic distance)	±1%	frequency
coordination number	±20%	magnitude
type of coordination atoms	±4 (in atomic no.)	amplitude envelope and phase shift
Debye-Waller factor ($\sigma^2 = \sigma_s^2 + \sigma_t^2$)	±20% (?)	oscillation damping speed

對於每一個配位層皆可透過 EXAFS 數據分析獲得上表中的四種結構參數，以及ΔE_0值。

(一) 吸收邊緣前端的背景扣除

(二) EXAFS 區域內平滑背景的扣除

(三) 正規化處理

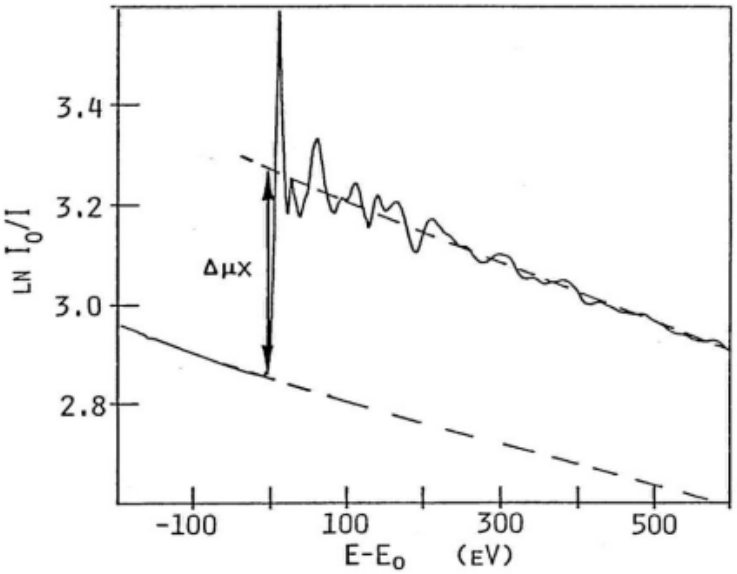

Fig. 6 Illustration of procedure for subtracting the pre-edge and post-edge backgrounds and dividing by the edge jump. The spectrum is measured at Ni K-edge using NiO as the sample.

(四) 將能量座標轉換至 k-空間並進行 k^n 之加權運算

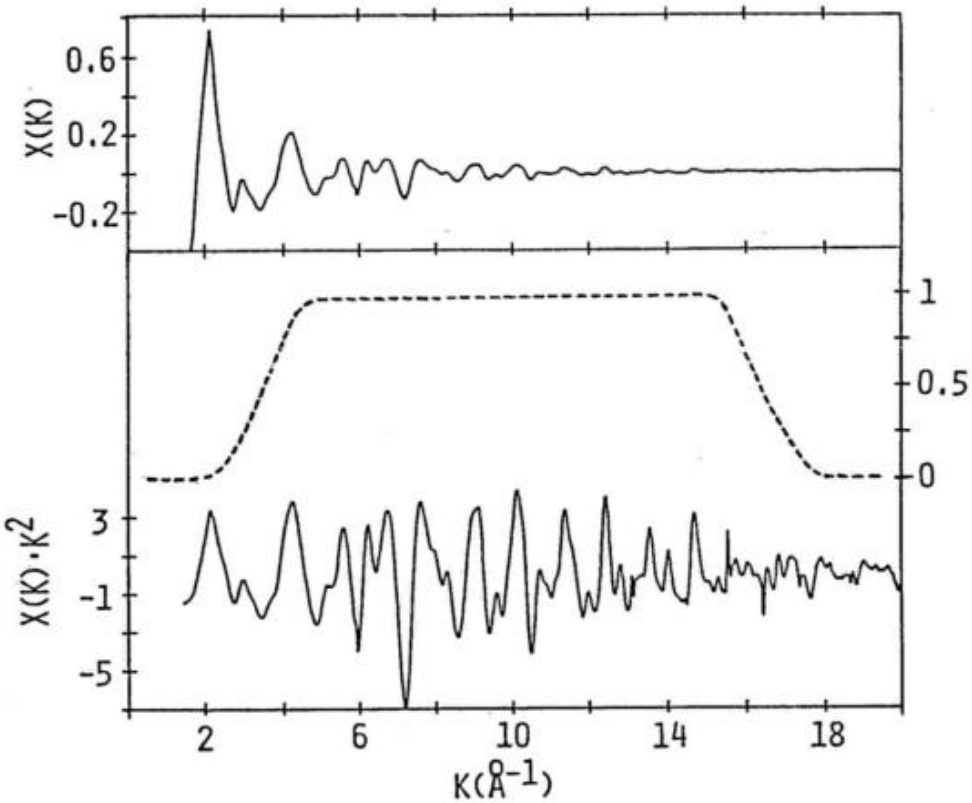

Fig. 7 Background-subtracted and normalized EXAFS function from Fig.6, multiplied by k^n (n = 0 and 2). Dotted curve represents the 40 % Hanning window function.

(五) 傅立葉變換

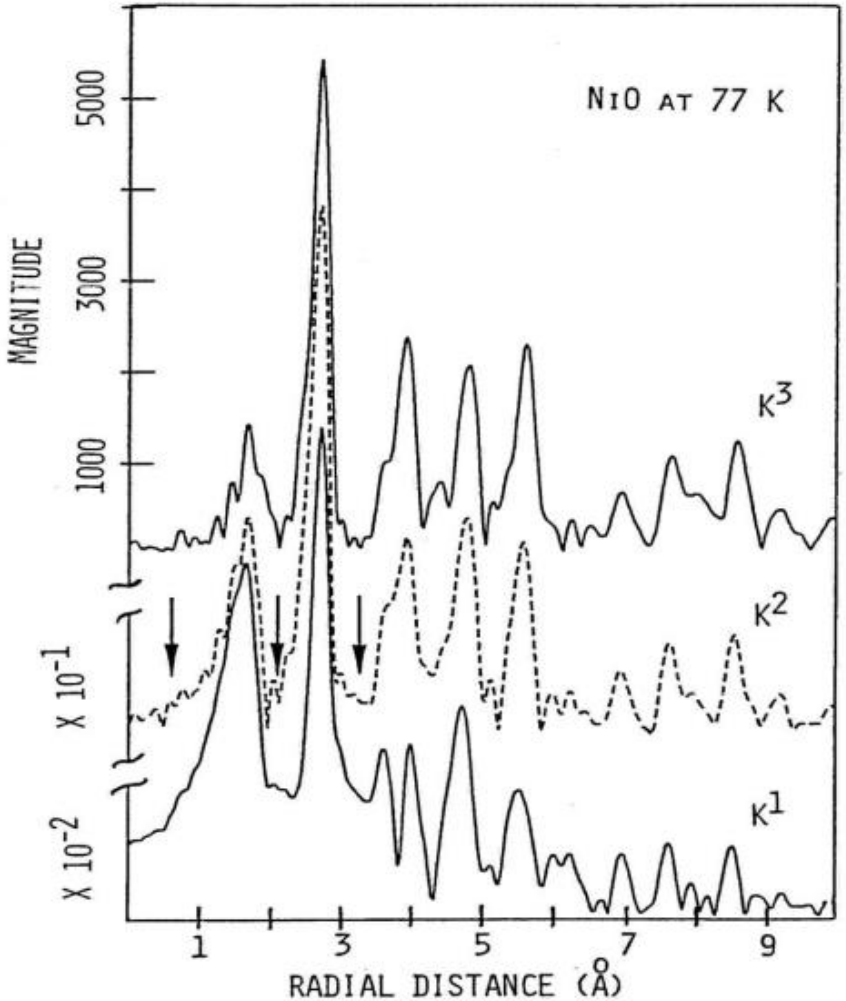

Fig. 8 Fourier transform of k^n-weighted NiO EXAFS. Vertical arrows indicate limits for inverse transform.

原始振盪

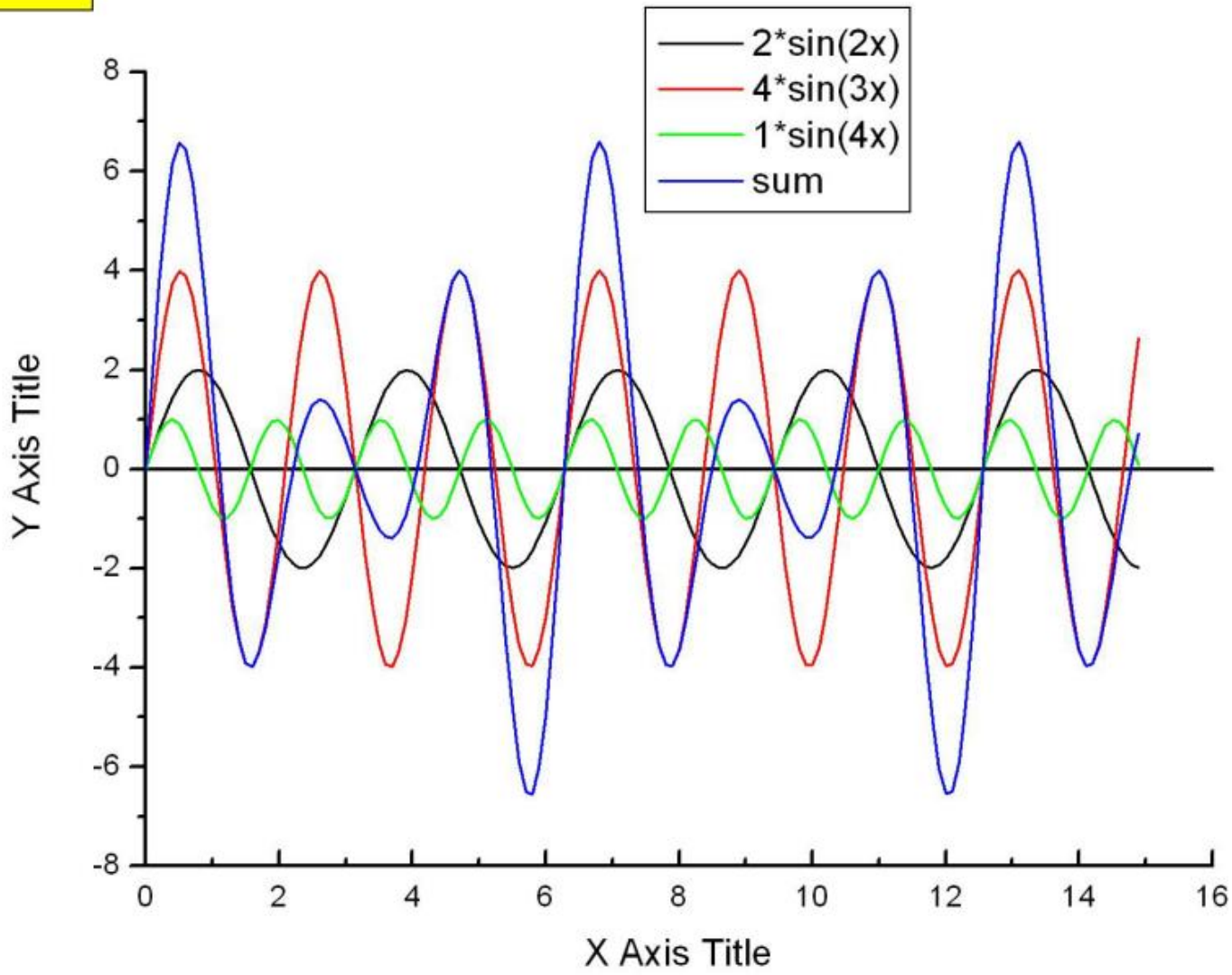
2*sin(2x)
4*sin(3x)
1*sin(4x)
sum
Y Axis Title
X Axis Title
8
6
4
2
0
-2
-4
-6
-8
0
2
4
6
8
10
12
14
16

傅立葉變換後

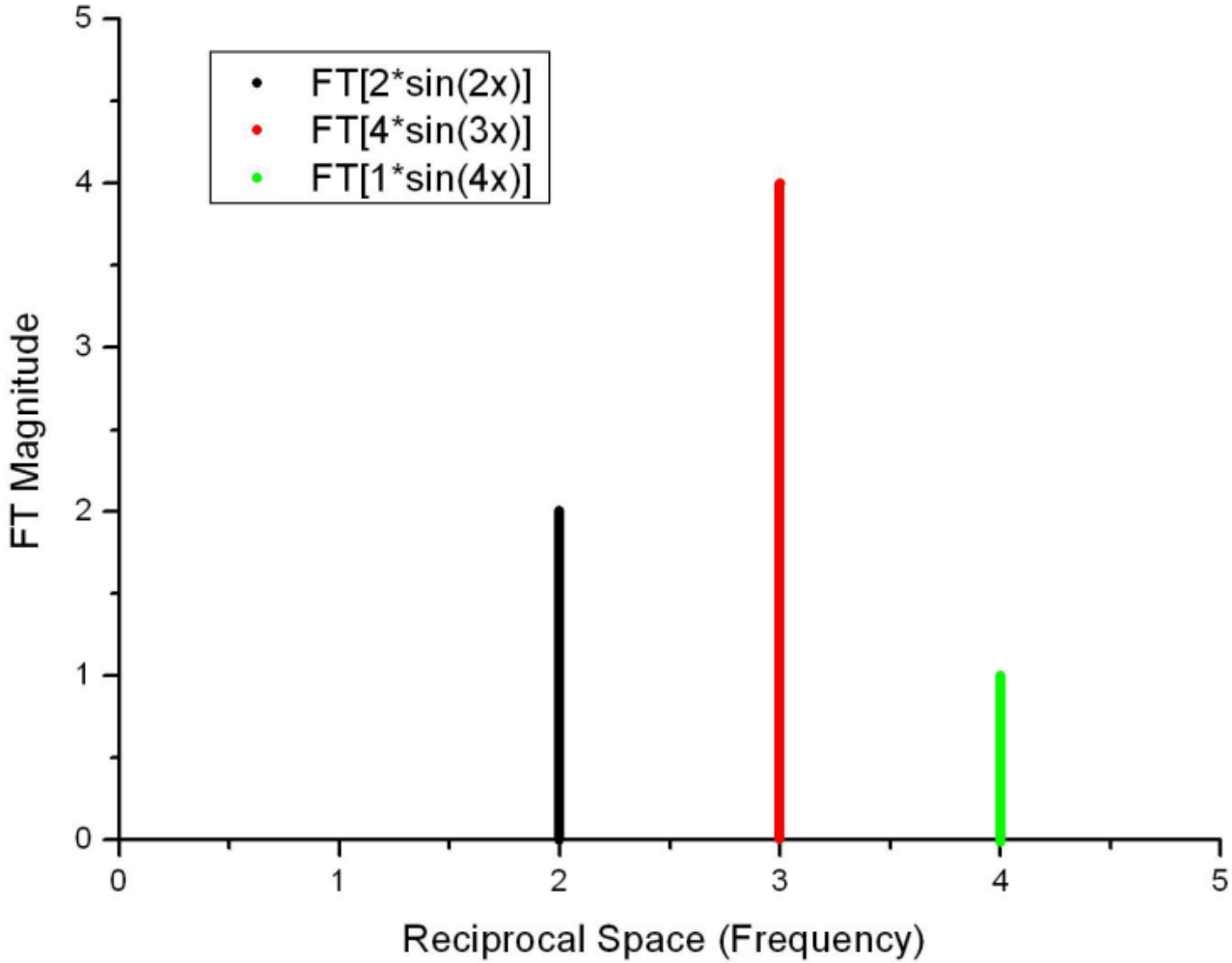
FT[2*sin(2x)]
FT[4*sin(3x)]
FT[1*sin(4x)]
FT Magnitude
Reciprocal Space (Frequency)
0
1
2
3
4
5

(六) 反傅立葉變換

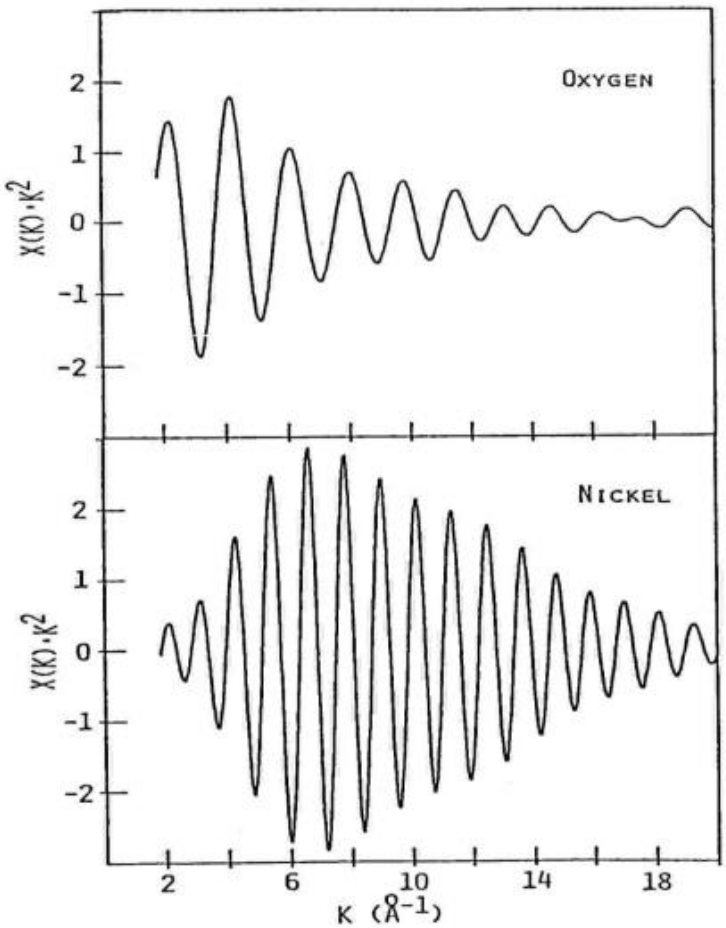

Fig. 9 Inverse transforms for the first two shells in NiO.

(七) 各配位層結構參數的計算

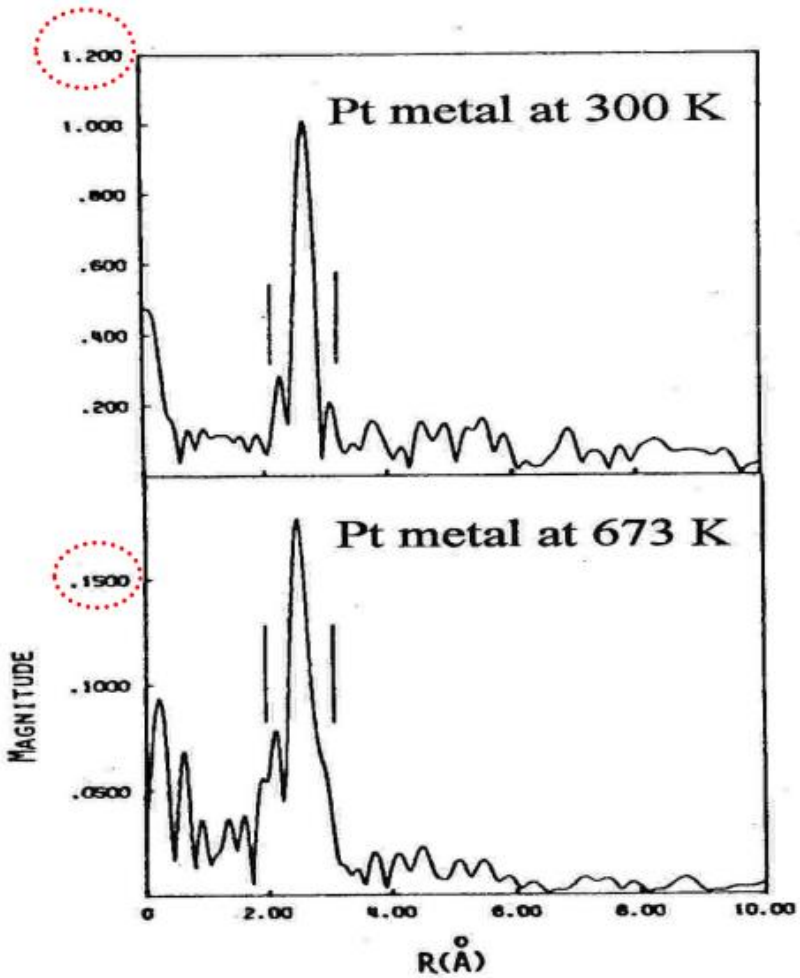

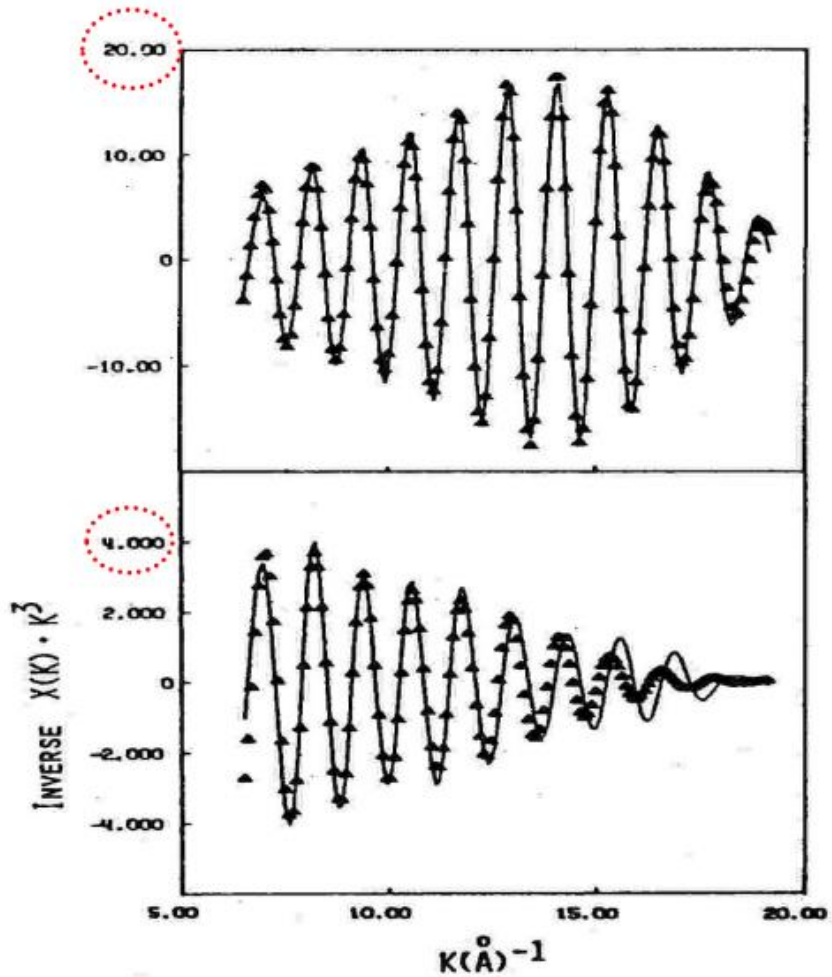

Ru Powder

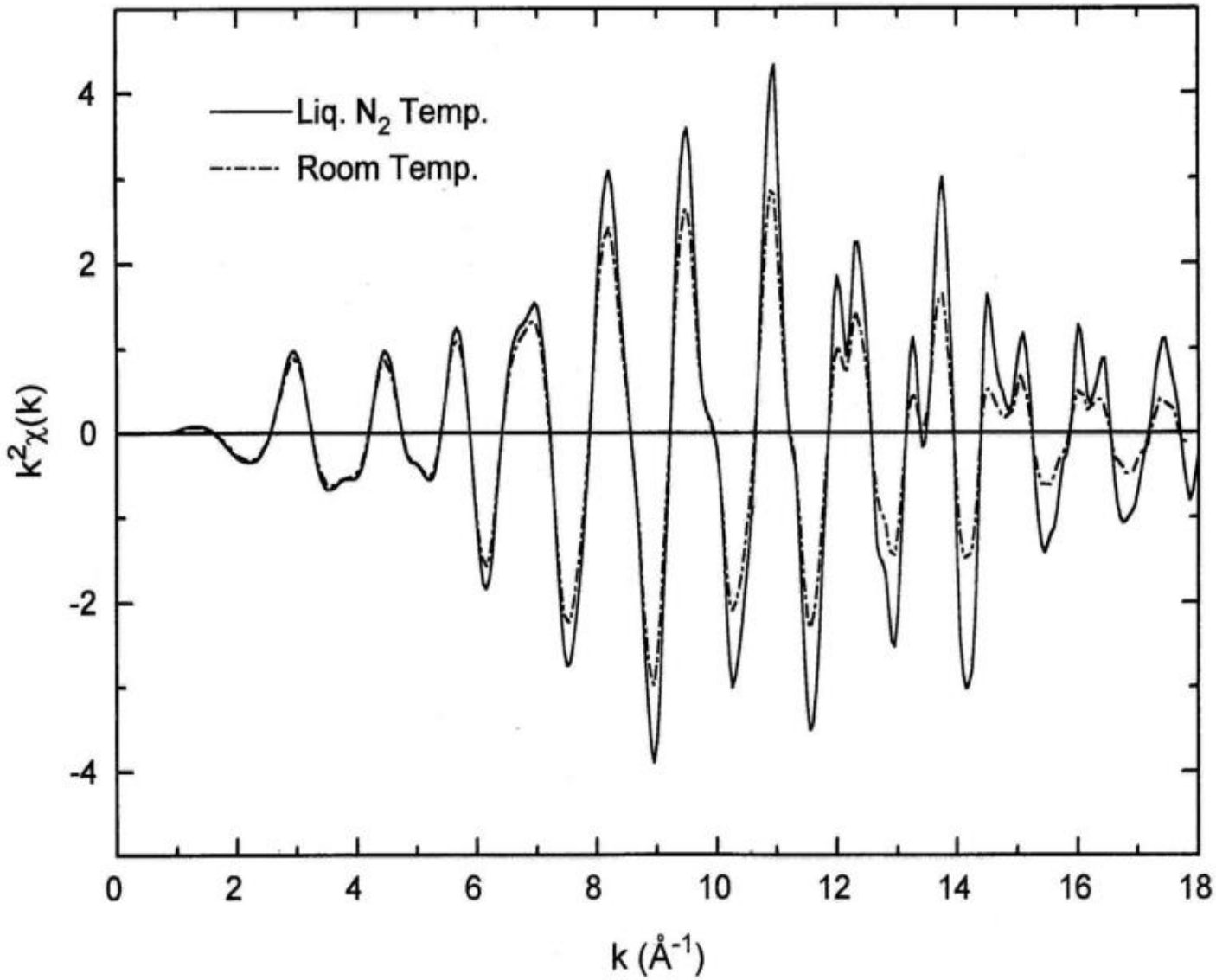

具有fcc晶格結構之三種不同顆粒形狀

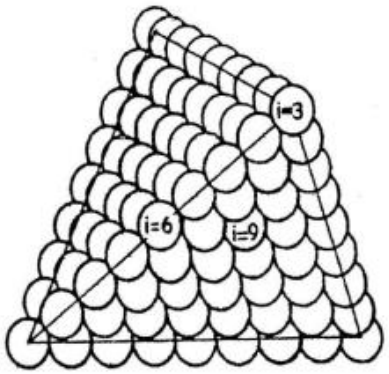

(a) Tetrahedron

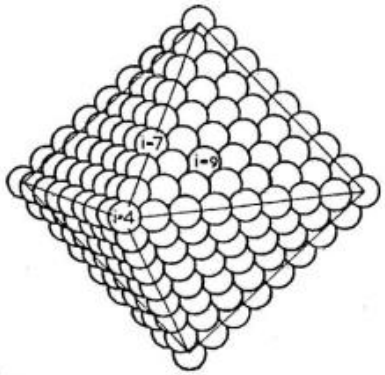

(b) Octahedron

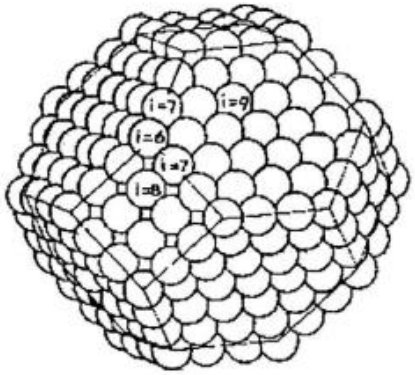

(c) Cuboctahedron

Particle size越小 ⇒ 平均的配位數(N_c)越低

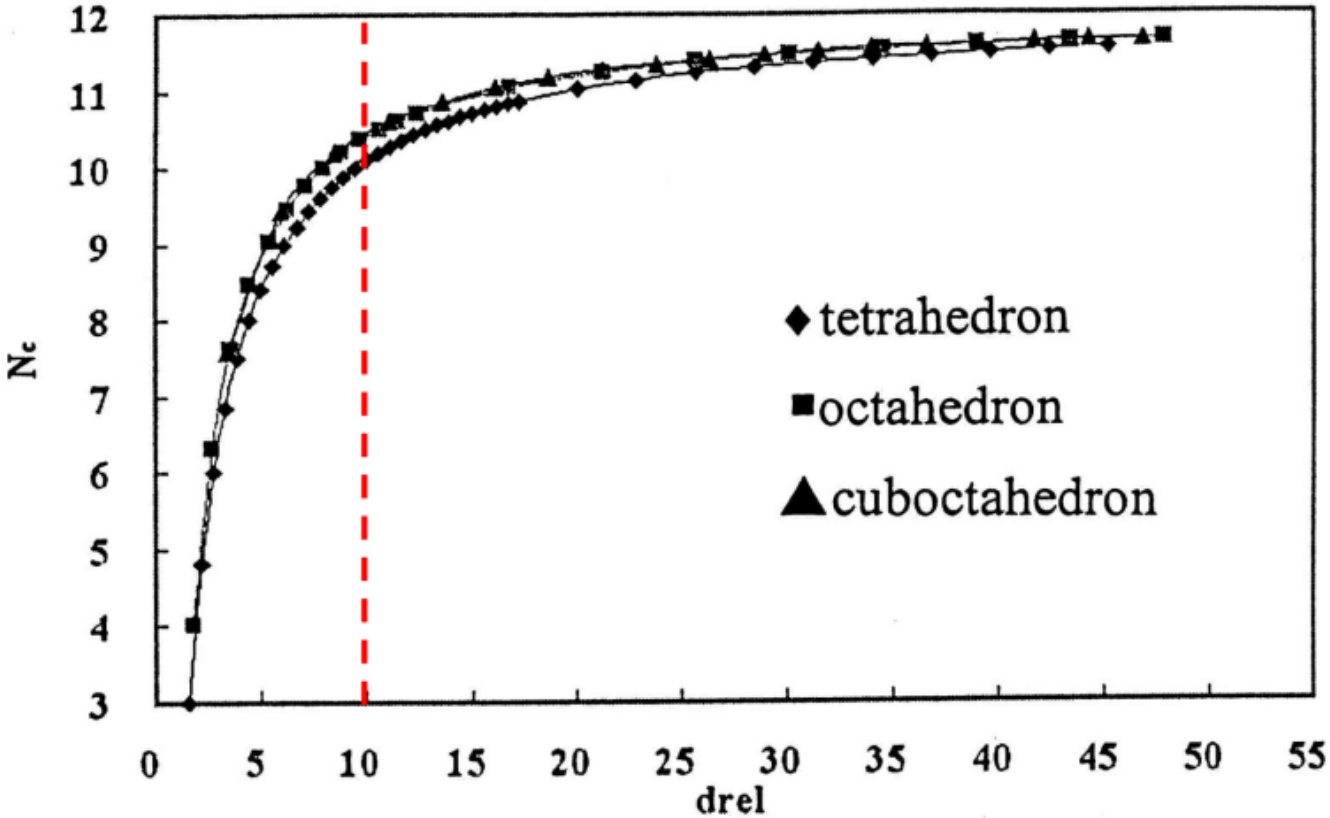

d_{rel} = (diameter of particle) / (diameter of atom)

三種理想 fcc 堆積模型之 N_c vs d_{rel} 關係圖

EXAFS to probe neighboring atoms of Ru-Cu nanoparticles

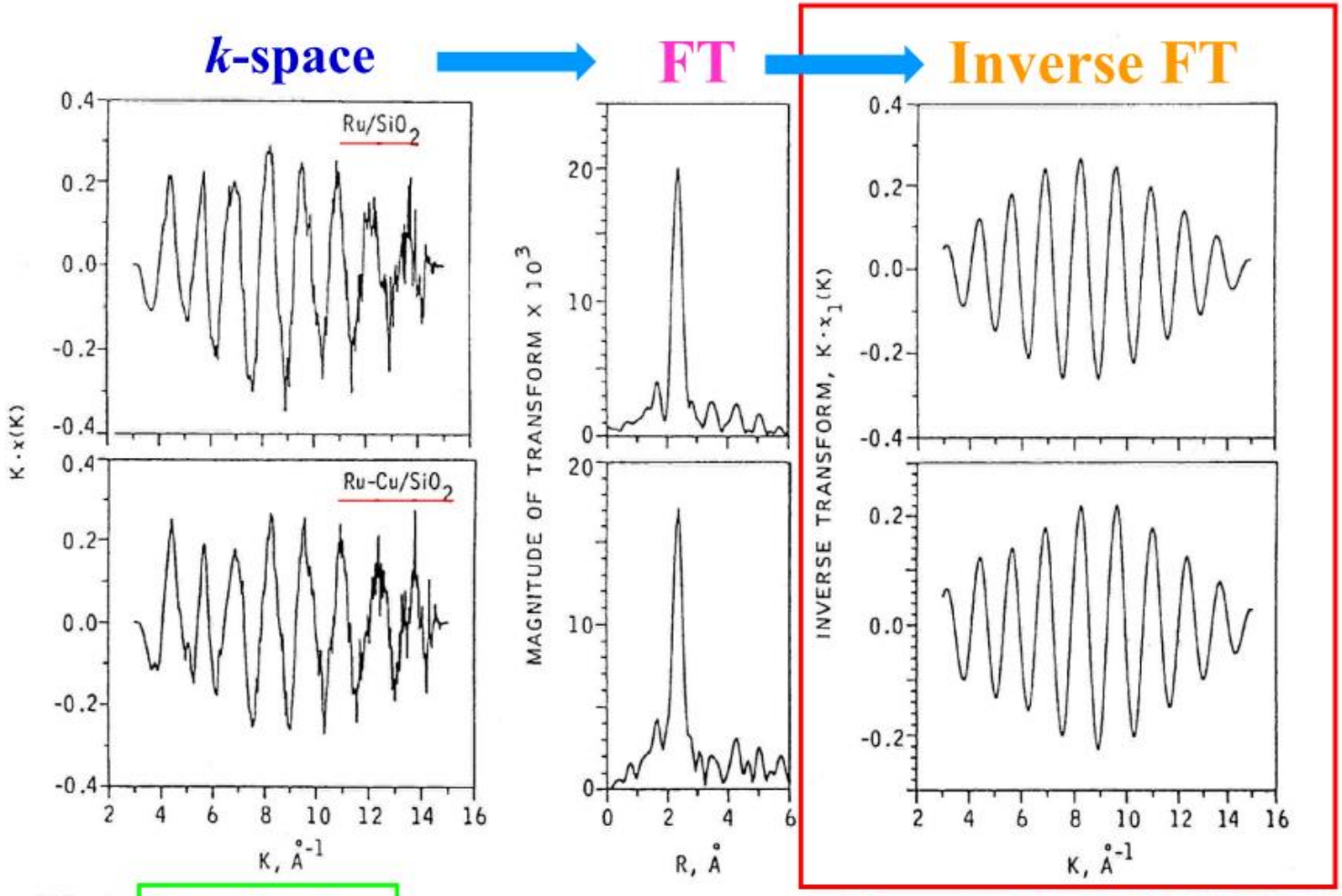

Ru *K*-edge

二者inverse FT之振盪趨勢差異不大，顯示Ru周圍幾乎沒有Cu

Reference: *J. Chem. Phys.* **72**, 4832 (1980).

EXAFS to probe neighboring atoms of Ru-Cu nanoparticles

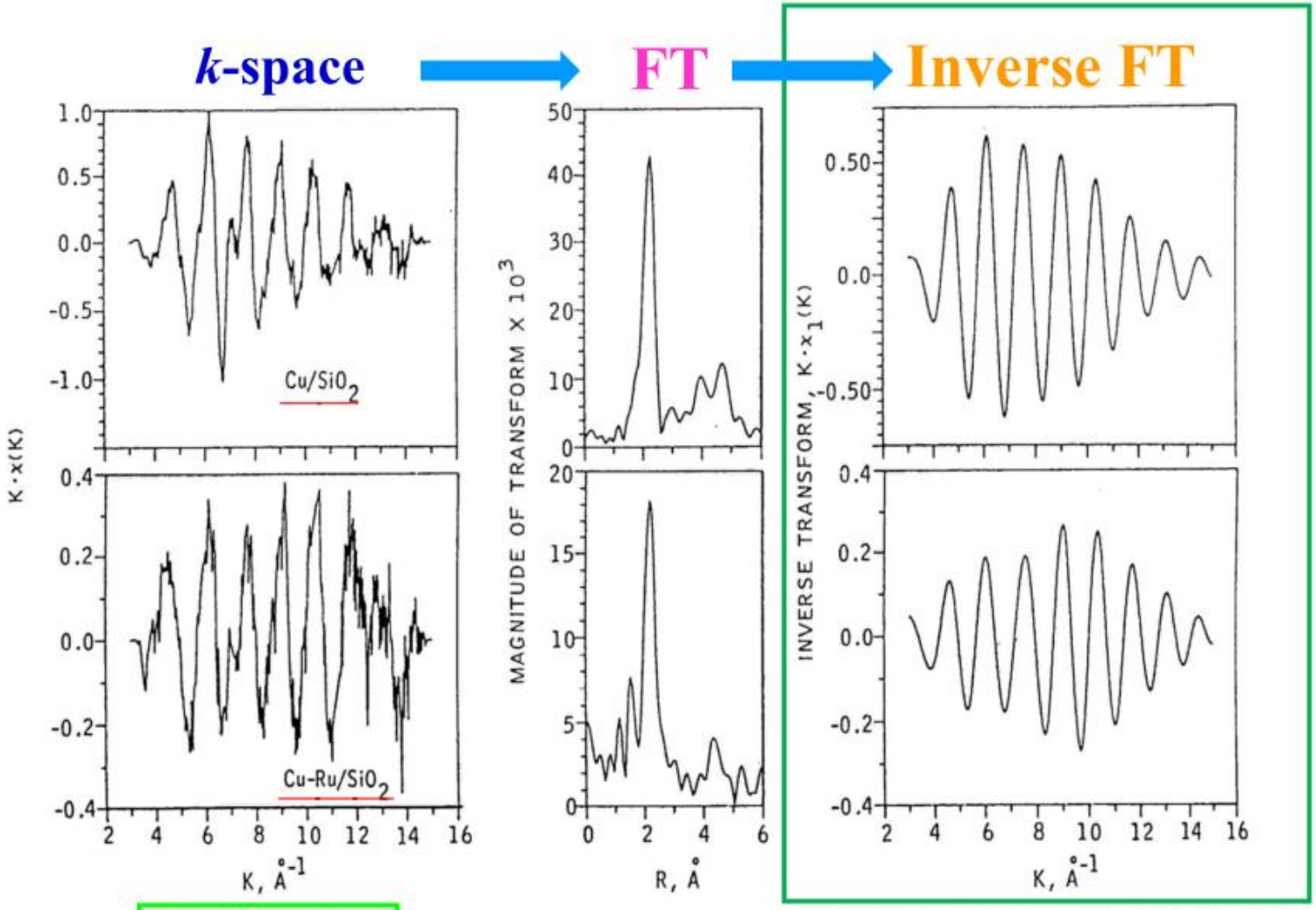

Cu *K*-edge

二者inverse FT之振盪趨勢差異很大，顯示Cu周圍可能有Ru

EXAFS to probe neighboring atoms of Ru-Cu nanoparticles

新鮮還原態　　吸附氧氣後

Ru *K*-edge

Cu *K*-edge

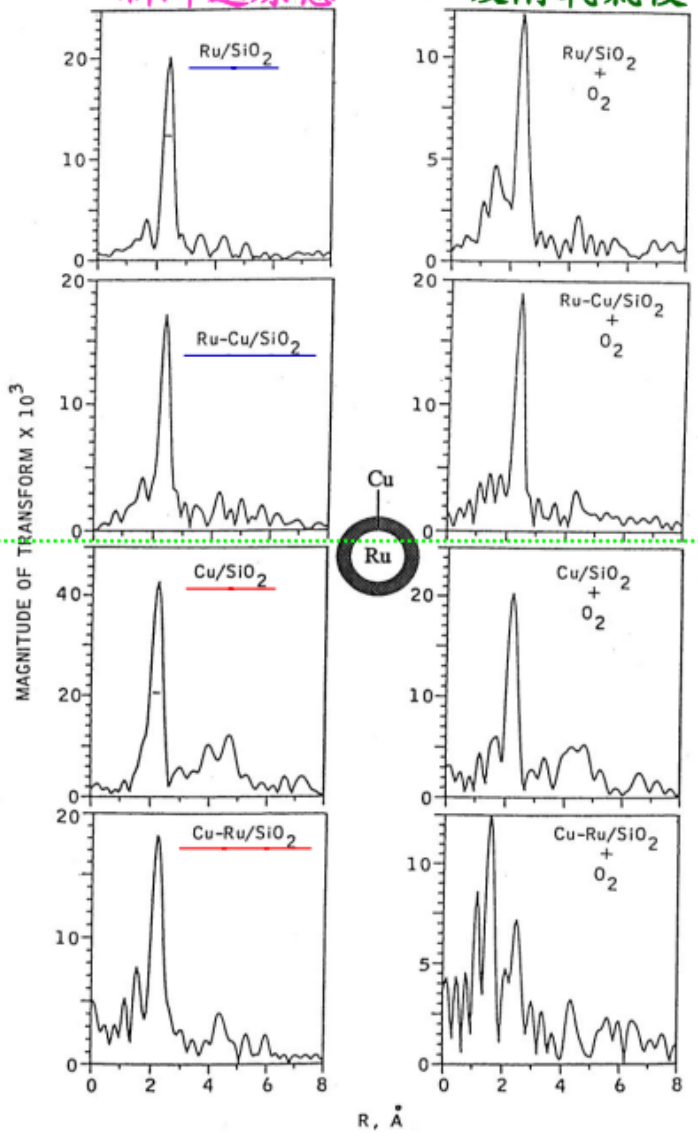

吸附氧氣前後,Ru之FT-EXAFS圖強度差異不大;顯示Ru-Cu奈米顆粒中的Ru可能存在核心,因此不易被氧化

吸附氧氣之後,Cu之FT-EXAFS圖明顯改變;顯示Ru-Cu奈米顆粒中的Cu可能存在表面,因此容易被氧化

Transformation of Co Monolayer on Pt/C

- Sample was prepared via under-potential deposition (UPD).
- The Co monolayer can modify the reaction mechanism and hence the sensitivity of oxygen sensors.

Cyclic voltammograms of Pt/C electrodes with and without monolayer Co in 1.0M KOH solution.

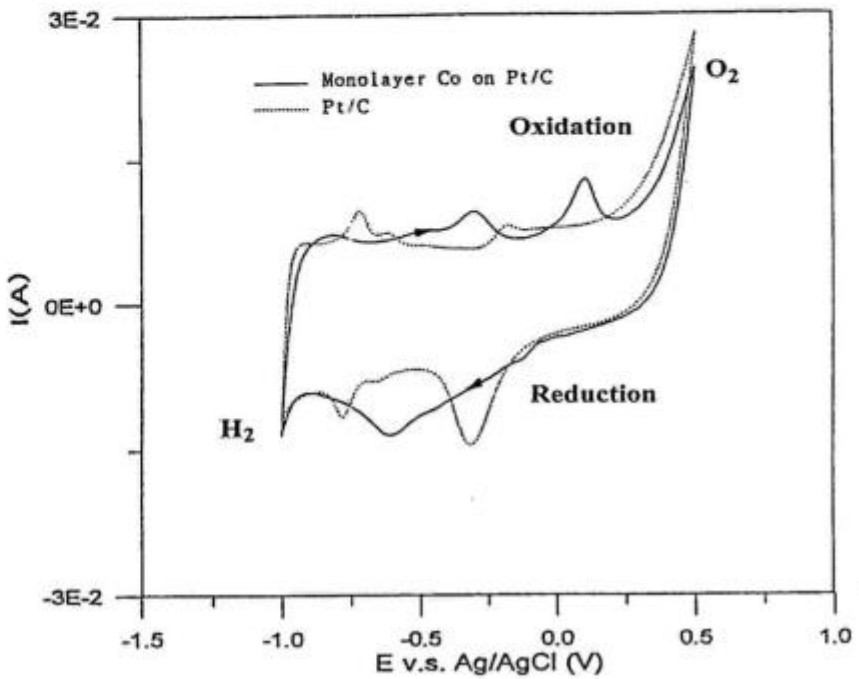

Transformation of Co Monolayer on Pt/C

- Both XANES and EXAFS data indicated that Co is present as Co^{2+} species when the applied voltage < -0.5 V.
- Co is present as Co^{3+} when the applied voltage > -0.2 V.
- The changes in electronic and structural properties are reversible.
- If the monolayer is Cu, the transformation will occur between Cu^0 and Cu^{2+}.

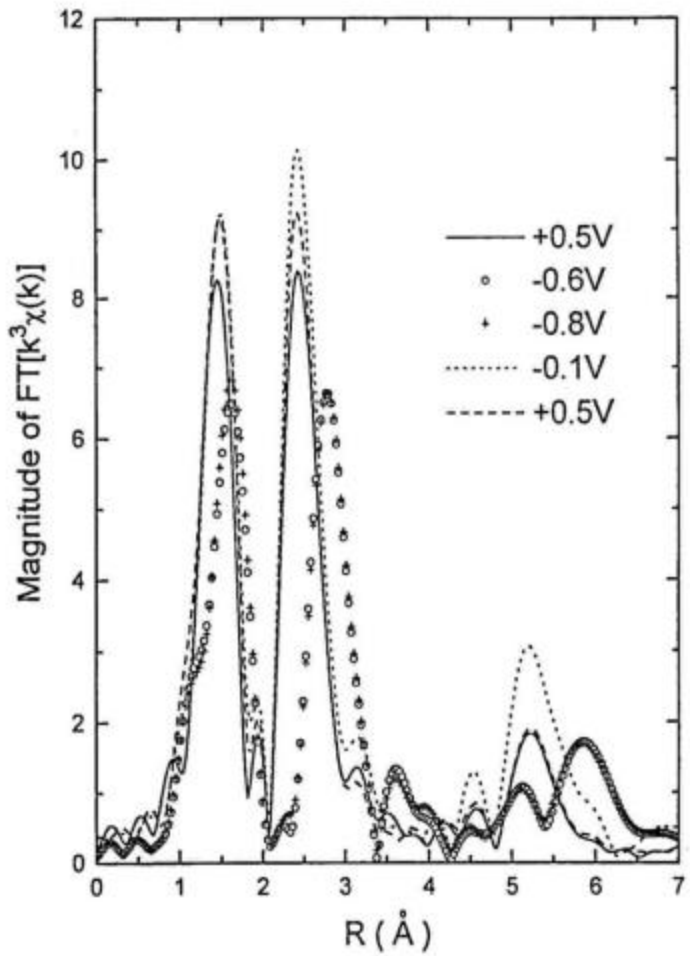

EXAFS to probe structural disorder of $LiCoO_2$ electrode

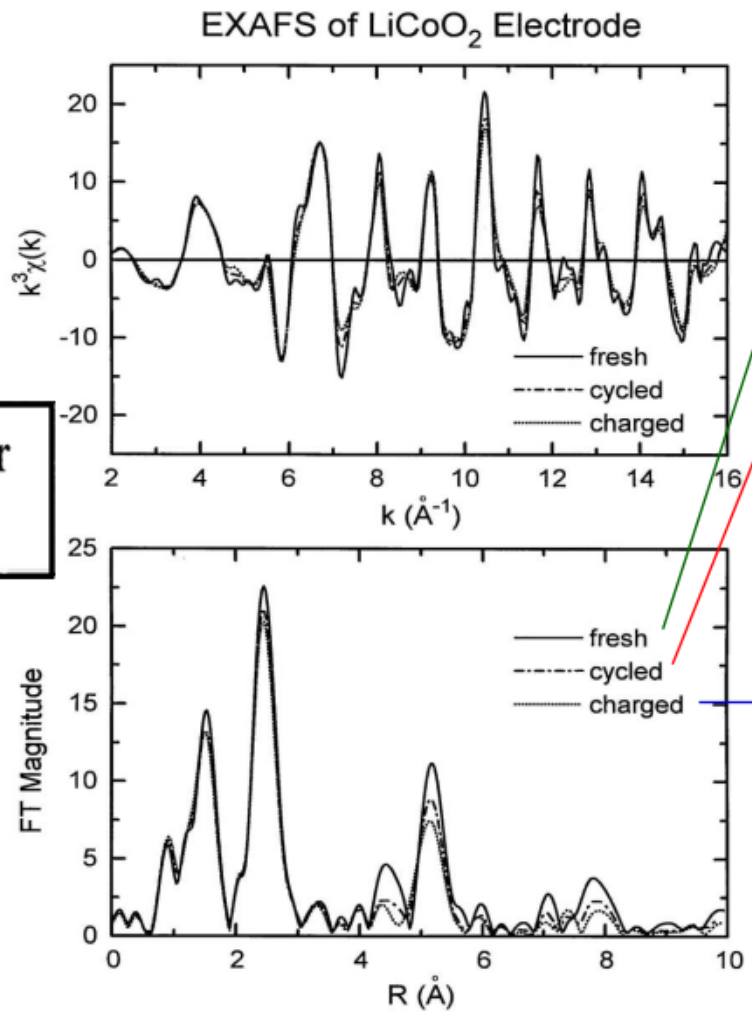

Debye-Waller factor

$(\sigma^2 = \sigma_s^2 + \sigma_t^2)$

原子靜態下的排列亂度

熱擾動

Fresh (初始態):
結構最有序

Cycled(充放電一次):
從圖上來看只能部分或接近回到初始狀態,無法完全回復;因此手機電池充放電循環多次後,將使結構整個破壞,無法繼續使用

Charged (充電):
Li 離子從晶格遷出,造成晶格部分扭曲,故結構趨於disorder

XANES to probe charge transfer of Li_2SrSiO_4:(Ce/Eu) yellow phosphor

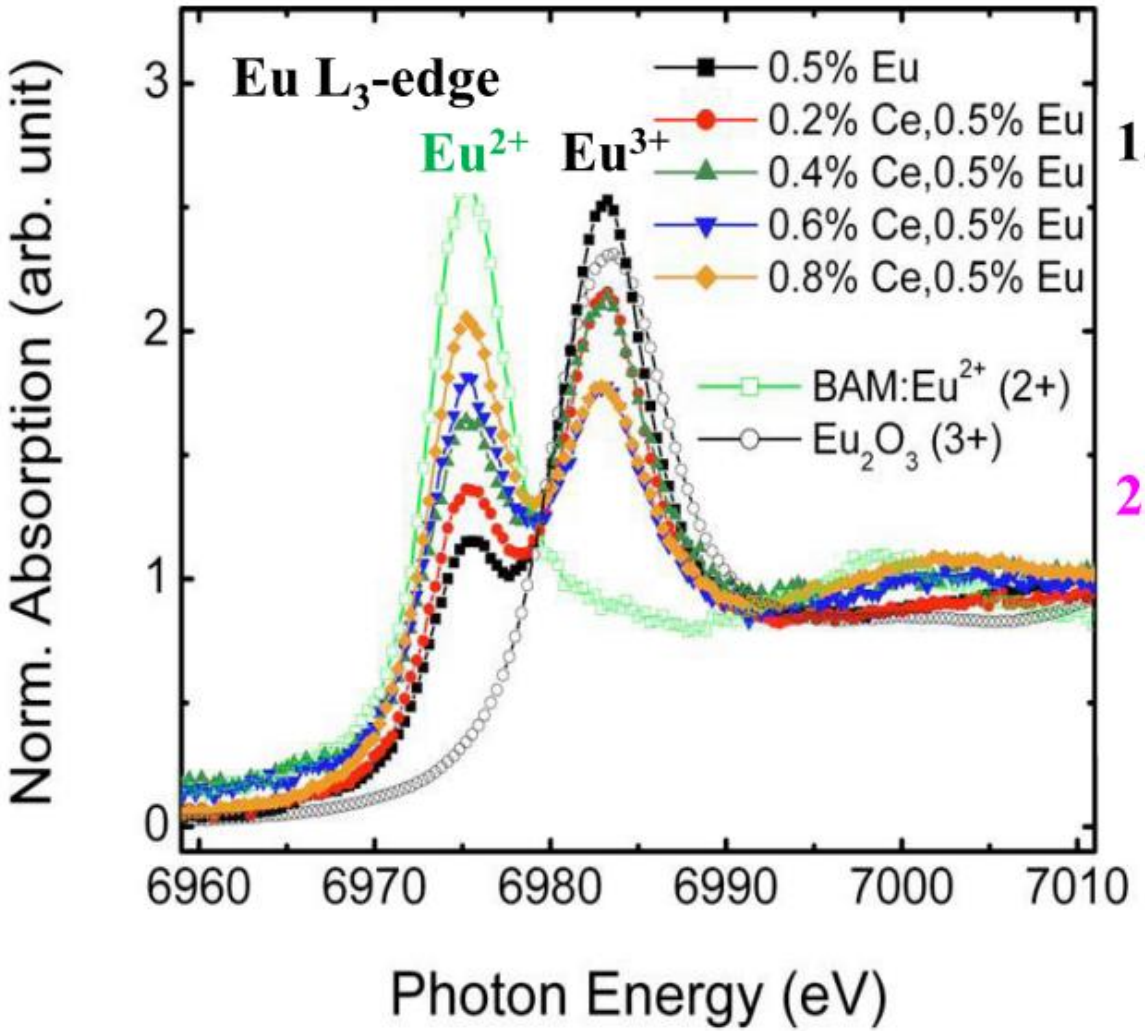

1. 螢光粉所含的Eu為混合價態，只摻雜0.5% Eu的樣品中Eu^{3+}明顯多於Eu^{2+}

2. 隨著Ce摻雜濃度的增加(Eu濃度保持固定)，Eu^{3+}的比例逐漸減少；顯示Ce將電子傳給Eu

Reference: *Appl. Phys. Lett.* **96**, 061904 (2010).

XANES to probe thickness of $LaNiO_3$ thin film

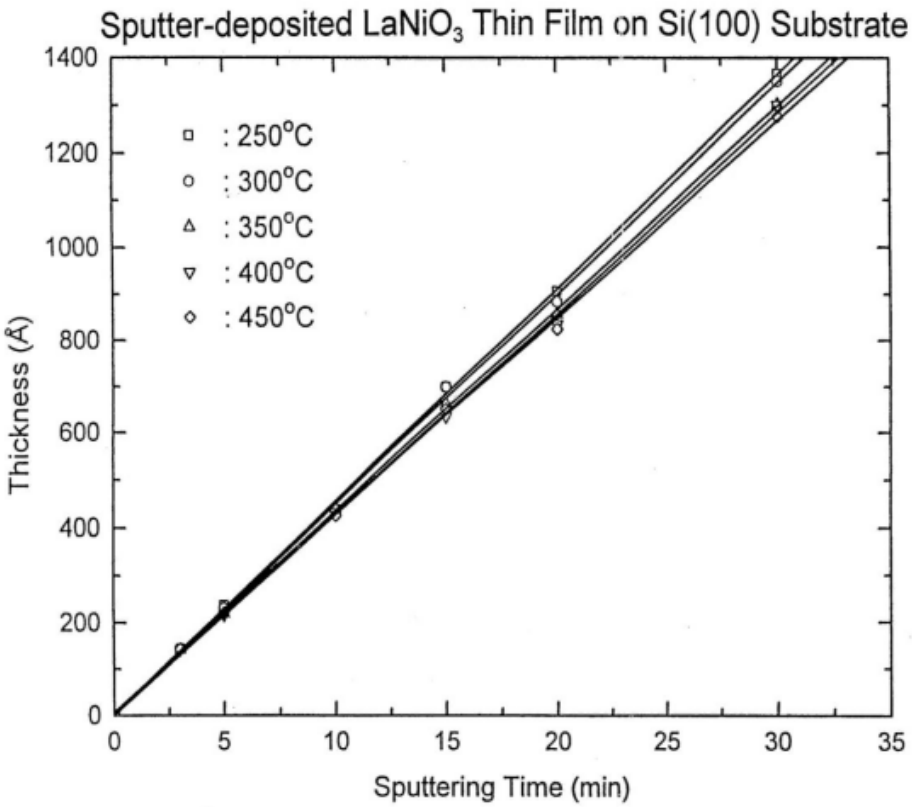

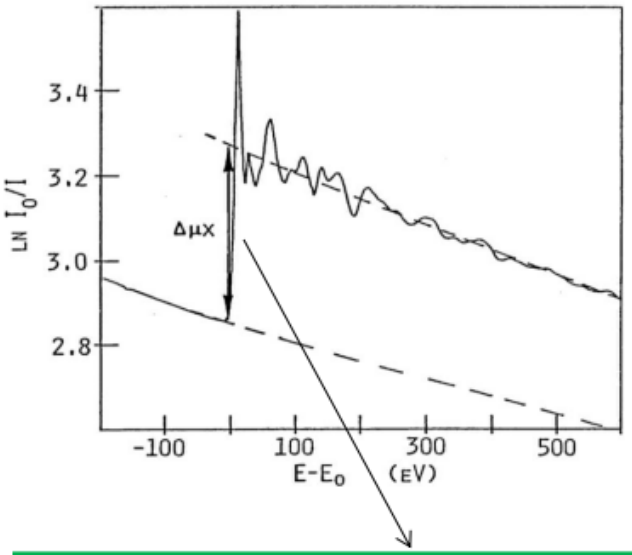

利用edge jump 推算薄膜厚度(或元素含量)與濺鍍時間之關係

1. 改變不同Si(100)基板之濺鍍溫度;其薄膜厚度與濺鍍時間均呈正比

2. 基板之濺鍍溫度越低,其薄膜厚度越大(成長速度越快)

XANES to probe thickness of $LaNiO_3$ thin film

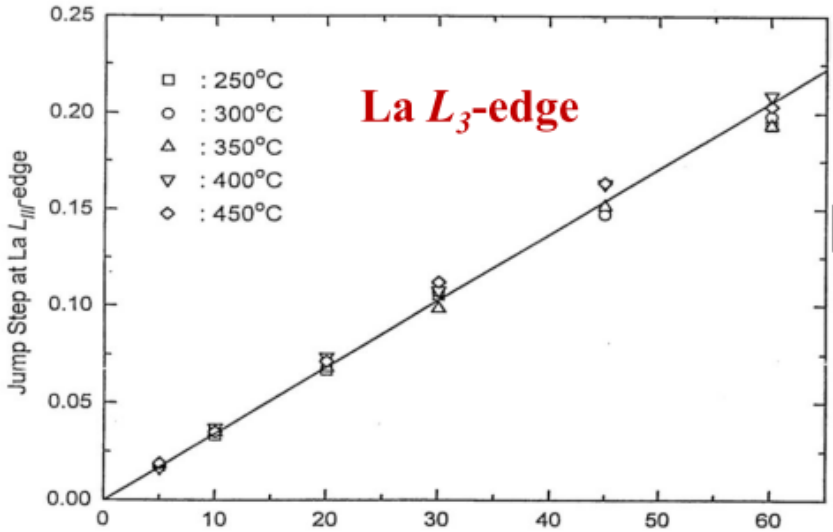

對比較重之La元素而言,改變濺鍍溫度其edge jump差異不大

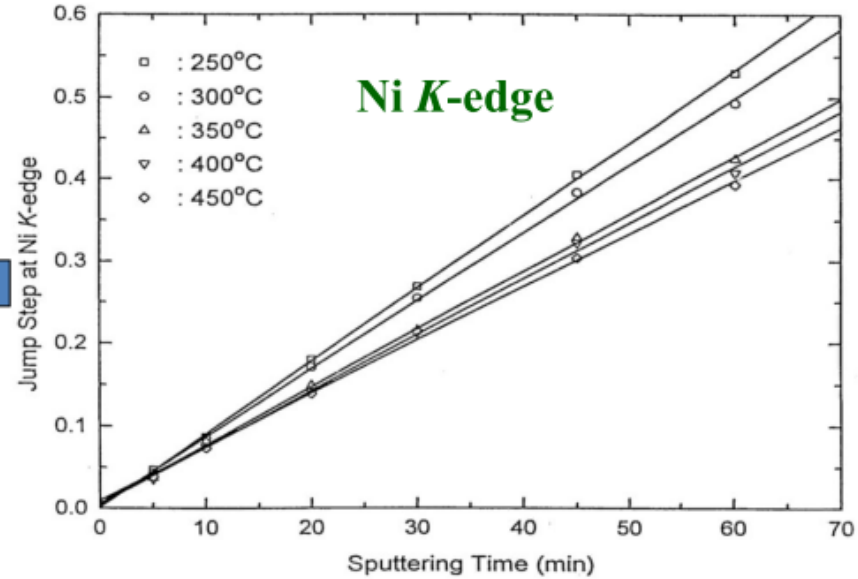

對比較輕之Ni元素而言,改變濺鍍溫度其edge jump有明顯變化,且250°C時斜率最大;換言之,造成其厚度變化主要是由Ni元素所控制

Reference: *J. Appl. Phys.* **80**, 2175 (1996).

Polarized XAS investigation of Br_2 adsorbed on graphoil sample

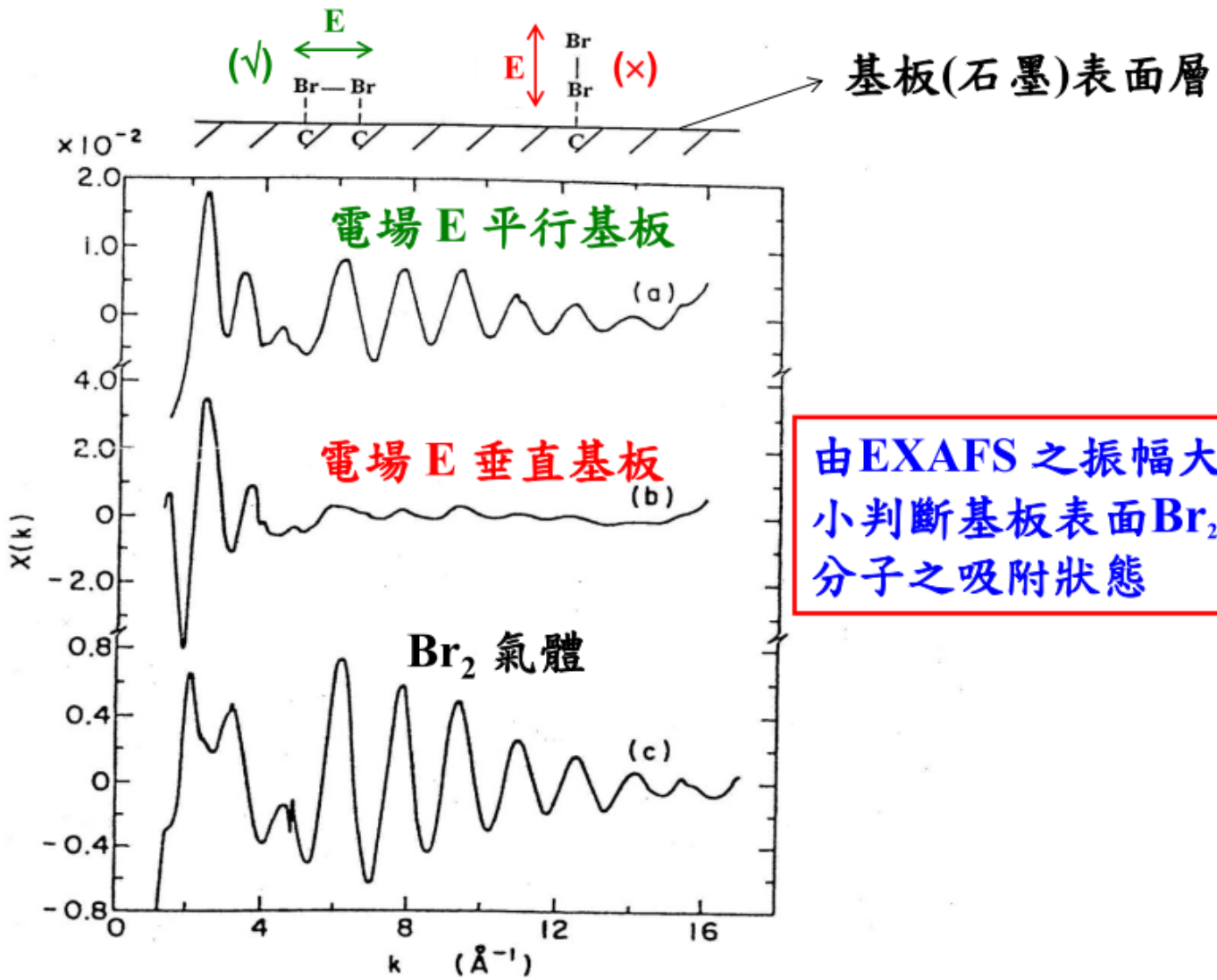

由EXAFS之振幅大小判斷基板表面Br_2分子之吸附狀態

Advantage of X-ray Absorption Spectroscopy

- A powerful structural tool for materials in various forms, including crystalline or amorphous solids, liquids, and gases. Sample is not required to have a structure of long-range order.
- XANES reflects effective charge density (oxidation state), electronic structure, and coordination symmetry of the absorber.
- EXAFS provides the information of local (< 10 Å) atomic structure.
- Element specific (element selective).
- Easy to perform *in-situ/operando* measurements.

X光吸收光譜之缺點與限制

獲得的訊息(包括氧化價數與配位數等)為樣品中所有吸收原子的平均值，因此當樣品含有不只一種狀態下的吸收原子(譬如存在不同晶相中)時，解讀數據分析結果需特別注意。

Thanks for your attentions